Title
Characterization of GFAP+ Islet Glial Cells

Author
Varonin, Jillian

Publication Date
2016

Peer reviewed|Thesis/dissertation

Characterization of GFAP+ Islet Glial Cells

by

Jillian Varonin

DISSERTATION

Submitted in partial satisfaction of the requirements for the degree of

DOCTOR OF PHILOSOPHY

in

Biomedical Sciences

in the

GRADUATE DIVISION

of the

UNIVERSITY OF CALIFORNIA, SAN FRANCISCO

Acknowledgments

First and foremost I would like to thank my PI, Michael German. Mike graciously took me into his lab when I needed a new home at the beginning of my 5th year in graduate school and helped me begin this new project on an understudied but fascinating cell type in the pancreatic islet: the GFAP+ glial cell. I would also like to thank the rest of the German lab members, past and present, including: Chester Chamberlain, Luc Baeyens, David Scheel, Zhongmei Li, Juehu Wang, Katherine Yang, Shuhong Zhao, Hector Macias, Stefani Nalle, and Shiue-Cheng (Tony) Tang, a professor at the Taiwanese National Tsing Hua University who took a sabbatical in German Lab.

A huge thank you, debt of gratitude, and acknowledgement is owed to Eleonora de Klerk, a postdoctoral scholar in the lab of Michael McManus, for her generous assistance with conducting the Drop-seq single cell RNA-seq experiments and computational analysis. I would also like the rest of the McManus lab for letting me camp out in their lab while I worked on those experiments. Without Vihn Nguyen, a specialist within the Division of Transplant Surgery and part of the Flow Cytometry Core, I'm not sure I could have conducted this project. Vihn isolated all my islets used for my project as well as assisted me with sorting cells on the complicated FACS machines. Vihn deserves the highest praise for his dedication, enthusiasm, and kindness. Additionally, as helpful lab neighbors are invaluable to conducing academic laboratory science, I would also like to acknowledge technical assistance and borrowing of lab supplies from Greg Ku and lab, Shingo Kajimura and lab, Katja Brückner and lab, as well as the rest of the Regenerative Medicine Building, Diabetes Center, and the labs listed in the Methods chapter for donating mice.

In addition to Mike, I would like to thank the rest of my thesis committee members, Ethan Weiss and Julie Sneddon. Along with Mike, Ethan has been a mentor to me since my

qualification exams, helping to see me through the highs and lows of completing my PhD. Julie has been a wonderful addition to the Diabetes Center and to my PhD mentorship. Ethan and Julie have provided much appreciated outside guidance and insight, in addition to being sources of motivation and support.

And last, but certainly not least, I would like to thank my family and friends for their encouragement and support while I have worked on my PhD. To my mom Linda, dad John, and brother Ian: thank you. I want to thank all my fellow 2010 entrance Biomedical Sciences PhD program cohort for the fun occasions away from lab, for answering my naïve questions about their research outside of my areas of expertise, and for struggling alongside of me. And thank you to my non-science friends who helped keep the sometimes crazy world of academic science in perspective. Thank you all!

Characterization of GFAP+ Islet Glial Cells

Jillian Varonin

Abstract

Besides the relatively well-studied endocrine cell types, such as the insulin producing-beta cell and glucagon-producing alpha cell, the pancreatic islet also includes multiple less-appreciated non-endocrine cells types. These non-endocrine cell types include blood vessel-related cells, including endothelial cells and pericytes, and nervous system related cells, including neurons and glial cells. While their existence has been recognized for decades, the GFAP+ glial cells that ensheath and extend into the islet are understudied and largely uncharacterized. The author of this thesis sought to define the GFAP+ cell population and its lineage, test potential mouse models and culturing systems that could be used to interrogate these cells, as well as perform single cell RNA-seq analysis on these cells by using the Drop-seq method. We found that the GFAP+ cells in the pancreas are of neural crest cell lineage and these cells remain and survive in ex vivo islet culturing systems. Additionally, through Drop-seq, we confirm that these GFAP+ cells express glial cell-associated genes as well as other cell markers that could be used experimentally to manipulate these seemingly genetically-intractable cells.

Table of Contents

List of Tables

List of Figures

Figure Legends:

Figures:

Chapter 1: Background

Diabetes and the Non-Endocrine Cells of the Pancreatic Islet

The pancreatic islet is made up of insulin-producing beta cells, glucagon-producing alpha cells, somatostatin-producing delta cells, pancreatic polypeptide producing PP cells, and the rare ghrelin-producing epsilon cell (Figure 1). Perhaps less appreciated, the islet also includes many non-endocrine cell types, including neurons and glial cells, blood vessel-associated cells, and immune cells (Figure 1). As both type I and type II diabetes ultimately result from beta cell dysfunction, death, and the lack of ability to adequately maintain or increase beta cell mass to meet the body's insulin demands, being able to improve beta cell function or control beta cell mass is a much sought after goal in the field of diabetes research. Intriguingly, the non-endocrine cell types of the pancreatic islet are known or thought to influence beta cell development, maturation, function and/or beta cell mass. Intact, isolated islets release insulin differently as compared dispersed islets in suspension or islets grown in 2D monolayers, likely due to differences in the islet 3D architecture and cellular and extracellular matrix (ECM) composition[1,2].

Islet Innervation: The pancreas is innervated by cells of the sensory system, sympathetic nervous system (SNS), and parasympathetic nervous system (PNS), and through the release of neurotransmitters and neuropeptides from nerve terminals at or near the islet endocrine cells, these neurons regulate the release of insulin, glucagon, somatostatin, and pancreatic polypeptide[3]. PNS activation increases insulin secretion via the release of acetylcholine, vasoactive intestinal polypeptide (VIP), gastrin-releasing peptide (GRP), and pituitary adenylate cyclase activating polypeptide (PACAP), while the SNS inhibits insulin secretion via the release norepinephrine and possibly neuropeptide Y (NPY) and galanin[3]. In addition to regulating endocrine cell secretion, neural inputs might also regulate beta cell mass. Nekrep et al. has

previously shown that mice lacking the transcription factor Phox2b do not develop cells of the neural crest cell lineage, including neurons and glia, and this loss of neural crest derived cells results in increased proliferation and number of beta cells and increased insulin content during embryonic development[4]. Additionally, Plank et al. show that signals from neural crest derived cells are required for proper beta cell maturation[5].

Islet Glial Cells: In addition to neurons, the pancreatic islet contains glial cells, which includes both myelinating and non-myelinating Schwann cells. Schwann cell is the name for peripheral nervous system glia. Glial fibrillary acidic protein (GFAP), an intermediate filament protein, is a widely used astrocytic and peripheral glial cell marker, in addition to calcium binding protein s100β[6]. Glial cells have been observed in the pancreatic islet for decades, going back as far as the 1950s in schematic drawings of the islets showing nerve fibers and specialized "interstitial cells of Cajal", which were later identified as Schwann cells[7]. Smith observed in 1975 that Schwann cells of the dog islet are interposed between the islet basal lamina and endocrine cells and have "cytoplasmic processes that encapsulated large expanses of the islet surface"[8]. Smith postulated that these cells may play a role "related to the transmission of electrotonic signals from nerves to the islet cells"[8]. Donev confirmed the presence of peri-islet glial in a variety of mammalian species, including dog, cat, sheep, guinea pig, rat, mouse, hamster, rabbit, and bat, and additional studies by other researches have observed these cells in monkeys and humans[7,9,10]. Glial cell processes have been observed in close contact with beta cells as well as alpha cells and capaillaries[7,9]. While existence of peri-islet glia has been observed for a long time, their exact function is still to be elucidated. As the authors of one recent review paper put it, "The study of glial cells in the pancreas is yet untraversed scientific territory"[11].

In contrast to neurons, glia do not fire action potentials, "but instead surround and ensheath neuronal cell bodies, axons and synapses throughout the nervous system"[12]. Astrocytes, and perhaps the akin perisynaptic, non-myelinating Schwann cells, play a role in synaptic

transmission, neurotransmitter clearance, and spatial buffering[12,13]. Astrocytes are thought to be important for metabolite and neurotransmitter recycling and breakdown, including in the so-called and much debated glutamate–glutamine cycle[14]. Additionally, astrocytes may regulate blood flow through interactions with blood vessels[15]. Dynamic interaction between astrocytes/neurons/blood vessels may be mediated by glial calcium signaling and sodium transients[15,16].

In the hypothalamus, there is an increasing amount of evidence that GFAP+ astrocytes may play a role in energy homeostasis and regulate feeding behavior by influencing agouti-related protein/neuropeptide Y (AgRP/NPY)-expressing neurons and pro-opiomelanocortin (POMC)-expressing neurons[17]. These hypothalamic glia express various hormone receptors, including for insulin and leptin[17] (and references therein). The authors of a recent paper looking at the role of glia in arcuate nucleus in regulating energy metabolism postulate that there are "a few possible mechanisms that may underlie the non-specific, glial activation-stimulation of AgRP neurons and POMC neurons. These include (1) astrocytic release of glutamate or D-serine gliotransmitters […] (2) regulation of extracellular transmitters or extracellular potassium"[17] (and references therein).

In sum, peri-islet glial cells may impact the endocrine cells of the islet directly or indirectly via their interactions with the parasympathetic, sympathetic, and sensory neurons or by modulating capillaries. Dissecting this cross-talk will be likely challenging.

Reactive Gliosis and Secreted Factors: In general, glial cells are known to become activated during neural injury or damage, including during Alzheimer's disease, stroke, traumatic injury, and ulcerative colitis, increasing their expression of GFAP, rates of proliferation, and synthesis of neurotrophins, mitogens, and extracellular matrix (ECM) components[18-21]. This reactive gliosis or glial scar formation may involve both the glial cells and pericytes[22]. Tang et al. show that peri-islet glia react to beta cell toxin streptozotocin (STZ)-induced islet injury by increasing GFAP+

fiber density inside the islet core[19]. Additionally, Teitelman et al. show that peri-islet glia of mice treated with STZ upregulate GFAP, rates of proliferation, and expression nerve growth factor (NGF)[18]. In further support of the possibility that peri-islet glia may release factors that influence beta cells, Mwangi et al. showed that treating a beta cell line with glial cell line-derived neurotrophic factor (GDNF) lead to increased beta cell proliferation and that transgenic mice overexpressing GDNF in glia under a GFAP promoter had increased beta cell mass, proliferation and insulin content[23]. Furthermore, peripheral nerve injury has been shown to induce GDNF expression in Schwann cells[24].

Autoimmune Targeting of Glial Cells in Type I Diabetes: The laboratory of Hans-Michael Dosch has investigated the immune system targeting and destruction of peri-islet glia during the onset of type I diabetes[25-28]. Autoimmune destruction of the pancreatic islet is not limited to just the insulin producing beta cells: the Dosch group has found that the glial sheath is destroyed during the pre-diabetes stage of nonobese diabetic (NOD) mice and potentially in pre-diabetic humans and that peri-islet glial destruction precedes invasive insulitis and beta cell death[25,27]. They show that NOD mice have peri-islet glia cell reactive T-cells and autoantibodies against GFAP and argue that the destruction of peri-islet glia is not simply the result of bystander damage during beta-cell attack[25,27]. Multiple sclerosis (MS) is also associated with GFAP autoimmunity[25]. Additional MS-associated autoantigens have been identified in NOD mice including myelin basic protein (MBP) and proteolipid protein (PLP), both of which are glial-cell related proteins[26]. Excitingly, a recent paper that tested a GFAP immune-tolerizing vaccine for a type I diabetes in NOD mice showed that “the GFAP vaccine successfully delays the progression of T1DM by regulating T-cell differentiation”[29].

Nervous System Tissue and Pancreatic Cancer/Pancreatitis: Pancreatic nerves and glial cells may also be involved in pancreatic cancer and pancreatitis. Researchers have observed increases in nerve size and number, as well as neural remodeling, immune infiltration and

cancer cell invasion of pancreatic nerves (called “neural invasion”)[11]. There may be an attraction between pancreatic Schwann cells and cancer cells, referred to as “Schwann cell carcinotropism”, thought to be primarily mediated by NGF secretion from pancreatic cancer cells and through p75 low affinity nerve growth factor receptor (p75NTR) on Schwann cells[11]. This Schwann cell carcinotropism may set the stage for neural invasion[11].

Glial Cells and Islet Transplantation: Regeneration of islet neurovascular network is important for the long-term survival of islets after transplantation[30]. As Juang et al. explains, understanding “the mechanisms and cellular players that participate in islet neurovascular regeneration holds the key to improving the outcome of transplantation”[30]. Juang et al. showed that donor glial cells and pericytes were major contributors to the formation of the glial sheath and perivascular population of islet grafts and the authors postulate that they may be releasing neurotropic and angiogenic factors to recruit host nerves and blood vessels to the transplanted islets[30]. Another group has also coated pancreatic islets with neural crest stem cells from the dorsal root ganglia and saw improved engraftment and function after liver intraportal transplantation[31].

Innervation of the Pancreas during Embryonic Development: Mouse pancreas innervation by the autonomic and sensory nerves develops before birth (neuron differentiation occurring between 13.5 and 15.5 dpc) while glial cell maturation, including the production of GFAP, likely occurs during the first postnatal week[5,32]. Glial cell encapsulation of the islet reaches adult morphology near the end of the second postnatal week[32].

Defining the Islet Glial Cell Population

Blood Vessel-Related Cells: As mentioned earlier, neurons and glial cells are known to interact with blood vessels. The embryonic development of islet capillaries is thought to precede and to guide islet innervation by providing a scaffold for the incoming neuronal processes[33]. Later in adulthood, the autonomic nervous system innervation of the pancreatic blood vessels

likely regulates blood flow[34]. Blood vessels are made up by multiple cells types, including blood-vessel lining endothelial cells and surrounding pericytes and vascular smooth muscle cells (vSMC) (Figure 1). Pericytes, also known as mural cells, express the marker NG2, a membrane-spanning chondroitin sulfate proteoglycan. NG2 stands for “neuron-glia antigen 2”; however, despite its name, in the context of the adult islet, NG2 is thought be to exclusively a pericyte marker[19]. Alpha-smooth muscle actin (αSMA) is a commonly used vSMC marker. Islets are highly vascularized and “receive approximately 10-times more blood than the exocrine part when expressed per unit weight of tissue (i.e., approximately 15% vs. 85% of total pancreas blood flow)”[35,36]. The role of blood perfusion, oxygen exposure, endothelial signaling, and pericytes on beta cell function is reviewed elsewhere[2,37-39].

Stellate Cells: The liver contains a special type of pericyte called a hepatic stellate cell (HSC), also known as an Ito cell or perisinusoidal cell, first described by Karl von Kupffer in 1876[40]. HSCs secrete and remodel the ECM both normally and pathologically in response to liver insults and have been associated with liver fibrosis, hepatocellular carcinoma (HCC), and various types of liver disease[41]. HSCs are characterized by vitamin A-storing lipid droplets and thought to express both mesenchymal and neural markers such as αSMA, vimentin, desmin, nestin, GFAP[41]; however, HSCs are thought to be of mesodermal origin from the results of various lineage tracing mouse models[42-44].

More recently, scientists claim that there are analogous pancreatic stellate cells that contain retinoid (vitamin A) containing lipid droplets and express both mesenchymal and neural markers such as αSMA, vimentin, desmin, nestin, GFAP, NGF, p75NTR, and neural cell adhesion molecule (NCAM)[45-49]. First described in 1982 as the cell type arose in the pancreas after excess vitamin A exposure and located near endothelial cells of blood vessels and “randomly in the connective tissues,” the authors postulated that these cells may come from pericytes and other undefined fibroblast cells types[50]. These authors also show that these cells are in close

contact with beta cells[50]. In 2012, Erkan et al. wrote a review on the current consensus of pancreatic stellate research[40]. These authors described the problems with various pancreatic stellate cell (PSC) markers, including vitamin-A containing lipid droplets (lost upon activation), α-SMA (expressed in pericytes and vSMCs), desmin (highly variable), nestin (not sufficient) and conclude that "a commonly used and reliable immunostaining marker selective for rat and human PSC (and absent in fibroblasts) is glial fibrillar acidic protein [GFAP]"[40]. Erkan et al. talk about stellate cells as a separate cell type from blood vessel pericytes and vSMCs and it appears that pancreatic stellate cells are viewed by pancreatic stellate cell researchers as their own distinct cell type[40]. The authors postulate the pancreatic stellate cells and HSCs may have a similar origins; however, they also explain that the origin of pancreatic stellate cells has not been defined like it has for HSC and "similar lineage tracing techniques need to be used to determine the exact origin of PSC"[40].

Pancreatic stellate cells have been described as myofibroblast-like cells and associated with pancreatic cancer, pancreatitis, and pancreatic fibrogenesis though ECM deposition[45,51,52]. Pancreatic stellate cells are said to respond to injury, inflammation, or exposure to oxidant stress[51,52]. Additionally, Sousa et al. showed that pancreatic stellate cell lines secrete non-essential amino acids, including alanine, as a fuel source for pancreatic ductal adenocarcinoma (PDAC)[53]. Sousa et al. used pancreatic stellate cell lines that were immortalized from outgrowth culture[53,54]. While most pancreatic stellate cell research focuses on the acinar portion of the pancreas, researchers claim to be able to isolate these cells by density gradients or outgrowth methods from pancreas blocks or isolated islets, asserting that they exist in the exocrine and endocrine parts of the pancreas[40,45,51,54]. Additionally, Yin et al. showed that hepatic stellate cells aided in the revascularization of transplanted islets, supporting the idea that pancreatic stellate cells may do the same[55].

Untangling and defining pericytes, stellate cells, and glia: There seems to be (at least) three separate bodies of literature and research that currently exist that focus on pancreatic glial cells, pancreatic pericytes/blood vessels, and pancreatic stellate cells. I argue that there is overlap between these research areas stemming from a poorly defined cell type: the pancreatic stellate cell. Pancreatic stellate cells are likely not one cell type but rather two or more cells types lumped together, including GFAP+ glial cells, NG2+ pericytes, αSMA+ vSMCs, and possibly another to-be-determined cell type (perhaps a true pancreatic stellate cell). In support of this idea, many of the characteristics of pancreatic glia are also attributed to pancreatic stellate cells, including many of the cellular markers such as GFAP and vimentin, the role in ECM deposition and in injury response, the possible association with pancreatic cancer and pancreatitis, the facilitation of islet transplantation, and potential metabolite secretion. Adding to this confusion, p75 low affinity nerve growth factor receptor has been used as a marker for purifying Schwann cells[56] and as a marker for HSCs and PSCs[48,49,57]. Alpha-SMA is said to be expressed by activated pancreatic (and hepatic) stellate cells; however, in response to CNS injury, reactive astrocytes seem to re-express genes seen during astrocyte development, including α-SMA (as well as nestin), as demonstrated in MS lesions[46,58]. The more one looks into these three bodies of literature, the more and more examples of confusing overlap and duplicate studies in supposedly different cell types one finds. There is a need to define these cell populations with unique, non-overlapping markers to aid in the experimental manipulation, characterization, and functional analysis of these non-endocrine cells of the pancreas.

Single Cell Sequencing

Single cell analysis is becoming more and more popular within biological research. In diabetes research, there have been multiple recent papers looking at the heterogeneity of beta cells, which previously were thought of as a homogeneous population, through the use of cell single sequencing to identify beta cell subtypes[59] (and references therein). To help define the peri-islet

glial cells, I decided to use single cell sequencing to identify previously unknown genes expressed by these enigmatic cells. Many single cell sequencing protocols rely on fluorescence activated cell sorting (FACS), which unfortunately is technically challenging for long-cellular-process-containing neurons and glia; however, use of FACS on neural tissue not unprecedented. For example, Cahoy et al. purified astrocytes and oligodendrocytes by FACS for gene expression analysis[60]. With a hopeful outlook on being able to sort islet glial cells from dissociated mouse islets, we chose to use the Drop-seq method for processing the cells for single cell sequencing in collaboration with the McManus lab.

Drop-seq: Drop-seq is a relatively new method of encapsulating thousands of single cells in the droplets of oil filled with a cell lysis buffer and an mRNA-capturing, barcoded bead[61]. All the beads contain a common PCR handle for PCR application after mRNA capture and reverse transcription, a bead-specific cell barcode that allows for the identification of all transcripts from a particular cell of origin, a string of 8 bases called a “unique molecular identifier” (UMI) that allows for each mRNA transcript to be “digitally” counted, and a 30 base oligo-dT for polyadenylated mRNA capturing and reverse transcriptase priming[61]. The UMI-aspect of the Drop-seq method is an advancement over the previous relative RNA-seq measures, like the reads per kilobase per million reads (RPKM)-based measurements, as the UMI method allows for absolute quantification of the mRNA transcript number (all sequenced and similar UMIs are collapse into a single count), thereby minimizing artifacts due to amplification bias. For further explanation of Drop-seq, please see the Macosko et al. paper[61]. The Methods section following this chapter also contains more detailed information on this RNA-seq technique.

Overview of Experimental Questions

During this thesis project, I sought to define the GFAP+ glial cell population in the pancreas through lineage tracing using a Wnt1-cre mouse line, which marks all cells of neural crest cell origin[62]. Generally, myelinating and non-myelinating Schwann cells of the peripheral nervous

system are thought to be of neural crest cell origin[63]. Additionally, mice lacking neural crest cells via a Phox2b disruption lack neurons and glia in the embryonic pancreas; however, it has not been previously shown that adult GFAP+ cells in the pancreas are of neural crest cell origin[4]. I also sought to assess several GFAP-based mouse lines, including GFAP-cre and GFAP-GFP, for their suitability for genetic ablation of peri-islet glia and for glial cell sorting. Lastly, I sought to perform gene expression analysis through the newly described Drop-seq method to identify new glial cell markers and potentially gain insights into glial cell function.

Chapter 2: Methods

Mice

Mice were housed in climate controlled rooms on a 12 hour light/dark cycle. All animal procedures were approved by the University of California, San Francisco (UCSF) Institutional Animal Care and Use Committee and were conducted in accordance with UCSF regulations. The following mouse lines were used: FVB/N-Tg(GFAP-GFP)14Mes/J (The Jackson Laboratory Stock Number: 003257; referred to as GFAP-GFP mice herein)[64], FVB-Tg(GFAP-cre)25Mes/J (Stock No: 004600; GFAP-cre)[65], Tg(Wnt1-cre)11Rth Tg(Wnt1-GAL4)11Rth/J (Stock No: 003829, Wnt1-cre)[62], Gt(ROSA)26Sor$^{tm4(ACTB-tdTomato,-EGFP)Luo}$/J (Stock No: 007576, mTmG)[66], B6.129X1-Gt(ROSA)26Sor$^{tm1(EYFP)Cos}$/J (Stock No: 006148, R26R eYFP)[67], and C57BL/6-Gt(ROSA)26Sor$^{tm1(HBEGF)Awai}$/J (Stock No: 007900, iDTR)[68]. The following UCSF labs kindly donated the following mouse lines to the German lab for these experiments: Jeffrey Bush: Wnt1-cre, Matthias Hebrok lab: iDTR (additional iDTR mice were purchased from Jackson Lab), Holger Willenbring: GFAP-cre, Arturo Alvarez-Buylla: GFAP-GFP. Note: Wnt1-cre mice were maintained as heterozygotes due to lethality problems associated with the homozygous mice. Additionally, unexpectedly, my Wnt1-cre female heterozygous mice seem to die spontaneously (and without apparent cause) as adults (various ages), while the males appear to be healthy.

This phenomenon has also been seen in the Bush Lab (the donating lab of this strain) as confirmed by personal communication.

Genotyping

To extract DNA from mouse tail samples for genotyping, the following master mix was made: 200 uL Chelex solution (to make Chelex solution: add 10 mL Chelex® 100 Chelating Resin (BioRad Catalog Number 142 1253) to a 50 mL falcon and then add water up to 45mL, mix thoroughly) per sample, 2 uL 10% Tween20 per sample, 2 uL Proteinase K (LifeTech Catalog Number 25530015) per sample. Two hundred uL of this master mix was added to each tail sample, vortexed and briefly spun down. Samples were incubated on a 55°C heat block overnight and then vortexed and briefly spun down. Samples were heat shocked at 95°C for 30 minutes, then vortexed and briefly spun down once more. Genotyping PCR reactions were made with 1 uL of this tail prep along with the Thermo Fisher Scientific DreamTaq Green PCR Master Mix (2x), primers (see Table 1 for genotyping primer sequences; primers ordered from Integrated DNA Technologies), and water up to 25 uL. With the exception of the mTmG genotyping protocol, primers were used at a final concentration of 0.5 uM; for the mTmG reactions, 1.25 uM final concentrations were used. PCR programs are listed in Table 2. All but the mTmG PCR products were run on a 1.5% agarose gel with the 1 Kb Plus DNA ladder (Thermo Fisher Scientific Catalog Number: 10787018) and visualized with ethidium bromide; the mTmG PCR products were run on 2.5% agarose gel. Expected band sizes are listed in Table 1.

Mouse Islet Isolation

Mouse pancreatic islets were isolated by Vihn Nguyen (see acknowledgments). Pancreases was perfused with 3 mL of HBSS (Hyclone) containing collagenase P (Roche). Distended pancreases were incubated in 37°C water bath for 14 minutes (for staining or culturing experiments, unless noted) or 16 minutes (for FACS experiments) and gently tapped to release

islets from pancreases. Islets were separated further by density gradients (Histopaque 1119, Sigma). Handpicked islets were transferred into RPMI (Gibco) supplemented with 10% FBS (Gibco), L-glutamine (Gibco), 2.5% HEPES buffer (Gibco), 1% Penicillin-Streptomycin (Gibco). Islets were either immediately fixed after this initial isolation for staining or used for culturing experiments.

Mouse Islet Culture

Mouse islets were cultured at 37°C in 5% CO_2 in RPMI 1640 without phenol red + L-glutamine (Gibco Catalog Number 11835-030) with 10% FBS, 1% penicillin streptomycin, 1% non-essential amino acids (UCSF Cell Culture Facility CCFGA001) and 2.5% HEPES. Occasionally RPMI with phenol red was used due to availability. Media was replaced every 24 hours for free floating, outgrowth, and Matrigel® experiments.

For free floating culture, Greiner CELLSTAR® 12 well suspension culture plates using ~25 islets per well in 2 mL of media was used, unless otherwise noted. Islets were transferred to new suspension culture plates during media changes to reduce islet adherence to plates.

For adhesion and outgrowth culture experiments, ~15 islets per well were added to 8 well Lab-Tek® Chamber Sides™ with Permanox® plastic (a tissue cultured treated plastic with excellent optical clarity and minimal autofluorescence to allow for immunofluorescence staining and imaging) with 200-400 uL of media. Adhered islets were cultured on the Permanox® plastic for 5 days before being washed once with PBS and fixed with 4% PFA for 25 minutes at room temperature for staining.

For experiments with islets grown in Matrigel®, ~25 islets were suspended in a mixture of 50% RPMI/50% thawed Corning Matrigel® Membrane Matrix Growth Factor Reduced (GFR) (Corning Catalog Number 354230) and pipetted with chilled pipet tips into 25 uL droplets onto the glass bottoms of room-temperature Nunc™ Lab-Tek™ 4 chamber slides (Thermo Fisher

Scientific Catalog Number 177399). Droplets were set in a 37°C incubator for 20 minutes before the addition of 700 uL warm media per chamber. To recover islets from the Matrigel® droplets, droplets were washed with cold PBS three times and dissolved using 800 uL Corning Cell Recovery Solution (Corning Catalog Number 354253) per droplet on ice for ~1 hour. Chamber contents were transferred into chilled 1.5 mL microcentrifuge tubes and spun at 4°C for 5 minutes at 1200 rpm to pellet islets. Liquid was removed and islets were gently washed twice in cold PBS before the addition of 4% PFA for overnight fixation and subsequent staining (as described in the whole islet staining section).

For diphtheria toxin treatment, islets were cultured in Matrigel® as described above but with the following changes: ~50 islets were embedded in 50 uL 100% Matrigel® droplets with 100 ng/mL diphtheria toxin (reconstituted lyophilized powder, Sigma Catalog Number D0564) and cultured in 700 uL media with 100 ng/mL diphtheria toxin.

Human Islets

Human islets were generously donated by a deceased patient and prepared by the UCSF Islet and Cellular Production Facility for research purposes only. The islets came from a male patient in his 40s with no history of diabetes. Prior to staining, the islets were cultured for one day in CMRL 1066 with glutamax, 1% nonessential amino acids, and 10% Gibco B-27® Serum-free Supplement (Thermo Fisher Scientific Catalog Number 17504044). Approximately 1000 islets were spun down at 1000 rpm for 3 minutes and media was removed. Islets were washed with PBS once before the addition of 4% PFA for overnight fixation and subsequent staining (as described in the whole islet staining section).

Tissue Fixation, Sectioning, and Staining

Extensive methodological details about heart perfusion, sectioning and staining be found in Appendix 1. Briefly, mouse pancreas tissue was fixed by heart perfusion with PBS followed by

4% PFA. Tissue was post-fixed overnight in 4% PFA in the 4°C cold room with “rotisserie” rotation, washed for 4 hours with PBS, and then sucrose protected in a 30% sucrose solution until the tissue sunk. Tissue was embedded in Tissue-Tek O.C.T Compound and frozen in an acetone-dry ice bath. Pancreas blocks was sectioned on the cryostat in 20 uM thick sections to preserve neuron, glial, and pericyte processes and morphology. Prior to primary antibody incubation, slides were fixed again for 10 minutes with 4% PFA, permeabilized for 30 minutes at room temperature with 0.5% Triton X-100 in PBS and blocked for one hour at room temperature with 0.1% triton/5% goat serum in PBS. Slides were stained using the following primary antibodies made up in blocking buffer using the following dilutions: mouse NKX6.1 at 1:100 (DSHB F55A10-c), guinea pig insulin at 1:500 (DAKO A0564), guinea pig glucagon at 1:2000 (LINCO, discontinued product line), chicken GFP at 1:500 (Aves GFP-1020; for eYFP or GFP reporter lines), rabbit GFAP at 1:500 (DAKO Ref Z0334), rabbit NG2 at 1:100 (EMDMillipore AB5320), rabbit TUJ1 at 1:500 (BioLegend 845502), and mouse TUJ1 at 1:700 (R&D Systems MAB1195-SP; stock reconstituted at 0.5 mg/mL in sterile PBS, used 1:700). Following primary antibody incubation and washing, the following Alexa Fluor® secondary antibodies were used at a 1:200 dilution, made up in blocking buffer containing a 1:1,000 dilution of a Hoechst nuclear stain: goat anti-chicken Alexa Fluor® 488 (Invitrogen Catalog Number A11039), donkey anti-mouse Alexa Fluor® 555 (A31570), goat anti-mouse Alexa Fluor® 488 (A11029), goat anti-mouse Alexa Fluor® 633 (A21052 and A21126), goat anti-guinea pig Alexa Fluor® 546 (A11074), goat anti-guinea pig Alexa Fluor® 633 (A21105), goat anti-rabbit Alexa Fluor® 488 (A11034), goat anti-rabbit Alexa Fluor® 633 (A21072), and donkey anti-rabbit Alexa Fluor® 488 (A21026). Slides were incubated in secondary antibodies for 1 hour in an opaque, humidified chamber at room temperature and then washed in PBS. Slides were mounted with Thermo Fisher Scientific ProLong Gold Antifade Reagent, cured for 24 hours, and imaged (see imaging section).

Whole Islet Staining

Islets, either immediately following islet isolation or at the end of a culturing experiment, were stained and imaged as intact, whole islets. For extensive whole islet staining methods, please see Appendix 2. Briefly, islets were transferred to low-retention siliconized 1.5 mL microcentrifuge tubes and gently spun down. After removing media, free floating islets were fixed in 1 mL of 4% PFA overnight on a rotisserie rotator, washed, and permeablized with 0.5% TritonX-100 in PBS at room temperature for 30 minutes with rotisserie rotation (all steps throughout are conducted using a rotisserie rotator). Islets were blocked in 0.1% TritonX-100/1% goat serum in PBS for 1 hour at room temperature and then incubated in primary antibodies made up in blocking buffer for 48 hours in the 4°C cold room. Primary antibodies and their concentrations used for whole islets match those used in pancreas sections except for insulin, which was used at a higher concentration (1:200 dilution). Following a 24 hour wash in the cold room, islets were incubated with secondary antibodies with a Hoechst stain for 48 hours. Secondary antibodies were made up in blocking buffer at a 1:200 dilution as described in the fixed frozen slide staining section above. After secondary antibody incubation, islets were washed for another 24 hours in the cold room before being mounted on slides with either ProLong Gold or with SunJin Lab RapiClear® clearing agent (courtesy of Tony Tang, please see acknowledgements)[30,69]. With either mounting medium, slides were cured or incubated for 24 hours before imaging. Note: the RapidClear clearing agent interferes with imaging the Hoechst stain. Propidium iodide (PI) can be used in its place; however, PI visualized in 488 channel on a florescent microscope, which would have prevented my ability to do GFP staining. Thus, cleared islets did not have Hoechst stain.

Imaging

Slides were imaged predominately in the Broad Center Microscopy Core on the Leica White Light Laser TCS SP5 X confocal microscope, running the LAS AF software, with additional

imaging done on the UCSF Diabetes Center Leica SP5 confocal microscope, a Leica DMI4000 B fluorescent tissue culture microscope, and the German lab's upright fluorescent scope, a Zeiss AxioImager Z1 with the Zeiss AxioVision software. Images can be assumed to be taken on a confocal microscope unless noted in the figure legend. Image processing was done using FIJI ("FIJI is just Imagej" with plugins).

Drop-seq

Drop-seq is a relatively new method of single cell encapsulation that allows for large-scale, parallel analysis of individual cells for RNA-seq[61] and was developed by the Harvard lab of Steve McCarroll. The McCarroll lab has made extensive information available on their laboratory website (http://mccarrolllab.com/dropseq/). The website includes a downloadable PDF of their latest version of their protocol; my collaborator Eleonora de Klerk and I followed v3.1 from December 2015. Additionally, their website has a separate computational protocol that can be followed once researchers have acquired either their raw miniSeq, miSeq, or HiSeq data to generate a digital gene expression (DGE) matrix; the January 2016 version that we used is available here. The computational protocol uses scripts that are also available for download from the McCarroll lab Drop-seq website. As such, methods described here will be an abbreviated version of the complete methods.

Isolated islets were dissociated to single cell suspension using Gibco® Cell Dissociation Buffer (Thermo Fisher Scientific Catalog Number 13151014) for 30 minutes with gentle tapping every 5 minutes. Dissociated islets were sorted using the BD FACSAria™ III into HBSS at 4°C and kept on ice until droplet making. For the sorting piloting experiment, islets were isolated, pooled and dissociated from four 4-5-month-old Wnt1-cre/mTmG mice and another set of islets were isolated and dissociated from one 5-month-old mTmG mouse lacking Wnt1-cre to serve as a negative control. For the pilot Drop-seq experiment, islets were isolated and pooled from three 3-month-old male littermates without any fluorescent protein transgenes (to conserve the

valuable transgenic mice); without tdTomato or GFP, FACS gating was simply set to collect single cells and exclude doublets and debris. Two tubes of islet cells were collected for this Drop-seq pilot: a “high” concentration of 225,000 cells and a “low” cell concentration around 50,000 cells, brought up to a total volume of 1.5 mL HBSS with 0.01% BSA (Sigma Catalog Number A8806). For the HiSeq Drop-seq sorting, isolated islets were pooled and dissociated from four 6-month-old Wnt1-cre/mTmG littermates (3 females and one male). Cells were sorted into two pools: tdTomato positive/GFP negative (control cells) and GFP positive/tdTomato negative (cells of neural-crest cell origin). Control cells and neural-crest-derived cells were collected in the same tube to reach a total of population of around 200,000 cells in 1.5 mL HBSS with 0.01% BSA. Exact numbers will be discussed in the results section.

Drop-seq droplet making set up included three syringe pumps each fitted with a 3 mL syringe: one filled with droplet generation oil (Bio-Rad Catalog Number 186-4006), a second with lysis buffer containing 120,000 Chemgene barcorded beads/mL (lysis buffer and beads as described in v3.1 from December 2015), and a third with the sorted cells. Tubing from the syringes was connected to a PDMS co-flow microfluidic droplet generation device placed on an inverted microscope to allow for visualization of the droplet making process. Beads were kept in suspension during droplet making through a magnetic mixing system. Droplets were collected in 50 mL falcon tubes with a limit of 1 mL collected droplets per falcon tube.

After collection, droplets were broken with the addition of 6X SSC and Perfluorooctanol (PFO; Sigma Catalog Number 370533) and handshaking. After removing the oil, the now-released beads were washed with more 6X SCC and 5X reverse transcriptase (RT) buffer. Beads were reverse transcribed with 200 uL per 90,000 beads of the following mixture: 75 uL H_2O, 40 uL Maxima™ 5X RT buffer, 40 uL 20% Ficoll PM-400, 20 uL 10 mM dNTPs, 5 uL NxGen™ RNase inhibitor (Lucigen Product 97065-224), 10 uL 50uM Template Switch Oligo (Exiqon; for primer sequence see Table 3) and 10 uL Maxima™ H Minus Reverse Transcriptase (Thermo Fisher

Scientific Catalog Number FEREP0753). RT reaction was carried out for 30 minutes at room temperature with rotation followed by 90 minutes at 42°C with rotation. After removing the RT mix and washing the beads with TE-SDS solution, TE-TW solution, and 10 mM Tris pH 8.0 (for solution composition, see v3.1), excess bead primers that did not capture RNA molecules were "chewed back" by exonuclease treatment. Two hundred uL of exonuclease mix was added per 90,000 beads, containing: 20 uL 10x Exo 1 buffer, 170 uL H_2O, and 10 uL Exonuclease I. This reaction was incubated at 37°C for 45 minutes with rotation. After removing exonuclease mix, beads were washed with TE-SDS, TE-TW, and H_2O.

For every Drop-seq run, the concentration of beads must be calculated before PCR amplification, which has a limit of 2,000 beads per PCR reaction tube. Twenty uL of the beads/H_2O mixture was removed and spun down. The water was removed and replaced with gel loading dye and this bead/loading dye mixture was loaded into an INCYTO C-Chip™ disposable Fuchs Rosenthal hemocytometer chamber (VWR Catalog Number 82030-472) for counting. Note: resuspension in loading dye is a deviation from the McCarroll lab protocol, which leaves the beads in water for the counting process. By using loading dye, the beads spread much more evenly across the hemocytometer to allow for accurate counting. Based on the bead concentration, water suspended beads were apportioned to 2,000 beads per PCR tube (for reference, with dissociated mouse islets and a 1.5 mL starting dissociated cell volume, one Drop-seq sample can generate upwards of 30 PCR reaction tubes based on this 2,000 beads/PCR reaction limit and current bead processing yields). PCR tubes were spun down to pellet beads and excess water was removed to from each tube to leave a bead/water volume of 24.6 uL. The following PCR mix was added per PCR tube: 0.4 ul 100 uM SMART PCR primer (for primer sequence see Table 3) and 25 uL KAPA HiFi HotStart ReadyMix (Kapa Biosystems, KK2601). The total PCR reaction volume was 50 uL. The McCarroll lab protocol lists a starting PCR program; however, this PCR program might not have enough cycles to sufficiently amplify

a particular experiment's cDNA, partly depending on the cell types being assayed. Table 3 lists all the PCR programs tried during the pilot Drop-seq and HiSeq Drop-seq experiments. Further discussion of PCR programs will be discussed in the results sections.

After PCR, 30 uL of AMPure XP magnetic beads (Beckman Coulter Catalog Number NC9959336) were added to each 50 uL PCR reaction (0.6x beads to sample ratio). Samples were mixed and incubated at 5 minutes at room temperature. After which, samples were placed on a magnetic stand for 2 minutes. Supernatant was removed and samples were washed twice with freshly made 70% ethanol. Samples were resuspended in 10 uL Qiagen EB buffer for 2 minutes before being placed back on magnetic stand. Eluate was transferred to a new tube. Purified cDNA PCR products were assessed by running 1 uL of each purified PCR sample on an Agilent High Sensitive DNA chip (Agilent Technology Catalog Number 5067-4626). Chips were prepared and run on a Bioanalyzer according to manufactures instructions.

Based on Bioanalyzer traces, PCR reactions with correct fragment size and concentration were pooled for tagmentation using the Nextera XT DNA Library Preparation Kit (Illumina Catalog Number FC-131-1024). To make PCR pools, 3 uL from 3-5 purified PCR reactions were combined and reanalyzed on the Bioanalyzer for their pooled DNA concentration. Pools were diluted 1:1 with Qiagen EB buffer to allow for accurate pipetting and 600 pg (HiSeq) or 1 ng (MiniSeq) of these pools were used for the tagmentation reactions. Tagmentation was conducted according to kit instructions, using the "New-P5-SMART PCR hybrid oligo" (for sequence see Table 3) and N701 Nextera Index Primer. Tagmented libraries were purified with AMPure XP beads twice, as described earlier; the first purification was eluted in 50 uL of EB buffer and the second purification was eluted in 10 uL of EB buffer. The McCarroll lab protocol only purifies their tagmented library once. One uL of each purified tagmentation reaction were analyzed on the Bioanalyzer and assessed for fragment size and concentration.

Based on Bioanalyzer concentrations, equimolar tagmentation reactions were pooled to generate samples to be sequenced either by Ilumina MiniSeq or HiSeq. For the Drop-seq pilot experiment, 1.8 picomoles from the “low” and the “high” cell concentration tagmented libraries were used for the Illumina MiniSeq reaction. For the HiSeq Drop-seq experiment, library samples of 10 uL at a 10 nmol/l concentration were sent to the UCSF Genomics Core for Illumina HiSeq 2500 sequencing. For HiSeq, two lanes were run using the Rapid PE 2x50bp flow cells, with the specification of read 1: 20 cycles and read 2: 80 cycles. Read 1 used a custom sequencing primer, as listed in Table 3.

MiniSeq and HiSeq raw data was processed using the computational protocol available for download on the McCarroll lab website, as mentioned earlier, to generate a digital gene expression (DGE) matrix. Gene expression heat maps were generated using the statistical software program and Microsoft Excel add-in XLSTAT. Gene ontology and pathway analysis was performed using the Max Planck Institute for Molecular Genetics’ ConsensusPathDB-mouse online software program (http://cpdb.molgen.mpg.de/MCPDB).

Chapter 3: Results

General Appearance of GFAP+ Islet Glial Cells

Sectioned adult mouse pancreases stained for GFAP and insulin show that pancreatic islets are surrounded by GFAP+ glial cells (Figure 2A). Islets can be found and identified in by GFAP staining alone as the GFAP+ cell bodies and processes circumscribe the mouse islet, as exemplified by the green GFAP+ ring in Figure 2Aiii. Additionally, GFAP+ glial cell bodies and processes exist in the interior the islet. Besides being observed in and surrounding the islet, GFAP+ cell bodies and processes are also found outside the islet along innervating nerve fibers and ganglia (Figure 3B) and surrounding blood vessels and ducts in the acinar portion of the pancreas as seen in Figure 2Aiv. In addition to being in contact with beta cells, GFAP+ cells

likely interact with glucagon-producing alpha cells (Figure 2B). GFAP+ cells were retained in both wild-type CD-1 (Figure 2C) and C57BL/6J adult mouse (not shown) isolated islets. GFAP+ cells are also seen inside isolated adult human islets (Figure 1D). Evidence of peri-islet glial cells in humans was also confirmed in a recent paper by Krivova et al. looking at sectioned pancreases from fetuses and children, and they claim that S100 is a better marker for human glial cells than GFAP[10].

Method Development for Studying Pancreatic Islet Glial Cells

Clearing: Incubating isolated and stained islets in a clearing solution allowed for improved visualization of the faint, intra-islet GFAP+ processes (Figure 3Ai-ii)[30,69]. While the difference between the cleared and standard mounted islet here is fairly subtle to see, the clearing solution also improved ability to image through the middle portions of the whole islet without as much loss of signal intensity. This is an important improvement as the islets were imaged whole to preserve the glial, neuronal, and pericyte morphology, and without sectioning, imaging though the entire islet is more difficult.

Islet Isolation: In addition to trying to improve my abilities to image the GFAP+ glia cells, I sought to improve the amount of retained glial cell bodies and processes on the isolated islets. The first mouse islets I stained, as shown in Figure 2, were isolated from the pancreas by a 14 minute collagenase digestion, a slightly shorter digestion time than the standard 16 minute digestion. Even so, the GFAP+ cells that were retained on the islet had a patchy appearance (for example, see Figure 2Cii, and compare the right and left sides of the upper islet). Furthermore, some isolated islets possessed numerous glial cells while other islets seemed devoid of much GFAP+ staining, if any. To test whether the length of collagenase digestion time effected the quality and number of retained GFAP+ cell bodies and processes, we tested 8, 10, and 12 minute digestion times (Figure 3B-D). However, shortening the collagenase digestion time did not improve GFAP+ cell retention. With a very short 8 minute digestion, islets were still

stuck to long nerve fibers, vessels, and surrounding pancreatic tissue (Figure 3B), yet the 5+ islets on this strand do not possess any more GFAP+ cells than those isolated with longer digestion times (Figure 3C-D). The longer the digestion time, the more islets were released from the pancreas and with less non-islet associated tissue. In addition to improving the number of islets harvested, the longer the digestion time, the larger the harvested islets tended to be. Generally, in all experiments, I found that larger isolated islets possessed more GFAP+ glial cells. So while digestion time effected the number, size, and amount of extra-islet tissue, islets of similar size did not appear to vary in the amount of retained GFAP+ cells or processes based on digestion time. Therefore, we continued to use the 14 minute digestion time for isolating islets for most experiments, unless noted.

Culturing: In an attempt to retain as many GFAP+ glial cells on the islet and maintain the "glial sheath" 3D structure as much as possible during culture, I tried culturing isolated islets in static suspension culture, rotation suspension culture, and embedded in Matrigel®. Rotation culture lead to excessive islet clumping (leading to necrotic cores in the middle of the clump), and Matrigel® was also fraught with necrosis issues. However, troubleshooting the problems associated with rotation or Matrigel® culture seemed not necessary in the end as static suspension culture in suspension culture plates with daily plate changes to prevent any islet-plate adhesion seemed to retain a sufficient quantity of GFAP+ cells relative to the number of cells seen before culture. Without seeing much loss of GFAP+ cells, static suspension culture appears to be a suitable manner in which to culture isolated islets to study GFAP+ glial cells. As mentioned in the "isolation" subsection above, there seems to be a positive correlation between isolated islet size and amount of retained GFAP+ cells seen immediately after isolation; however, the larger the islet, the more difficult it is to culture without seeing cell death in the middle of the islet. Also of note, in all culturing systems I tried, the islets with necrotic cores, visible damage (as defined by irregular edges) or that clumped with other islets, the GFAP+

cells seemed to undergo some sort of reactive gliosis as extensive GFAP+ processes could be seen in those islets around the areas of damage and in-between islet clumps. It is unclear whether the clumping of islets is the result of “sticky” GFAP+ cells or if that the GFAP+ cells are responding to the clumping (or some combination of these possibilities).

Lineage Tracing GFAP+ Glial Cells

To determine if the GFAP+ cells in the adult mouse pancreas were of neural crest cell origin, I bred Wnt1-cre mice to two different reporter lines: mTmG and R26R eYFP. Both mTmG and R26R eYFP pancreases were stained for GFP as the GFP antibody used recognizes both fluorescent proteins; therefore, “eYFP” and “GFP” can be considered to be synonymous when reading figure legends. While the eYFP and mGFP proteins retained some of their signal after tissue processing, staining with a GFP primary antibody and Alexa Fluor 488 secondary antibody served to enhance the GFP signal for more robust imaging. GFAP was visualized using an Alexa Fluor 633 secondary to minimize spectral overlap with the Alexa Fluor 488 signal or any remaining endogenous GFP or eYFP signals. While GFAP staining is shown as red in Figure 4 images, this is only due to pseudo-coloring and not a reflection of tdTomato signal. In both Wnt1-cre/mTmG and Wnt1-cre/eYFP sectioned and stained pancreases, nearly all GFAP+ staining co-localized with GFP staining (Figure 4A-D), indicating that all GFAP+ cells are of neural crest cell lineage. I did not see any GFAP+ cells in the pancreas, either in or around the islet, near blood vessels and ducts or in the acinar portions of the pancreas, which did not co-localize with GFP signal. As Wnt1-cre marks all cells of neural crest cell lineage, including both glial cells and neurons, I did see some GFP staining that did not co-localize with GFAP staining. Also worth noting, in the mTmG mice, the GFP protein is a membrane-targeted eGFP mutant version of the protein, which outlines the cell’s membranes; GFAP is an intracellular filament protein. This difference in fluorescent protein localization can also be seen in Figure 4.

To make sure that the co-localization of GFP and GFAP staining was not simply a reflection of the close physical association of neurons and glial cells, I identified clearly nucleated cells that are GFAP and GFP co-positive in single z-layers from the z-stack images of the Wnt1-cre/mTmG and eYFP pancreas sections. Figure 5A shows a GFAP+ glial cell (here shown in blue) from a Wnt1-cre/mTmG pancreas section that stains positive for GFP, in addition to being beta-cell marker Nkx6.1 negative (Figure 5A). Looking at Figure 5B, one can see that the cells in the white ovals are clearly nucleated GFAP+ cells that also stain for GFP.

To differentiate GFAP+ glial cells from islet pericytes, I stained the Wnt1-cre/mTmG pancreas sections with NG2, a pericyte marker and integral membrane proteoglycan. As one can see in Figure 6, islet-associated, NG2+ pericytes do not co-localize with GFP and are therefore not neural crest cell derived. This staining also serves as a fortuitous negative control for the co-localization images in Figure 5, demonstrating a cell type that does not overlap with the GFP signal.

Unsuitable Mouse Models for Studying GFAP+ Islet Glial Cells

GFAP-cre: I evaluated several mouse models that turned out to not be suitable for studying GFAP+ cells in the pancreas despite their potential utility for studying these cells in CNS or in other organs or tissues. One such model was the GFAP-cre mouse, which has been used to study glial cells in the CNS[65]. I bred the GFAP-cre mouse to the R26R eYFP reporter to verify Cre expression in adult pancreatic islets. While some GFAP+ cell bodies and processes stained for GFP (indicating Cre recombination; example highlighted by Figure 7B arrowhead), most cells that stained for GFP were not GFAP+ (example highlighted by Figure 7B arrow). The duct-like structures in the acinar area of the pancreas dramatically stained for GFP, as seen in Figure 7C-D, and the close-up of a cross-section of a duct Figure 8. The GFP+ structures do not co-localize with the blood-vessel associated pericytes (Figure 7D).

GFAP-cre/iDTR: GFAP-cre/iDTR mice were bred concurrently with the eYFP reporter mice, so while the previous section's experiments were ongoing, I also performed a pilot ablation study before knowing the above section's results. The iDTR mice contain a transgene for the diphtheria toxin receptor (DTR); however its expression is blocked by an upstream *loxP*-flanked STOP sequence. In the presence of Cre recombinase, the STOP sequence is deleted and DTR expression is turned on. Upon diphtheria toxin (DT) treatment, only those cells that express DTR die; cells that do not express the DTR should not be effected by the DT treatment. As the GFAP-cre/iDTR mice would ultimately prove unsuitable for this ablation experiment due to the problems with the Cre expression, only islets from control treated GFAP-cre/iDTR and GFAP-cre-negative/iDTR mice and from DT treated GFAP-cre-negative/iDTR mice are shown in Figure 9. Isolated islets were embedded in Matrigel® and cultured for 72 hours in 100 ng/mL diphtheria toxin-containing media or DT-free media. There does not appear to be a difference in the overall islet health or GFAP+ cells' appearance between control treated islets (Figure 9A) and the representative GFAP-cre-negative/iDTR DT-treated islet (Figure 9B). While this cohort of mice were not able to be used for glial cell ablation studies, the lack of impact of DT treatment on islets without the DT receptor bodes well for future DT ablation studies using a different, to-be-determined Cre (see Discussion section).

GFAP-GFP: Another model tested was the GFAP-GFP mouse. I cultured isolated islets for 72 hours from both male and female 10-15 week-old GFAP-GFP mice, both in Matrigel® droplets and in suspension culture. Islets were visualized during culture using a fluorescent tissue culture microscope, but very minimal GFP signal could be seen live (Figure 10A). This lack of GFP signal was reflected in the GFP staining performed on the fixed islets at the end of the culture period in Figure 10B. These same fixed islets were co-stained for GFAP, which revealed that there were in fact many GFAP+ cells in these islets. Therefore, it appears that GFP signal in the GFAP-GFP mice is not strong enough to be useful to monitor GFAP+ glial cells in culture.

Additionally, the degree of difference between GFP transgene live signal and staining and the 'true' GFAP staining was too great to feel confident enough to use this mouse for fluorescent activated cell sorting (FACS).

Neurons in the Pancreatic Islet

As both the GFAP-cre and GFAP-GFP mouse models proved unsuitable for the various experiments we had planned to interrogate these cells, including GFAP-cre/iDTR glial cell ablation or GFAP-cre/mTmG (or GFAP-cre/R26R eYFP or GFAP-GFP) glial cell sorting, we turned to the next best thing available: Wnt1-cre mice. While the Cre recombinase in Wnt1-cre mouse would mark all neural crest cell derived cells, including both glial cells and neurons, it was unclear how many neurons are retained in isolated islets, especially compared to GFAP+ glial cells, or if those neurons would persist in culture.

TUJ1 antibody: As the pancreas contains three types of neurons: parasympathetic, sympathetic, and sensory, I needed a marker that would identify all neurons, regardless of neuron type, and would not cross-react with beta cells or other endocrine cell types, as islet endocrine cells have been found to express a variety of neuronal cell markers, such as tyrosine hydrolase[24] (and references therein). Therefore, the first task was to confirm the reliability of the pan-neuronal marker I chose: Neuron-specific class III β-tubulin (TUJ1). Figure 11A-C shows sectioned pancreases from Wnt1-cre/R26R eYFP mice stained for GFP, TUJ1, insulin, and DNA. Figure 11A confirms that these nucleated TUJ1+ cells are of neural crest cell lineage, as reiterated in C, and Figure 11B shows that these nucleated TUJ1+ cells are insulin negative. Next, I tested TUJ1 staining in isolated, wild-type C57BL/6J mouse islets (Figure 11D-F). The staining revealed long neuronal processes in the islet (Figure 11D). The TUJ1+ cells are Nkx6.1 negative (Figure 11E). The islet in F is shown as a maximum projection while the small inset in the white box shows the single z-plane to allow for visualization of the Hoechst-stained nuclei of the TUJ1+ cells in the attached peri-islet ganglia.

TUJ1+ neurons in isolated islets survive islet culture: By co-staining for GFAP in addition to TUJ1 in isolated islets, one can see that where there are TUJ1+ cell bodies and processes, there are also GFAP+ cell bodies and processes (Figure 13A) and that these TUJ1+ neurons and GFAP+ glial cells are in tight physical association with each other (Figure 12). It does not appear that GFAP+ cell bodies or processes exist in areas of the freshly isolated islet without associated neuronal processes or cell bodies.

To test whether these TUJ1+ neurons survive in islet culture and to assess their survival as compared to GFAP+ glial cells, islets were isolated from 12 week old wild-type C57BL/6J mice and either fixed immediately (Time 0 h) or cultured for 72 hours in suspension culture with daily media and plate changes. The neurons appear to survive as well, if not better, than the GFAP+ glial cells (Figure 13B). The TUJ1+ cells respond to culture with the appearance of many fine TUJ1+ processes that are no longer associated with nearby GFAP+ staining (Figure 13B).

Figure 14A islets i-iii show a range of retained GFAP+ and TUJ1+ cells from dense patches to sparse. Despite the neurite outgrowth phenomenon, even after culture, one does not see islets with many TUJ1+ cells and few GFAP+ cells or many GFAP+ cells and few TUJ1+ cells. For example, if one finds an islet with only a few TUJ1+ neurons, it invariably contained only a few GFAP+ cells (Figure 14B).

A Mixed-Origin Cell Population Outgrows From Adhered Islets

Other research groups have published papers looking at the cells that outgrow from cultured iselts[25,51]. To determine if any of those outgrowing cells were glial cells of neural crest cell origin, isolated islets from Wnt1-cre/R26R eYFP mice were grown on Permanox® plastic chamber slides. After 5 days in culture, islets had adhered to the plastic and cells had grown out from the islets onto the plastic surface. The slides were fixed and stained for GFP and GFAP (Figure 15). The cells that grew out from the islet were, unsurprisingly, a mixed-origin population of cells.

Some islets were surrounded by cells mostly of non-neural crest cell origin (GFP negative), while other islets were surrounded by cells that mostly stained for GFP. This range of amount of outgrown neural crest derived cells is most likely a reflection of the amount of retained glial and neuronal cells on the isolated islets at the start of culture. GFAP staining was faint in the outgrown cells, which could be enhanced with increased brightness and contrast (Figure 15B; GFAP+ cells in Figure 15B overlap with the eYFP+ cells in the panel directly above in Figure 15A); this faint GFAP staining may be a reflection of reduced GFAP content or altered cytoskeleton structure but this would require further investigation. While it was not done at the time of this particular experiment, it would have also been useful to stain these slides for TUJ1. Outgrowth culturing methods clearly do not generate even a roughly uniform population of cells, so this does not seem like a suitable method to isolate islet glial cells.

Drop-seq Experiments

As GFAP-cre and GFAP-GFP mice were not suitable mouse models for sorting GFAP+ islet glial cells, we decided to use Wnt1-cre/mTmG mice to sort islet glial cells for RNA-seq. However, as Wnt1-cre/mTmG mice label all neurons and glial cells with GFP and as isolated islets contain TUJ1+ neurons in roughly equal proportion to GFAP+ glial cells, sorted GFP+ cells from Wnt1-cre/mTmG mice could contain both neurons and glial cells. Therefore, to perform RNA-seq on islet glial cells, I needed to do single cell sequencing. There are a variety single cell sequencing techniques currently available, each with their own benefits and drawbacks. Here, we decided to use the relatively new method of Drop-seq, for reasons discussed in the Introduction. Additionally, I was able to perform these experiments in collaboration with the Diabetes Center lab of Dr. Michael McManus.

Sorting Pilot: To determine how many GFP+ cells could be isolated from one mouse pancreas, we performed a pilot sorting experiment using pooled, dissociated islets from four 4-5-month-old, mixed-sex Wnt1-cre/mTmG mice. By FACS, we sorted a total of 4,205 GFP+ cells, which

translates to approximately 1,051 eGFP+ cells per mouse (Table 5). An excess of 500,000 tdTomato+ cells were also sorted from the four mice, representing a large potential “control” population of endocrine and non-endocrine islet cells from non-neural crest cell lineages. Figure 16 shows the FACS scatter plots from the Wnt1-cre/mTmG dissociated islet cells (A) and from the negative control mouse, an mTmG mouse without Wnt1-cre, which should not possess GFP+ cells (B).

Drop-seq Pilot: As Wnt1-cre/mTmG mice were a limiting factor due to issues surrounding breeding, genotyping and death (see Methods sections), we used mice that lacked any fluorescent transgenes to practice the technically-challenging Drop-seq protocol on dissociated mouse islets for the first time. For the planned HiSeq Drop-seq experiment, I had a second cohort of four adult mTmG mice, which, based on the FACS pilot described in the previous section, would conservatively generate around 4,000 GFP+ cells. Because Drop-seq requires are large starting cell concentration and minimum volume of 1.5 mL to create the droplets, I would need to add in an appropriate amount of tdTomato+ control cells to make up the difference between the number of GFP+ cells collected and the desired total cell population. However, the more tdTomato+ cells added into the single cell mixture at the start of droplet making, the more the GFP+ cells of interest would be diluted. Therefore, we wished to determine the minimum number of control cells we could use to generate sufficient sequencing data. We decided to try two starting cell concentrations: a “high” cell concentration of 225,000 cells/1.5 mL (150 cells/uL) that had been previously and empirically determined by the McManus lab as a suitable cell concentration for MiniSeq data generation using cell lines and a “low” cell concentration of 50,000 cells/1.5 mL (33 cells/uL) that had not been tried but, if it worked, would allow me to use less control cells in my HiSeq experiment.

From dissociated islets pooled from three 13 week old male mice, we generated a “high” cell concentration of 225,000 cells/1.5mL (150 cells/uL) and “low” cell concentration at 49,571

cells/1.5 mL (33 cells/uL). The flow gating and scatter plots are shown in Figure 16C. After generating cell and bead oil droplets using the microfluidic device, lysing the droplets, performing reverse transcription, and manually counting the bead concentration via a hemocytometer counter, the cDNA-coated beads were ready for amplification by PCR. Approximately 32,500 beads (32.5 beads/uL) were recovered for the “high” cell concentration sample and 52,800 beads (52.8 beads/uL) were recovered from the low cell concentration sample. The first PCR program tried on an aliquot of 2000 beads from each sample was the McCarroll v3.1 protocol (Table 4); however; this 13 cycle protocol did not generate any amplified cDNA, as determined by Bioanalyzer High Sensitivity DNA Chip. An additional PCR reaction using 6,000 beads from the “low” cell concentration was also tried and this too failed to generate any cDNA using the 13 cycles. This failure was not entirely unexpected as the Drop-seq PCR program must be empirically determined based on the cell type(s) being assayed and their starting origin (i.e. cell line vs intact organ). Therefore, we next tried PCR program J (Table 4) with 26 cycles, double the number of PCR cycles tried during the first PCR attempt, only using a 2000 and a 6000 bead aliquot from “high” cell concentration sample to save on beads and reagents. This generated 6,952.67 pg/uL amplified cDNA from 2,000 beads, which is over the desired 1-2.5 ng/uL cDNA concentration (based on McManus lab empirical experience; McCarroll lab protocol estimates a 400-1000 pg/uL amplified cDNA yield from a 2000 bead PCR reaction and 100 cells/uL starting concentration, but also mentions this yield can vary by experiment). This meant that the properly amplifying PCR program was somewhere in between 13 and 26 cycles, so next we tried PCR programs A (“high” cell concentration sample only), B (“high” cell concentration sample only), C, F, H, I, and J (“low” cell concentration sample only) (Table 4) on 2000 bead aliquots from the “high” and “low” cell concentration samples. From the Bioanalyzer High Sensitivity DNA Chip results, PCR program F (21 cycles) generated the desired concentration and peak sizes (a predominant peak around 1200 bp and with minimal ~100-500 bp peaks) for the “high” cell concentration sample, so the rest of the beads from the

“high” cell concentration sample were processed with 21 PCR cycles; and, although untested during this PCR optimization experiment, Program G (22 cycles) was chosen as the PCR program to process the rest of the “low” concentration sample (21 cycles did not generate enough cDNA product and 23 cycles did not generate the correct Bioanalyzer profile as assessed by peak sizes).

Based on Bioanalyzer results of the 21 and 22 cycle PCR reactions, 3 uL aliquots from four PCR reactions with the correct cDNA concentration and peak profiles were pooled from the “high” and “low” cell concentration samples and 1 ng of these pools were used for the tagmentation reactions used to prepare the libraries for MiniSeq. 1.8 picomoles (pM) from each tagmented library was sequenced by MiniSeq and generated approximately 22.5 million reads.

After computational processing of the MiniSeq data, 68 cells from the “high” cell concentration sample had been sequenced with more than or equal to 1000 total transcripts (101 cells with over 500 transcripts) and 25 cells had over 1000 total transcripts from the “low” cell concentration sample (36 cells with over 500 transcripts). From the “high” cell concentration, 54 cells had over 500 genes sequenced and from the “low” cell concentration, 23 cells had over 500 genes sequenced. Some of the most highly expressed genes included glucagon, insulin (1 and 2), Malat1, mt-Rnr2, somatostatin, transthyretin, pancreatic polypeptide (PPY), chromogranin A, peptide YY (PYY), carboxypeptidase E (Cpe3), Meg3, and islet amyloid polypeptide (for a complete list of the top 35 genes by all cell-total transcript number, see the left-most column of Table 6). As the cells used for this pilot were from dissociated islets, finding endocrine-associated genes as the most highly expressed genes was reassuring. Additionally, it was possible to identify a cell as either, for example, a beta cell or an alpha cell, based on its transcriptional profile. Furthermore, the most highly expressed genes in the two samples (“high” and “low” cell concentrations) were similar, which was reassuring as the samples came from the

same flow preparation yet had been processed as separate samples for the remainder the Drop-seq protocol.

The “low” cell concentration had more fickle PCR reactions (more “failed” PCR reactions based on Bioanalyzer profiles peak sizes and cDNA concentrations as compared to the “high” cell concentration sample), which did not inspire confidence going into the HiSeq experiment. Balancing increasing the dilution of my GFP+ cells with the likelihood of technical success, I decided to try around 200,000 cells/1.5 mL as my starting cell concentration for droplet making for the HiSeq experiment, which was just slightly lower than the 225,000 cells/1.5 mL of the “high” cell concentration test sample.

HiSeq Drop-seq: Isolated and dissociated islets from four ~6 month old, mixed-sex Wnt1-cre/mTmG mice (three females and one male) were sorted by FACS (Figure 17). Cells were sorted to exclude doublets and cellular debris and then sorted for FITC-high/dsRed-low cells (i.e. GFP-high/tdTomato-low cells; containing glial cells) and FITC-low/dsRed-high cells (i.e. GFP-low/tdTomato-high cells; control cells containing non-endocrine and endocrine cells types from non-neural crest cell lineages). A total of 204,251 cells were collected and brought up to 1.5 mL with a HBSS/BSA solution (136 cells/uL) for Drop-seq droplet making. Only 4,251 of the collected cells (~2.1%) were GFP-high/tdTomato-low cells. The total number of GFP+ cells collected from these four Wnt1-cre/mTmG mice was consistent with the total number of GFP+ cells collected from the four Wnt1-cre/mTmG mice in the sorting pilot (4,205 cells) (Table 5).

Based on the results from the Drop-seq “high” cell concentration sample, the first cDNA PCR amplification attempt was done using PCR programs E and F (20 cycles and 21 cycles). However, these PCR programs had issues of over-amplification (predominant small sized peaks), so I tried a two different 19 cycle PCR programs, C and D. PCR program D over-amplified small sized peaks, while PCR program C generated 2,033.08 pg/uL cDNA from a 2000 bead aliquot with a predominant peak around 1241 bp; therefore, program C was used to

process the rest of the 26 aliquots of 2000 the beads. Eleven PCR reactions were pooled into three tagmentation reactions to prepare the libraries for sequencing (two pools of three PCR reactions and one pool of four PCR reactions). Six PCR reactions were ran in one HiSeq lane (from two pooled tagmentation reactions) and four PCR reactions (from one tagmentation reaction) was run in a second HiSeq lane.

Combining the data from both HiSeq lanes (i.e. all 11 PCR reactions), 338 cells were sequenced with over 1000 transcripts. Between these 338 cells, 16,489 unique genes were sequenced. Within these 338 cells, four cells perfectly matched the glial cell profile: GFP+, tdTomato negative, GFAP+, and TUJ1 negative. GFAP transcripts were only found in these four cells; in other words, GFAP was only found in GFP+ cells and not found in any cells that contained tdTomato.

Unexpectedly, many of the clearly endocrine cells lacked tdTomato, most likely because this red fluorescent protein had a low number of unique transcripts captured per cell. Only 45 cells out of these 338 cells had 1 or more transcripts of tdTomato with an average of 2 transcripts per positive cell (range 1-7 transcripts per cell). GFP was expressed at a similar transcript level as tdTomato: 25 cells out of these 338 cells had 1 or more eGFP transcripts with an average of around 2 transcripts per positive cell (range 1-10 transcripts per cell). Also worth noting that four of the tdTomato positive cells were also positive for GFP, which likely is the result of two (or more) cells or cell fragments being encapsulated in the same droplet of oil during the original droplet formation at the start of the Drop-seq protocol. Nine cells contained TUJ1 transcripts, with only one of those cells being TUJ1+/GFP+ double positive. One TUJ1 transcript was found in a tdTomato+ cell that was likely the result of a cellular clump (this particular cell had over twice as many total transcripts than the cell with the second most total transcripts). With only 66 cells having one or more fluorescent transcripts, 272 cells lacked any fluorescent transcripts.

Therefore, it appears that transcripts expressed at low levels may not always be “captured” by Drop-seq.

To identify other glial cells that did not express GFAP, which also had a low total transcript count per cell (of the four cells that contained GFAP, they only had 1-2 transcripts per cell), clustering analysis was run on 284 cells with at least 1000 total transcripts and using the 11,766 genes with at least 5 total transcripts in at least 5 cells (i.e. the sum of the transcripts across all cells was equal to or greater than 5 and expressed in at least 5 five cells; this excluded transcripts expressed at very low levels in very few cells). This identified a total of seven glial cells, including the four “perfect” matching glial cells and three additional cells expressing many of the genes found in the four “perfect” matching glial cells and that are glial-associated, including GFP, Vim, Apoe, Plp1, Sparc, Timp3, and s100b. The seven glial cells had an average of 3,384 total transcripts per cell (range: 1,998-4,498 total transcripts). A heat map including those seven glial cells and 67 other control cells within a similar range of total transcripts is shown in Figure 18. This heat map was run using and is shown with 567 genes for visual clarity. The glial cells cluster on the right most edge of the graphic; other endocrine cells are identified in the figure legend. Endothelial and duct cells form two clusters between the islet cells and glial cells, and three immune cells were identified that cluster between the beta and alpha cells on the heat map (Figure 18).

Average gene expression for each gene was calculated in the seven glial cells and in 168 control cells that spanned the range of total transcript counts found in the seven glial cells and that did not have any GFP transcripts. Note: to normalize transcript counts, the transcript count of each gene was divided by the total number of transcripts per cell; this normalization method was used throughout data analysis on this HiSeq data. Table 7 shows the top glial genes expressed in at least four of the seven glial cells and that have an average expression at least

20 fold higher than the average control cell expression or is uniquely expressed in the glial cells (i.e. no expression in the control cells). GFAP and GFP are highlighted in green in Table 7.

Gene ontology and pathway analysis was run on the top glial expressed genes (expressed in at least 5 glial cells and had either a greater than 20 fold ratio over average control cell expression or an “infinite” fold induction due to lack of control cell expression. Average expression was calculated using the seven glial cells and 178 control cells that lacked GFAP and/or GFP). Ontology and pathway analysis graphics are shown in Figure 19.

Top genes based on total transcript across the entire 338 HiSeq cells included many mitochondrially encoded genes (Table 6). Many of these same mitochondrially encoded genes are also among the top MiniSeq pilot genes. The significance of these genes are this is unclear. The HiSeq heat map also includes many ribosomal genes, which also have unclear significance.

Overall, the top genes by total transcript number in the HiSeq run and in the MiniSeq pilot are similar, which indicates a confidence-boosting level of consistency between Drop-seq runs (Table 6). Looking back at the pilot Drop-seq data, while I did not sequence any GFAP transcripts, there may be a few glial cells that were sequenced based on the transcription profile established in the HiSeq run. One cell in particular with 2,251 transcripts had a glial-like expression profile, expressing 66 of the 138 top HiSeq glial genes listed in Table 7, including Apoe, Sparc, Prnp, Plp1, Timp3, Ifi27l2a, Sfrp1, Kcna1, Vim, Iqgap2, Abca8b, Chl1, Synm, Scn7a, B2m, Dbi, Pmepa1, Cryab, and Lpar1. Table 8 lists the top 34 genes within those 66 HiSeq-identified glial genes (cut-off: 3 or more transcripts) in this possible glia cell.

Chapter 4: Discussion and Future Directions

Discussion

Lineage tracing: All GFAP+ cells in healthy adult mouse pancreas that I observed are of neural crest cell origin; therefore, I argue that GFAP is not a suitable pancreatic stellate cell marker and should only be used as a glial cell marker in the pancreas. While I focused primarily on the islet, the GFAP+ processes I saw around blood vessels, ducts, and elsewhere in the acinar portions of the pancreas all co-localized with GFP staining in Wnt1-cre/mTmG and Wnt1-cre/eYFP mice. However, it would be worth more closely assessing these non-islet areas as they were outside the scope of this project. It would also be worth looking at GFAP staining in the adult Wnt1-cre/mTmG or eYFP pancreases in other physiological and pathophysiological conditions (eg. experimentally induced-pancreas injury or cancer models) to see if GFAP may be turned on in non-neural crest cell origin cells under certain perturbations.

GFAP-cre mice: While GFAP staining in the pancreas seems to be a reliable neural crest cell-derived glial cell marker; unfortunately, GFAP-cre does not seem to be a suitable glial cell-specific mouse line. Cre recombination was seen in duct-like cells of the pancreas that do not stain for positive for GFAP and only sporadically/faintly in GFAP+ glial cells. This non-glial cell expression of Cre may have occurred during embryonic development or at some point prior to adulthood.

Searching the literature on the GFAP-cre line, I can find pieces of evidence in several papers that support my findings. In the 2001 paper describing the creation of the GFAP-cre mice, the authors show images from the liver of GFAP-cre/R26R-lacZ reporter adult mice showing labeling of some of the cells in the periportal region[65]. The authors write, “We did not pursue final identification of the lacZ-positive cells in the liver, but note that their distribution did not correspond to that of stellate cells, the hepatic cell previously reported to express GFAP (Gard

et al., 1985; Buniatian et al., 1996). It is interesting that non-myelinating Schwann cells of the peripheral nervous system, (Jessen et al., 1984; Feinstein et al., 1992), were not affected by the hGFAP-cre transgene, even though the hGFAP promoter has occasionally directed expression to these cells when lacZ or green fluorescent protein were used as reporters"[65].

Additional researchers using a GFAP-cre/GFP mouse "unexpectedly" found expression of GFAP, Cre-recombinase, and GFP "in bile duct cells and ductular-appearing cells in peri-portal canals of Hering in GFAP-Cre/GFP mice"[70]. Looking into the expression of GFAP in these unexpected cells, they report that "expression of GFAP was demonstrated at the RNA level in freshly isolated primary cholangiocytes and HSC, but not hepatocytes, from healthy adult rats"[70]. Others have also seen that GFAP-cre/ZsGreen labels bile ducts and cytokeratin 19-expressing cholangiocytes and that the line does not label "a significant amount of HSCs, suggest[ing] that previous studies employing GFAP-cre are likely to be not HSC-specific"[71].

Another paper assessing the cell specificity of various cre-lines argues for the need of more comprehensive characterization of cre-driver lines for the benefit of the scientific community[72]. The authors explain that "several cre strains, specifically neuro-specific strains, exhibited significant unexpected and unreported deletion outside of their targeted tissue or cell types"[72]. These authors tested GFAP-cre and found that it was expressed in the periportal regions of the liver in addition to pancreatic ducts[72]. In sum, my findings, as well as the findings of these other researchers, call into question using GFAP-cre to study either pancreatic glial cells or hepatic (or pancreatic) stellate cells as there is likely Cre recombination occurring in unwanted cell types.

Neurons in pancreas: As explained in the results section, as both the GFAP-cre and GFAP-GFP mouse models proved unsuitable for the various experiments we had planned to interrogate the peri-islet glial cells, including using the GFAP-cre/iDTR mice for glial cell ablation and the GFAP-cre/mTmG (or GFAP-cre/R26R eYFP or GFAP-GFP) for glial cell sorting, I

decided to use the Wnt1-cre line instead. Besides GFAP, the other known peri-islet glial cell marker is s100β; however, s100β may also be a non-suitable glial-cell specific gene to use for transgenic mouse lines. s100β-eGFP transgenic reporter mice labels alpha cells and this unexpected labeling has exploited as a method to sort alpha cells by FACS, despite alpha cells lack of expression of s100b at the transcript level[73]. While the Cre recombinase in the Wnt1-cre mouse would mark all neural crest cell derived cells, including both glial cells and neurons, it was unclear how many neurons would be retained in isolated islets, especially compared to GFAP+ glial cells, or if those neurons would persist in culture.

PNS neurons emanate from intrapancreatic ganglia, which are connected to the vagus nerves, while the SNS nerve cell bodies are located in the paravertebral or celiac ganglia[3,74]. A special type of intrapancreatic ganglia has been termed the "'neuroinsular complex (NIC) type I" containing both neuron cell bodies ("perikarya") and endocrine cells, often found near pancreatic ducts[75]. Serizawa et al. wrote in 1979 that "There seems to be every gradation between pure ganglia, mixed forms representing the neuro-insular complexes, and pure islets"[76] which later lead to the development of classification scheme of islets, NICs, and ganglia, reviewed by Proshchina et al.[77] According to Persson–Sjögren, a "quantitative analysis of mouse pancreas revealed that a substantial number of the islets do in fact contain perikarya"[75]. Persson–Sjögren goes on to postulate that "If not destroyed by too harsh a treatment during the collagenase isolation procedure, the nerve cell bodies intrinsic to the neuroinsular complex type I should accompany the endocrine cells"[75]. Indeed, I did find that nucleated neurons were retained in isolated mouse islets. Furthermore, these neurons persisted and survived in culture. Juang et al. only traced donor pericytes and glial cells in their transplanted islets; however, considering my findings, I wonder if there were also transplanted neurons on those islets as well[30]. The survival of neurons on isolated islets left us without a suitable mouse model for experimental

manipulation of peri-islet glia; providing further justification for the need to perform single cell sequencing.

Glial genes of interest: The Drop-seq HiSeq experiment sequenced seven presumed peri-islet glial cells based on their gene expression profiles. Encouragingly, the glial cells expressed known astrocyte, oligodendrocyte, and Schwann cells related genes, including Myelin and lymphocyte protein (Mal), Proteolipid Protein (PLP), GFAP, s100β, Vim, fatty acid binding protein 7 (FABP7), SRY-box 10 (Sox10), Apolipoprotein E (ApoE), and Osteonectin/secreted protein acidic and rich in cysteine (Sparc)[60].

The data set from this experiment is fascinating and contains many potentially interesting genes worthy of literature searches and potential experimental follow-up. For example, Serpine2 (Protease Nexin-1; PN-1), which was found in six of the seven glial cells at an average ~40 fold higher expression than control cells, is a secreted serine protease inhibitor that has been associated with glial cells, neurite outgrowth, blood vessel growth and pancreatic cancer; additionally, related genes SERPINE1 and SERPINI2 are claimed to be part of the secreted pancreatic stellate cell proteome generated by an immortalized GFAP+ PSC cell line originally isolated from outgrowth culture[78-81]. Another serpin family member, Serpinh1, was also expressed in six of the seven glial cells at an average ~20 fold higher expression than control cells; interestingly, siRNA against serpineh1 was just licensed to Bristol-Myers Squibb (BMS) to be developed as a therapy for non-alcoholic steatohepatitis (NASH) as this gene is thought to be responsible for collagen scar formation in the liver by hepatic stellate cells. Annexin 2 (Anxa2) is also claimed to be part of the secreted pancreatic stellate cell proteome and found to be expressed in 4 of the 7 Drop-seq HiSeq glial cells at a ratio of almost 20 fold higher than the expression found in control cells[79]. Annexin 2 is known to bind to S100-family proteins and regulate GFAP polymerization[82]. Other genes associated with pancreatic stellate cells, such as the ECM-regulating tissue inhibitor of metalloproteinases (TIMPs), were found in the Drop-seq

HiSeq glial cells, including TIMP3, which was expressed in all seven of the glial cells at an average 87 fold higher expression than control cells. With so many of my presumed glial cell genes coming up as pancreatic stellate cell genes in literature searches, I am still left contemplating if pancreatic stellate cell studies include GFAP+ glial cells.

One of the most interesting genes found in the Drop-seq HiSeq glial cells was Sparc, which was found in all seven of the glial cells at an almost 75 fold higher expression than control cells. Sparc has also been attributed to pancreatic stellate cells[83,84] and is associated with pancreatic cancer (PDAC)[85] and the pathogenesis of obesity and diabetes[86]. Sparc (secreted protein acidic and rich in cysteine), also known as osteonectin and/or BM-40 (basement membrane 40), is a secreted, ECM-associated glycoprotein. In astrocytes, Sparc is thought to regulate synapse formation and growth factor signaling cascades (including VEGF (vascular endothelial growth factor), PDGF (platelet-derived growth factor), FGF2 (fibroblast growth factor-2), and TGFβ (transforming growth factor beta)) and to be upregulated during reactive gliosis[87,88].

Glial cell line derived neurotrophic factor receptor alpha 3 (GFRα3) was found in five of the seven glial cells at an average ~50 fold higher expression than control cells and encouragingly, has just recently been studied by others in the context of the pancreatic islet, including in peri-islet glial cells[89]. However, while GFRα3 seems to be expressed in peri-islet glial cells in adult mice as seen by immunostaining, GFRα3 also seems to be expressed in endocrine progenitor cells during mouse embryonic development, thus limiting its potential as a Cre driver[89].

Drawbacks to Drop-seq: While the Drop-seq method generated a large amount of interesting data; this method is not without its caveats. Drawbacks of Drop-seq include the high starting volume and cell concentration needed (this technique seems most suitable for sequencing a large or unlimited quantity of cells rather than a rare cell type), repeated need to manually and tediously count the beads, the 2000 bead/PCR reaction tube limit (which is under-emphasized in the original paper and dramatically limits the supposedly “high-throughput” nature of this

method), and the empirically-determined PCR program and its fickle success rate at generating the desired fragment sizes and concentrations. Interestingly, we ran two HiSeq lanes, one with pooled tagmentation reactions from the PCR reactions that had optimal Bioanalyzer profiles and a second lane with “less than ideal” Bioanalyzer profiles. However, both lanes seemed to generate similar quality data, so perhaps less stringency on Bioanalyzer profile screening is possible. Additionally, 10x Genomics has a new tabletop machine that automates and performs a Drop-seq-like single cell sequencing and may be another avenue to pursue for sequencing more peri-islet glia. While the 10x Genomics machine is not currently able to process the large numbers of cells that the Drop-seq method is theoretically able to, one of the benefits of the 10x Genomics machine is that it can use a smaller number of cells to start and is more suited for rare cell types.

Future Directions

Data Mining My initial retrospective look at the Drop-Seq pilot data and finding one likely glial cell and a handful of other cells with many of the HiSeq identified glial-associated genes raises the exciting possibility of acquiring other islet single cell sequencing data sets, from papers such as Lawlor et al.[90], and identifying more glial cells. As this pilot data was from islets not enriched for glial cells and only sorted for single, intact cells, there is likely enough of a chance that other data sets on dissociated islets would include glial cells too.

Mouse lines and genetic ablation Genes that seem glial cell specific could be used as Cre drivers for crossing with iDTR mice for islet glial cell ablation experiments. The first step in evaluating a new Cre driver would be to stain sectioned mouse pancreases (and later isolated mouse islets) for candidate genes, like Sparc, and then assess their co-localization with GFAP to determine glial-cell specificity. In addition to using these Cre drivers to conduct ablation studies, the new glial markers could be used with mTmG mice for FACS experiments to isolate more peri-islet glia for sequencing. Even more intriguing are the apparent glial-cell-specific cell

surface markers as these markers could be used for cell sorting using antibodies. This type of sorting could be done on WT mice, which would be a great boon to experiments as one would not need to breed, genotype and age mice with specific multi-transgene genotypes, as I did with the Wnt1-cre mTmG mice. One such cell surface marker is tetraspanin family gene CD9, a gene previously studied in Schwann cells and found in 6 of the 7 Drop-seq HiSeq glial cells at an average 200 fold higher expression than control cells[91].

Similarly to peri-islet glia, the impact of islet pericytes on beta cell function is also largely unknown. Employing a similar method as we had planned to ablate glia cells, Sasson et al. recently used a Nkx3.2-cre/iDTR mouse to ablate islet pericytes and observed changes in glucose stimulated insulin secretion (GSIS) and beta cell maturity genes[92]. Likewise, I would test GSIS, beta cell proliferation and death, as well as glucagon secretion due to GFAP+ cells close association with glucagon-expression alpha cells, in isolated and glial-cell ablated islets. These ablation studies may yield further insight into the function of these fascinating-yet-frustrating peri-islet glial cells.

References

1 Weir, G. C. *et al.* Dispersed adult rat pancreatic islet cells in culture: A, B, and D cell function. *Metabolism* **33**, 447-453, doi:http://dx.doi.org/10.1016/0026-0495(84)90146-X (1984).

2 Roscioni, S. S., Migliorini, A., Gegg, M. & Lickert, H. Impact of islet architecture on [beta]-cell heterogeneity, plasticity and function. *Nat Rev Endocrinol* **12**, 695-709, doi:10.1038/nrendo.2016.147 (2016).

3 Ahrén, B. Autonomic regulation of islet hormone secretion – Implications for health and disease. *Diabetologia* **43**, 393-410, doi:10.1007/s001250051322 (2000).

4 Nekrep, N., Wang, J., Miyatsuka, T. & German, M. S. Signals from the neural crest regulate beta-cell mass in the pancreas. *Development (Cambridge, England)* **135**, 2151-2160, doi:10.1242/dev.015859 (2008).

5 Plank, J. L. *et al.* Influence and timing of arrival of murine neural crest on pancreatic beta cell development and maturation. *Developmental biology* **349**, 321-330, doi:http://dx.doi.org/10.1016/j.ydbio.2010.11.013 (2011).

6 Uchida, T. & Endo, T. Identification of cell types containing S-100b protein-like immunoreactivity in the islets of Langerhans of the guinea pig pancreas with light and electron microscopy. *Cell and tissue research* **255**, 379-384 (1989).

7 Sunami, E. *et al.* Morphological characteristics of Schwann cells in the islets of Langerhans of the murine pancreas. *Archives of histology and cytology* **64**, 191-201 (2001).

8 Smith, P. H. Structural modification of Schwann cells in the pancreatic islets of the dog. *The American journal of anatomy* **144**, 513-517, doi:10.1002/aja.1001440412 (1975).

9 Donev, S. R. Ultrastructural evidence for the presence of a glial sheath investing the islets of Langerhans in the pancreas of mammals. *Cell and tissue research* **237**, 343-348 (1984).

10 Krivova, Y. S., Proshchina, A. E., Chernikov, V. P., Barabanov, V. M. & Savel'ev, S. V. Immunohistochemical Analysis and Electron Microscopy of Glial Cells in the Pancreas of Fetuses and Children. *Bull. Exp. Biol. Med.* **159**, 666-669, doi:10.1007/s10517-015-3043-1 (2015).

11 Demir, I. E., Friess, H. & Ceyhan, G. O. Neural plasticity in pancreatitis and pancreatic cancer. *Nat Rev Gastroenterol Hepatol* **12**, 649-659, doi:10.1038/nrgastro.2015.166 (2015).

12 Allen, N. J. & Barres, B. A. Neuroscience: Glia [mdash] more than just brain glue. *Nature* **457**, 675-677 (2009).

13 Ko, C. P. & Robitaille, R. Perisynaptic Schwann Cells at the Neuromuscular Synapse: Adaptable, Multitasking Glial Cells. *Cold Spring Harbor perspectives in biology* **7**, a020503, doi:10.1101/cshperspect.a020503 (2015).

14 McKenna, M. C. *et al.* Glutamate oxidation in astrocytes: Roles of glutamate dehydrogenase and aminotransferases. *Journal of neuroscience research* **94**, 1561-1571, doi:10.1002/jnr.23908 (2016).

15 Bazargani, N. & Attwell, D. Astrocyte calcium signaling: the third wave. *Nat Neurosci* **19**, 182-189, doi:10.1038/nn.4201 (2016).

16 Rose, C. R. & Chatton, J. Y. Astrocyte sodium signaling and neuro-metabolic coupling in the brain. *Neuroscience* **323**, 121-134, doi:http://dx.doi.org/10.1016/j.neuroscience.2015.03.002 (2016).

17 Chen, N. *et al.* Direct modulation of GFAP-expressing glia in the arcuate nucleus bi-directionally regulates feeding. *eLife* **5**, doi:10.7554/eLife.18716 (2016).

18 Teitelman, G., Guz, Y., Ivkovic, S. & Ehrlich, M. Islet injury induces neurotrophin expression in pancreatic cells and reactive gliosis of peri-islet Schwann cells. *Journal of neurobiology* **34**, 304-318 (1998).

19 Tang, S. C., Chiu, Y. C., Hsu, C. T., Peng, S. J. & Fu, Y. Y. Plasticity of Schwann cells and pericytes in response to islet injury in mice. *Diabetologia* **56**, 2424-2434, doi:10.1007/s00125-013-2977-y (2013).

20 Pekny, M. & Nilsson, M. Astrocyte activation and reactive gliosis. *Glia* **50**, 427-434, doi:10.1002/glia.20207 (2005).

21 Wiese, S., Karus, M. & Faissner, A. Astrocytes as a Source for Extracellular Matrix Molecules and Cytokines. *Frontiers in Pharmacology* **3**, doi:10.3389/fphar.2012.00120 (2012).

22 Goritz, C. *et al.* A pericyte origin of spinal cord scar tissue. *Science (New York, N.Y.)* **333**, 238-242, doi:10.1126/science.1203165 (2011).

23 Mwangi, S. *et al.* Glial cell line-derived neurotrophic factor increases beta-cell mass and improves glucose tolerance. *Gastroenterology* **134**, 727-737, doi:10.1053/j.gastro.2007.12.033 (2008).

24 Atouf, F., Czernichow, P. & Scharfmann, R. Expression of neuronal traits in pancreatic beta cells. Implication of neuron-restrictive silencing factor/repressor element silencing transcription factor, a neuron-restrictive silencer. *The Journal of biological chemistry* **272**, 1929-1934 (1997).

25 Tsui, H. *et al.* Targeting of pancreatic glia in type 1 diabetes. *Diabetes* **57**, 918-928, doi:10.2337/db07-0226 (2008).

26 Tsui, H. *et al.* Islet glia, neurons, and beta cells. *Annals of the New York Academy of Sciences* **1150**, 32-42, doi:10.1196/annals.1447.033 (2008).

27 Winer, S. *et al.* Autoimmune islet destruction in spontaneous type 1 diabetes is not beta-cell exclusive. *Nature medicine* **9**, 198-205, doi:10.1038/nm818 (2003).

28 Yantha, J. *et al.* Unexpected acceleration of type 1 diabetes by transgenic expression of B7-H1 in NOD mouse peri-islet glia. *Diabetes* **59**, 2588-2596, doi:10.2337/db09-1209 (2010).

29 Pang, Z. *et al.* Evaluating the potential of the GFAP-KLH immune-tolerizing vaccine for type 1 diabetes in mice. *FEBS letters*, doi:10.1002/1873-3468.12511 (2016).

30 Juang, J. H., Kuo, C. H., Peng, S. J. & Tang, S. C. 3-D Imaging Reveals Participation of Donor Islet Schwann Cells and Pericytes in Islet Transplantation and Graft Neurovascular Regeneration. *EBioMedicine* **2**, 109-119, doi:10.1016/j.ebiom.2015.01.014 (2015).

31 Lau, J., Vasylovska, S., Kozlova, E. N. & Carlsson, P. O. Surface Coating of Pancreatic Islets With Neural Crest Stem Cells Improves Engraftment and Function After Intraportal Transplantation. *Cell Transplant.* **24**, 2263-2272, doi:10.3727/096368915x686184 (2015).

32 Burris, R. E. & Hebrok, M. Pancreatic innervation in mouse development and beta-cell regeneration. *Neuroscience* **150**, 592-602, doi:10.1016/j.neuroscience.2007.09.079 (2007).

33 Reinert, R. B. *et al.* Vascular endothelial growth factor coordinates islet innervation via vascular scaffolding. *Development (Cambridge, England)* **141**, 1480-1491, doi:10.1242/dev.098657 (2014).

34 Rodriguez-Diaz, R. *et al.* Innervation patterns of autonomic axons in the human endocrine pancreas. *Cell Metab* **14**, doi:10.1016/j.cmet.2011.05.008 (2011).

35 Henderson, J. R. & Moss, M. C. A morphometric study of the endocrine and exocrine capillaries of the pancreas. *Quarterly journal of experimental physiology (Cambridge, England)* **70**, 347-356 (1985).

36 Dolensek, J., Rupnik, M. S. & Stozer, A. Structural similarities and differences between the human and the mouse pancreas. *Islets* **7**, e1024405, doi:10.1080/19382014.2015.1024405 (2015).

37 Lau, J., Svensson, J., Grapensparr, L., Johansson, Å. & Carlsson, P.-O. Superior beta cell proliferation, function and gene expression in a subpopulation of rat islets identified by high blood perfusion. *Diabetologia* **55**, 1390-1399, doi:10.1007/s00125-012-2476-6 (2012).

38 Richards, O. C., Raines, S. M. & Attie, A. D. The Role of Blood Vessels, Endothelial Cells, and Vascular Pericytes in Insulin Secretion and Peripheral Insulin Action. *Endocrine Reviews* **31**, 343-363, doi:doi:10.1210/er.2009-0035 (2010).

39 Schaeffer, M., Hodson, D. J., Lafont, C. & Mollard, P. Endocrine cells and blood vessels work in tandem to generate hormone pulses. *Journal of molecular endocrinology* **47**, R59-66, doi:10.1530/jme-11-0035 (2011).

40 Erkan, M. *et al.* StellaTUM: current consensus and discussion on pancreatic stellate cell research. *Gut* **61**, 172-178, doi:10.1136/gutjnl-2011-301220 (2012).

41 Hellerbrand, C. Hepatic stellate cells—the pericytes in the liver. *Pflügers Archiv - European Journal of Physiology* **465**, 775-778, doi:10.1007/s00424-012-1209-5 (2013).

42 Asahina, K., Zhou, B., Pu, W. T. & Tsukamoto, H. Septum transversum-derived mesothelium gives rise to hepatic stellate cells and perivascular mesenchymal cells in developing mouse liver. *Hepatology (Baltimore, Md.)* **53**, 983-995, doi:10.1002/hep.24119 (2011).

43 Cassiman, D., Barlow, A., Vander Borght, S., Libbrecht, L. & Pachnis, V. Hepatic stellate cells do not derive from the neural crest. *Journal of hepatology* **44**, 1098-1104, doi:10.1016/j.jhep.2005.09.023 (2006).

44 Asahina, K. *et al.* Mesenchymal origin of hepatic stellate cells, submesothelial cells, and perivascular mesenchymal cells during mouse liver development. *Hepatology (Baltimore, Md.)* **49**, 998-1011, doi:10.1002/hep.22721 (2009).

45 Rosendahl, A. H. *et al.* Conditionally immortalized human pancreatic stellate cell lines demonstrate enhanced proliferation and migration in response to IGF-I. *Experimental cell research* **330**, 300-310, doi:10.1016/j.yexcr.2014.09.033 (2015).

46 Apte, M. V., Pirola, R. C. & Wilson, J. S. Pancreatic stellate cells: a starring role in normal and diseased pancreas. *Frontiers in physiology* **3**, 344, doi:10.3389/fphys.2012.00344 (2012).

47 Omary, M. B., Lugea, A., Lowe, A. W. & Pandol, S. J. The pancreatic stellate cell: a star on the rise in pancreatic diseases. *J Clin Invest* **117**, 50-59, doi:10.1172/jci30082 (2007).

48 Fujiwara, K. *et al.* CD271(+) subpopulation of pancreatic stellate cells correlates with prognosis of pancreatic cancer and is regulated by interaction with cancer cells. *PLoS One* **7**, e52682, doi:10.1371/journal.pone.0052682 (2012).

49 Trim, N. *et al.* Hepatic Stellate Cells Express the Low Affinity Nerve Growth Factor Receptor p75 and Undergo Apoptosis in Response to Nerve Growth Factor Stimulation. *The American Journal of Pathology* **156**, 1235-1243, doi:10.1016/S0002-9440(10)64994-2.

50 Watari, N., Hotta, Y. & Mabuchi, Y. Morphological studies on a vitamin A-storing cell and its complex with macrophage observed in mouse pancreatic tissues following excess vitamin A administration. *Okajimas folia anatomica Japonica* **58**, 837-858 (1982).

51 Zha, M., Li, F., Xu, W., Chen, B. & Sun, Z. Isolation and characterization of islet stellate cells in rat. *Islets* **6**, e28701, doi:10.4161/isl.28701 (2014).

52 Vonlaufen, A. *et al.* Pancreatic stellate cells and pancreatic cancer cells: an unholy alliance. *Cancer research* **68**, 7707-7710, doi:10.1158/0008-5472.can-08-1132 (2008).

53 Sousa, C. M. *et al.* Pancreatic stellate cells support tumour metabolism through autophagic alanine secretion. *Nature* **536**, 479-483, doi:10.1038/nature19084 (2016).

54 Hwang, R. F. *et al.* Cancer-associated stromal fibroblasts promote pancreatic tumor progression. *Cancer research* **68**, 918-926, doi:10.1158/0008-5472.can-07-5714 (2008).

55 Yin, Z., Wu, W., Fung, J. J., Lu, L. & Qian, S. Cotransplanted hepatic stellate cells enhance vascularization of islet allografts. *Microsurgery* **27**, 324-327, doi:10.1002/micr.20365 (2007).

56 Vroemen, M. & Weidner, N. Purification of Schwann cells by selection of p75 low affinity nerve growth factor receptor expressing cells from adult peripheral nerve. *Journal of neuroscience methods* **124**, 135-143 (2003).

57 Suzuki, K. *et al.* p75 Neurotrophin Receptor Is a Marker for Precursors of Stellate Cells and Portal Fibroblasts in Mouse Fetal Liver. *Gastroenterology* **135**, 270-281.e273, doi:http://dx.doi.org/10.1053/j.gastro.2008.03.075 (2008).

58 Moreels, M., Vandenabeele, F., Dumont, D., Robben, J. & Lambrichts, I. Alpha-smooth muscle actin (alpha-SMA) and nestin expression in reactive astrocytes in multiple sclerosis lesions: potential regulatory role of transforming growth factor-beta 1 (TGF-beta1). *Neuropathology and applied neurobiology* **34**, 532-546, doi:10.1111/j.1365-2990.2007.00910.x (2008).

59 Prasad, Rashmi B. & Groop, L. Single-Cell Sequencing of Human Pancreatic Islets—New Kids on the Block. *Cell Metabolism* **24**, 523-524, doi:http://dx.doi.org/10.1016/j.cmet.2016.09.012 (2016).

60 Cahoy, J. D. *et al.* A transcriptome database for astrocytes, neurons, and oligodendrocytes: a new resource for understanding brain development and function. *J Neurosci* **28**, 264-278, doi:10.1523/jneurosci.4178-07.2008 (2008).

61 Macosko, E. Z. *et al.* Highly Parallel Genome-wide Expression Profiling of Individual Cells Using Nanoliter Droplets. *Cell* **161**, 1202-1214, doi:10.1016/j.cell.2015.05.002 (2015).

62 Danielian, P. S., Muccino, D., Rowitch, D. H., Michael, S. K. & McMahon, A. P. Modification of gene activity in mouse embryos in utero by a tamoxifen-inducible form of Cre recombinase. *Current biology : CB* **8**, 1323-1326 (1998).

63 Woodhoo, A. & Sommer, L. Development of the Schwann cell lineage: from the neural crest to the myelinated nerve. *Glia* **56**, 1481-1490, doi:10.1002/glia.20723 (2008).

64 Zhuo, L. *et al.* Live astrocytes visualized by green fluorescent protein in transgenic mice. *Developmental biology* **187**, 36-42, doi:10.1006/dbio.1997.8601 (1997).

65 Zhuo, L. *et al.* hGFAP-cre transgenic mice for manipulation of glial and neuronal function in vivo. *Genesis (New York, N.Y. : 2000)* **31**, 85-94 (2001).

66 Muzumdar, M. D., Tasic, B., Miyamichi, K., Li, L. & Luo, L. A global double-fluorescent Cre reporter mouse. *Genesis (New York, N.Y. : 2000)* **45**, 593-605, doi:10.1002/dvg.20335 (2007).

67 Srinivas, S. *et al.* Cre reporter strains produced by targeted insertion of EYFP and ECFP into the ROSA26 locus. *BMC developmental biology* **1**, 4 (2001).

68 Buch, T. *et al.* A Cre-inducible diphtheria toxin receptor mediates cell lineage ablation after toxin administration. *Nature methods* **2**, 419-426, doi:10.1038/nmeth762 (2005).

69 Tang, S. C., Peng, S. J. & Chien, H. J. Imaging of the islet neural network. *Diabetes, obesity & metabolism* **16 Suppl 1**, 77-86, doi:10.1111/dom.12342 (2014).

70 Yang, L. *et al.* Fate-mapping evidence that hepatic stellate cells are epithelial progenitors in adult mouse livers. *Stem cells (Dayton, Ohio)* **26**, 2104-2113, doi:10.1634/stemcells.2008-0115 (2008).

71 Mederacke, I. *et al.* Fate tracing reveals hepatic stellate cells as dominant contributors to liver fibrosis independent of its aetiology. *Nat Commun* **4**, 2823, doi:10.1038/ncomms3823 (2013).

72 Heffner, C. S. *et al.* Supporting conditional mouse mutagenesis with a comprehensive cre characterization resource. *Nat Commun* **3**, 1218, doi:10.1038/ncomms2186 (2012).

73 Benner, C. *et al.* The transcriptional landscape of mouse beta cells compared to human beta cells reveals notable species differences in long non-coding RNA and protein-coding gene expression. *BMC Genomics* **15**, 620, doi:10.1186/1471-2164-15-620 (2014).

74 Kiba, T. Relationships between the autonomic nervous system and the pancreas including regulation of regeneration and apoptosis: recent developments. *Pancreas* **29**, e51-58 (2004).

75 Persson–Sjögren, S., Forsgren, S. & Täljedal, I.-B. Peptides and other neuronal markers in transplanted pancreatic islets☆. *Peptides* **21**, 741-752, doi:http://dx.doi.org/10.1016/S0196-9781(00)00186-8 (2000).

76 Serizawa, Y., Kobayashi, S. & Fujita, T. Neuro-insular complex type I in the mouse. Re-evaluation of the pancreatic islet as a modified ganglion. *Archivum histologicum Japonicum = Nihon soshikigaku kiroku* **42**, 389-394 (1979).

77 Proshchina, A. E., Krivova, Y. S., Barabanov, V. M. & Saveliev, S. V. Ontogeny of Neuro-Insular Complexes and Islets Innervation in the Human Pancreas. *Frontiers in Endocrinology* **5**, doi:10.3389/fendo.2014.00057 (2014).

78 Neesse, A. *et al.* Pancreatic stellate cells potentiate proinvasive effects of SERPINE2 expression in pancreatic cancer xenograft tumors. *Pancreatology : official journal of the International Association of Pancreatology (IAP) ... [et al.]* **7**, 380-385, doi:10.1159/000107400 (2007).

79 Wehr, A. Y., Furth, E. E., Sangar, V., Blair, I. A. & Yu, K. H. Analysis of the human pancreatic stellate cell secreted proteome. *Pancreas* **40**, 557-566, doi:10.1097/MPA.0b013e318214efaf (2011).

80 Monard, D. SERPINE2/Protease Nexin-1 in vivo multiple functions: Does the puzzle make sense? *Seminars in cell & developmental biology*, doi:10.1016/j.semcdb.2016.08.012 (2016).

81 Buchholz, M. *et al.* SERPINE2 (protease nexin I) promotes extracellular matrix production and local invasion of pancreatic tumors in vivo. *Cancer research* **63**, 4945-4951 (2003).

82 Hagemann, T. L. *et al.* Gene expression analysis in mice with elevated glial fibrillary acidic protein and Rosenthal fibers reveals a stress response followed by glial activation and neuronal dysfunction. *Human molecular genetics* **14**, 2443-2458, doi:10.1093/hmg/ddi248 (2005).

83 Sato, N. *et al.* SPARC/osteonectin is a frequent target for aberrant methylation in pancreatic adenocarcinoma and a mediator of tumor-stromal interactions. *Oncogene* **22**, 5021-5030, doi:10.1038/sj.onc.1206807 (2003).

84 Pothula, S. P. *et al.* Key role of pancreatic stellate cells in pancreatic cancer. *Cancer Letters* **381**, 194-200, doi:http://dx.doi.org/10.1016/j.canlet.2015.10.035 (2016).

85 Vaz, J., Ansari, D., Sasor, A. & Andersson, R. SPARC: A Potential Prognostic and Therapeutic Target in Pancreatic Cancer. *Pancreas* **44**, 1024-1035, doi:10.1097/mpa.0000000000000409 (2015).

86 Aseer, K. R., Kim, S. W., Choi, M. S. & Yun, J. W. Opposite Expression of SPARC between the Liver and Pancreas in Streptozotocin-Induced Diabetic Rats. *PLoS One* **10**, e0131189, doi:10.1371/journal.pone.0131189 (2015).

87 Clarke, L. E. & Barres, B. A. Emerging roles of astrocytes in neural circuit development. *Nature reviews. Neuroscience* **14**, 311-321, doi:10.1038/nrn3484 (2013).

88 Jones, E. V. & Bouvier, D. S. Astrocyte-secreted matricellular proteins in CNS remodelling during development and disease. *Neural plasticity* **2014**, 321209, doi:10.1155/2014/321209 (2014).

89 Nivlet, L. *et al.* Expression and functional studies of the GDNF family receptor alpha 3 in the pancreas. *Journal of molecular endocrinology* **56**, 77-90, doi:10.1530/jme-15-0213 (2016).

90 Lawlor, N. *et al.* Single cell transcriptomes identify human islet cell signatures and reveal cell-type-specific expression changes in type 2 diabetes. *Genome Res*, doi:10.1101/gr.212720.116 (2016).

91 Chernousov, M. A., Stahl, R. C. & Carey, D. J. Tetraspanins are involved in Schwann cell-axon interaction. *Journal of neuroscience research* **91**, 1419-1428, doi:10.1002/jnr.23272 (2013).

92 Sasson, A. *et al.* Islet Pericytes Are Required for beta-Cell Maturity. *Diabetes* **65**, 3008-3014, doi:10.2337/db16-0365 (2016).

Appendix 1. Heart Perfusion, Sectioning and Staining of the Mouse Pancreas

Heart Perfusion:

Supplies Needed:

- Pan (to collect blood/PBS/PFA) with Styrofoam board wrapped in blue diaper
- Needles to pin arms/legs (recommend 26G3/8)
- Winged infusion set (Terumo REF SV*27EL; needle gauge is 27G1/2)
- Two 10 mL syringes (BD Luer-Lock 309604): label one for PBS and one for PFA
- Two 50 mL conical tubes: fill with cold PBS and cold 4% PFA

  To make PFA: Use a glass ampule of 16% PFA from Electron Microscopy Services 15710. Break glass ampule and empty all 10 mL into 50 mL falcon tube. Add PBS up to 40 mL and vortex. Keep on ice. Wear eye protection when breaking glass ampule and only work with open PFA in the chemical hood.
- Post-fix PFA tubes: add 30-40 mL 4% PFA to 50 mL falcon tubes (one falcon per mouse), on ice
- Isoflurane anesthesia equipment
- Surgical tools: Scissors, forceps (sharp and dull)
- Clean plastic petri dishes for dissecting
- 70% ethanol spray bottle

Procedure:

Day 1

1) Anesthetize mouse using isoflurane, transfer mouse to Styrofoam board and place nose inside isoflurane nose cone to maintain anesthesia during the procedure. Toe pinch test to make sure mouse is sufficiently anesthetized.

2) Pin mouse down and spray fur with 70% ethanol.
3) Open mouse (including diaphragm and rib cage to expose heart).
4) Cut the right atria of the heart with the super-sharp forceps.
5) Insert butterfly needle into the left ventricle. Butterfly needle should be connected to the PBS syringe (pre-filled with 10 mL PBS). Push all 10 mL PBS through the mouse.
6) Switch to the PFA syringe (prefilled with 10 mL PFA). Push all 10 mL PFA through mouse.
7) Remove pancreas with spleen still attached.
8) Add tissue to PFA post-fix tube. Leave in 4°C cold room overnight with gentle rotation on a rotisserie rotator (Barnstead Thermolyne Labquake Shaker/Rotisserie).

Day 2

9) **Wash tissue with PBS:** Transfer tissue to a new falcon tube filled with cold PBS. Change the PBS once an hour for 4 hours total. Perform washes in the cold room with gentle rotation.
10) **Sucrose protect:** Trim off fat, spleen, and separate into "head" and "tail" pancreas pieces (under dissecting scope; easier to fit adult mouse pancreas into two cyromolds if cut pancreas in half. "Head" refers to portion of pancreas that follows the stomach/duodenum/GI tract and "tail" refers to the portion of the pancreas closest to the spleen) and transfer to sucrose solution. Leave in sucrose solution in 4°C cold room with gentle rotation until tissue sinks (takes around 1 day).

    To make sucrose solution: Weigh 12g of sucrose and add to 50 mL conical. Add PBS to 40 mL. Dissolve.

Day 3

11) **Embed:** Remove pancreas from sucrose solution and rinse tissue in OCT (Tissue-Tek O.C.T Compound) using 3 prefilled cyromolds. Move the tissue from rinse-mold to rinse-

mold with forceps, gently swirling the tissue in the compound. Embed in square Peel-A-Way Disposable Plastic Tissue Embedding Molds 70182 filled two-thirds full with OCT; swirl tissue in OCT one final time and place tissue at the bottom on the mold. Freeze in acetone/dry ice bath. Store in plastic baggie in -80°C freezer to section later (or can section same day).

Sectioning:

Supplies Needed:

- Slides (Product: Fisherbrand Superfrost Plus Precleaned Microscope Slides)
- Blades (Product: Thermo Shandon MB35 Premier 35°/80mm microtome blades)
- Pencil to label slides
- Slide boxes
- Extra OCT to mount block on chuck and razor blade to remove block from chuck
- Cyrostat
- Paint brushes to smooth sections onto slide

Procedure:

1) **Remove blocks from -80°C freezer**: Put on dry ice to carry to the cryostat. Place blocks in cryostat, set the temp to the cutting range (see below), and let equilibrate for about a half hour before starting to section.
2) **Prepare chuck:** Attach block to chuck with a dime-sized blob of OCT on the chuck, add an extra seam of OCT around the base of the block (on the outside), and let OCT freeze/block attach firmly to the chuck for at least 5 minutes before starting to cut (not waiting long enough risks the block moving when cutting these thick sections). Trim off excess block OCT with a razor before starting to section.

3) **Cut:** Cut sections 20 uM thick (these are fairly thick sections to allow for preservation of pericyte, neural and glial cell processes). **Cutting temp range:** -11°C to -13°C (start with -12° C; can play with temperature a bit. If sections curl up or shatter: too cold. If sections wrinkle: too warm. Try block: -13°C and chamber: -12°C to start). I can fit about 3 sections per slide (without overlapping sections). I generally cut about ~20+ slides per block.
4) **Freeze:** Leave slides sit at room temp for ½ hour after finished cutting before storing in -80°C freezer.

Staining fixed-frozen sections of mouse pancreas:

1) **Warm and pap pen:** Remove slides from freezer and let slides warm to room temperature. Circle tissue with pap pen.
2) **Wash:** Wash the slides 3x with PBS, "quick washes": With slides lying flat, add ~1-2mL PBS per slide (DPBS, 1X without calcium and magnesium, Corning cellgro REF 21-031-CV). Aspirate liquid off of the slide using a vacuum tube fitted with a p200 non-filtered tip. These washes are "quick," meaning they last about the amount of time it takes to add the wash buffer to each slide and remove it.
3) **Fix:** Fix the slides with 4% PFA (freshly made up in PBS), 10 minutes: let sit at room temperature, on bench top.
4) **Wash:** Wash the slides 3x with PBS, 5 min per wash.
5) **Permeabilize:** 10 min in permeabilization buffer (0.5% Triton X-100 in PBS).

   For 10 mL of permeabilization buffer:

   50 uL of Triton X-100

   9.950 mL PBS (same PBS as described in step 2)
6) **Block:** Remove permeabilization buffer and block with blocking buffer (0.1% triton/5% goat serum in PBS) for 1 hour at room temperature in a humidified chamber (an opaque

shallow plastic tub with lid lined with damp paper towels. I add a pipet tip rack (that plastic insert in the tip box that holds the tips) on top of the paper towels to make a flat platform for the slides).

For 10 mL of blocking buffer:

10 uL of Triton X-100

500 uL goat serum (UCSF Cell Culture Facility (CCF): Invitrogen 16210-064, UCSF CCF Code INVZR118; aliquot in 15 mL falcon tube and freeze. Thaw out aliquots as needed; discard thawed aliquot after ~1 month)

9.490 mL PBS

7) **Primary antibody:** Remove blocking buffer and add ~300-400uL/per slide primary antibody made up in blocking buffer (make ~500 uL/per slide, can add any remaining 1° antibody buffer to slides). Place slides in closed humidity chamber in 4°C cold room on a level/flat shelf (check to make sure liquid is flat and evenly spread on slide), overnight.

1° Antibody Concentrations:

Mouse **NKX6.1** 1:100 (Product: DSHB F55A10-c)

Guinea Pig **Insulin** 1:500 (Product: DAKO A0564)

Guinea Pig **Glucagon** 1:2000 (Product: LINCO)

Chicken **GFP** 1:500 (Product: aves GFP-1020) (for eYFP or GFP reporter lines)

Rabbit **GFAP** 1:500 (Product: DAKO Ref Z0334)

Rabbit **NG2** 1:100 (Product: EMDMillipore AB5320)

Rabbit **TUJ1** 1:500 (BioLegend 845502)

Mouse **TUJ1** 1:700 (R&D Systems MAB1195-SP; stock reconstituted at 0.5 mg/mL in sterile PBS, used 1:700)

8) **Wash:** Remove primary antibody and wash 3x with PBS for 5 min per wash.

9) **Secondary Antibody:** Add ~300 uL secondary antibody to slides. We use the Life Technologies Alexa Fluor® secondaries in the correct species according to the primary antibody. All secondaries are used 1:200, made up in blocking buffer (make about 400uL/slide). Add Hoechst stain 1:1,000 for nuclear stain (Product: Life Technologies H3570). Leave at room temperature (on bench) in humidity chamber for 1 hour. Make sure no light gets into chamber.

    2° Antibody Product Information:

    Goat Anti-Chicken: Alexa Fluor® 488 (Invitrogen Catalog Number A11039)

    Donkey Anti-Mouse: 555 (A31570)

    Goat Anti-Mouse: 488 (A11029), 633 (A21052 and A21126)

    Goat Anti-Guinea pig: 546 (A11074), 633 (A21105)

    Goat Anti-Rabbit: 488 (A11034), 633 (A21072)

    Donkey Anti-Rabbit: 488 (A21026)

10) **Wash:** Wash the slides 3x with PBS, 5 min per wash.

11) **Coverslip:** Remove last wash and add Thermo Fisher Scientific ProLong Gold Antifade Reagent (Product: Thermo Fisher Scientific P36934). Need about 3 drops ProLong Gold per slide (less is better for imaging but adding too little can generate air bubbles). Add cover slip (Product: FisherFinest Premium Cover Glass 12-548-5M 24 x 50-1) and place slide flat (don't tip vertical yet) in slide box to **cure** for 24 hours at room temperature. After "curing" period, slides can be stored in 4°C refrigerator.

12) **Image:** Image slides on confocal.

Appendix 2. Staining Whole Islets

1) **Collect islets in microcentrifuge tube:** For moving islets from one location to another, removing liquid from islet-containing tubes, and other instances where the islets may

come in contact with the pipet tip, I recommend to using the Rainin low-retention tips (P200: Rainin Catalog Number 17007959 and P1000: 17007953) to prevent islet loss due to plastic adhesion. To start the staining process, add islets to siliconized 1.5 mL low-retention microcentrifuge tubes (Fisherbrand 02-681-320). Gently spin down (1000 rpm, 1 minute) the islets and remove media. To remove media, I recommend pipetting out as much liquid as possible without disrupting the islet pellet at the bottom of the tube or aspirating up any islets in the pipet tip (visually check the tip by eye). (*Optional step*: wash with 1 mL PBS, gently spin down and remove wash. This step may result in the loss of islets so proceed with caution/step can be skipped)

2) **Fix:** add 1 mL of freshly made 4% PFA to each 1.5 mL tube of islets. Place tubes in the 4°C cold room on a rotisserie rotator (Barnstead Thermolyne Labquake Shaker/Rotisserie), overnight. See “Supplies needed” section for heart perfusion in Appendix 1 for 4% PFA preparations.
3) **Wash:** Remove islets from cold room, gently spin down and remove PFA as described in Step 1. Wash islets with PBS with ~0.2% goat serum 3x, 5 minutes per wash. Place on a bench top rotisserie rotator (at room temperature) for each wash. **Useful tip:** Adding small amount of goat serum to PBS will dramatically reduce islet sticking to plastic tubes and tips.
4) **Permeabilization:** Spin down, remove last wash and permeabilize with 0.5% TritonX 100 in PBS for 30 minutes at room temperature on rotisserie rotator. Add 1 mL of permeabilization buffer to each tube of islets.

    <u>For 10 mL of permeabilization buffer:</u>

    50 uL of Triton X-100

    9.950 mL PBS

5) **Block:** Spin down, remove permeabilization buffer, and block with 0.1% TritonX100 and 1% goat serum for 1 hour at room temperature on rotisserie rotator. Add 1 mL of blocking buffer to each tube of islets.

   For 14 mL of blocking buffer:

   14 uL of triton X-100

   140 uL goat serum

   13.846 mL PBS

6) **Primary antibody:** Spin down, remove blocking buffer and add 1 mL of 1° antibody buffer per tube of islets. Let tubes rotate in cold room for 48 hours (long incubation to increase antibody penetration of large, whole islets. Insulin is especially difficult to achieve penetration through whole islet). 1° and 2° antibodies made up in blocking buffer from Step 5. Use 1° antibody concentrations listed in my Appendix 1 section for staining fixed-frozen pancreas sections with the exception of insulin. For guinea pig insulin, use at 1:200.

7) **Wash:** Remove islets from cold room, spin down and remove 1° antibody. Add 1 mL of wash buffer per tube of islets and wash for 5 minutes (on rotisserie rotator, either in cold room or at room temperature). Spin, remove wash and add fresh wash buffer. Place in cold room rotisserie rotator for 1 hour and then repeat this 1 hour wash once more (total of 2x, 1 hour washes). Remove wash buffer, add fresh wash buffer and place back in cold room rotisserie rotator for around 22 hours (24 hour total wash time).

   For 20 mL of wash buffer:

   20 uL of TritonX 100

   19.980 mL of PBS

8) **Secondary antibody:** Remove islets from cold room, spin down, and remove wash buffer. Add 1 mL of 2° antibody per tube of islets and cover tube with foil to block all

light. Let tubes rotate in cold room for 24 hours. Use the Life Technologies Alexa Fluor® secondaries at 1:200 (see staining fixed-frozen pancreas sections protocol for Alexa Fluor product information) and add Hoechst stain 1:1,000 for nuclear stain (Product: Life Technologies H3570).

9) **Wash:** Remove islets from cold room, spin down and remove 2° antibody. Repeat wash steps of Step 7 except this time, wrap tubes in foil to protect from light. (Recap of Step 7: 1x 5 minute wash, 2x 1 hour washes, 22 hours more in cold room for a total of 24 hour total wash time).

10) **Mount islets on slides:** Remove islets from cold room, spin down, and remove wash buffer. Add 1 mL of fresh PBS to each islet tube. Gently spin down to pellet all islets at the bottom of the tube and remove all but around 50 uL of PBS. Resuspend islets in this PBS and pipet this islet-PBS mixture out onto a glass slide (Product: Fisherbrand Superfrost Plus Precleaned Microscope Slides). Islets will stick to slide, allowing PBS to be carefully pippeted off, leaving islets behind. Wash microcentifuge tube out with another ~50 uL of PBS to recover any remaining islets and pipet out onto another slide. Remove PBS from second slide. Make sure no islets are remaining in tube (they may stick to the tube sides and lid). Add Thermo Scientific ProLong Gold Antifade Reagent (Product: P36934). Need about 3 drops ProLong Gold per slide (less is better for imaging but adding too little can generate air bubbles). Add cover slip (Product: FisherFinest Premium Cover Glass 12-548-5M 24 x 50-1) and place slide flat (don't tip vertical yet) in slide box to cure for 24 hours at room temperature. After "curing" period, slides can be stored in 4°C refrigerator.

    Alternative mounting method for islet clearing: Instead of adding ProLong Gold, pipet a small quantity of SunJin Lab RapiClear® clearing agent (courtesy of Tong Tang, see acknowledgements) on top of islets. Cover slip and add nail polish around coverslip

perimeter to prevent slide from drying out. Let incubate at room temperature in the dark for 24 hours. Can also use 250 uM SunJin Lab iSpacer® (an adhesive border that is placed on the slide before adding islets) to maintain islet shape during cover slipping. Attach coverslip on top of iSpacer® with nail polish. Note: the RapidClear® clearing agent kills Hoechst stain. Propidium iodide (PI) can be used in its place.

11) **Image:** Image whole islets through entire z-stack on confocal.

Tables

Table 1. Genotyping primers

Mouse Line	Primer Sequence 5'->3'	Expected Band Sizes
GFAP-GFP and R26R eYFP	GAC GTA AAC GGC CAC AAG TT GGT CTT GTA GTT GCC GTC GT	GFP: 260 bp (presence or absence)
GFAP-cre	ACT CCT TCA TAA AGC CCT ATC ACT CGT TGC ATC GAC CG	Cre: 190 bp WT: 700 bp Het: both bands
Wnt1-cre	CTG GTG TAG CTG ATG ATC CG ATG GCT AAT CGC CAT CTT CC	Cre: ~350 bp (presence or absence)
mTmG	CTC TGC TGC CTC CTG GCT TCT CGA GGC GGA TCA CAA GCA ATA TCA ATG GGC GGG GGT CGT T	mTmG: 250 bp WT: 330 bp Het: both bands
iDTR	GCG AAG AGT TTG TCC TCA ACC AAA GTC GCT CTG AGT TGT TAT GGA GCG GGA GAA ATG GAT ATG	iDTR: 340 bp WT: 650 bp Het: both bands

Table 2. Genotyping PCR programs

GFAP-GFP and R26R eYFP	**Temp (c)**	**Time (s)**
Step 1	94	120
Step 2	94	30
Step 3	58	30
Step 4	72	45
Step 5	*Go to 2, 34x*	
Step 6	72	300
GFAP-cre	**Temp (c)**	**Time (s)**
Step 1	94	180
Step 2	94	30
Step 3	51	60
Step 4	72	60
Step 5	*Go to 2, 35x*	
Step 6	72	120
mTmG	**Temp (c)**	**Time (s)**
Step 1	95	180
Step 2	95	30
Step 3	61	60
Step 4	72	60
Step 5	*Go to 2, 35x*	
Step 6	72	600
Wnt1-cre	**Temp (c)**	**Time (s)**
Step 1	95	180
Step 2	95	30
Step 3	62	60
Step 4	72	60
Step 5	*Go to 2, 35x*	
Step 6	72	300
iDTR	**Temp (c)**	**Time (s)**
Step 1	94	120
Step 2	94	20
Step 3	65 (-0.5 C per cycle)	15
Step 4	68	10
Step 5	*Go to 2, 10x*	
Step 6	94	15
Step 7	60	15
Step 8	72	10
Step 9	*Got to 6, 28x*	
Step 10	72	120

Table 3. Drop-seq primers

Primer Name	Sequence 5'->3'
Template Switch Oligo (TSO)	AAGCAGTGGTATCAACGCAGAGTGAATrGrGrG
Smart PCR primer	AAGCAGTGGTATCAACGCAGAGT
New-P5-SMART PCR hybrid oligo	AATGATACGGCGACCACCGAGATCTACACGCCTG TCCGCGGAAGCAGTGGTATCAACGCAGAGT*A*C
Custom Read 1 primer	GCCTGTCCGCGGAAGCAGTGGTATCAACGCAG AGTAC

Notes: r indicates RNA base; * indicates phosphorothioate bond; Custom Read 1 primer is HPLC purified

Table 4. Drop-seq PCR programs

PCR Program:	**v3.1**	**A**	**B**	**C**	**D**	**E**	**F**	**G**	**H**	**I**	**J**
Total Number of Cycles	*13c*	*15c*	*17c*	*19c*	*19c*	*20c*	*21c*	*22c*	*23c*	*25c*	*26c*
		95C for 180 s									
X Number of Cycles of: 98 C 20 s 65 C 45 s 72 C 180 s	4	5	6	7	8	8	8	8	8	8	8
X Number of Cycles of: 98 C 20 s 67 C 20 s 72 C 180 s	9	10	11	12	11	12	13	14	15	17	18
		72 C 300 s									
		4 C Forever									

Table 5. Wnt1-cre/mTmG dissociated islets FACS numbers

Experiment	Number of eGFP+ cells/mouse	Number of tdTomato cells/mouse
Sorting Pilot	1,051	Excess of 125,000
Drop-seq for HiSeq	1,063	Excess of 50,000

Table 6. Top expressed genes based on total transcript number in Drop-seq MiniSeq pilot and Drop-seq HiSeq experiment

MiniSeq	HiSeq
mt-Rnr2	mt-Rnr2
Gcg	Gcg
Ins2	Ins2
Malat1	Malat1
Ppy	Ppy
Ins1	Pyy
Pyy	Ins1
mt-Rnr1	Ttr
Ttr	Sst
Iapp	Iapp
Chga	Chga
Meg3	Meg3
Gm26924	TAOK1
mt-Cytb	mt-Cytb
mt-Nd2	Pcsk2
mt-Nd5	Gnas
Pcsk2	Chgb
Scg2	mt-Nd1
mt-Nd1	Scg2
Gnas	mt-Rnr1
mt-Nd4	mt-Nd2
Hsp90b1	Hsp90ab1
Peg3	Resp18
Hsp90ab1	mt-Nd5
Chgb	mt-Nd4
Resp18	Hsp90b1
Golgb1	Cst3
Cpe	Cpe
Atrx	Peg3
mt-Co1	mt-Co1
Pcsk1n	Rpl41
Golga4	Pcsk1n
Cst3	Scg5
Scg3	Rbm25
Calm1	Rps24

Note: MiniSeq data is from the top 400 cells in the “high” cell concentration (150 cells/uL) sample only for the purposes of this comparison.

Table 7. Top glial expressed genes in Drop-seq HiSeq experiment using Wnt1-cre/mTmG islets

Gene	Mean Glial Cell Expression	Mean Control Cell Expression	Ratio Glial/Control Expression	Number of Glial Cells Expressing Gene
S100b	6.998	0	#DIV/0!	6
EGFP	5.023	0	#DIV/0!	7
Fabp7	4.342	0	#DIV/0!	5
Sema3b	3.800	0	#DIV/0!	7
Mal	3.254	0	#DIV/0!	7
Art3	3.093	0	#DIV/0!	6
Fam129a	2.545	0	#DIV/0!	5
Sostdc1	2.318	0	#DIV/0!	5
Kcna6	2.287	0	#DIV/0!	4
Gfra2	2.028	0	#DIV/0!	6
Cyp2j9	1.775	0	#DIV/0!	5
Cmtm5	1.669	0	#DIV/0!	4
Lrrc4c	1.425	0	#DIV/0!	6
Gm12688	1.398	0	#DIV/0!	4
Gpr37l1	1.380	0	#DIV/0!	4
Synm	1.312	0	#DIV/0!	4
Sox10	1.302	0	#DIV/0!	5
Pdzd2	1.008	0	#DIV/0!	4
Gfap	0.995	0	#DIV/0!	4
Apoe	50.027	0.227	220.1	7
Plp1	39.156	0.267	146.5	7
Sparc	34.361	0.460	74.7	7
Timp3	28.229	0.323	87.3	7
Scn7a	24.476	0.074	329.2	7
Prnp	20.904	0.690	30.3	7
Sfrp1	17.723	0.046	387.4	6
Apod	17.416	0.054	323.6	6
B2m	16.611	0.782	21.3	7
Marcks	16.542	0.800	20.7	7
Kcna1	13.329	0.038	354.1	7
Cd59a	12.711	0.105	121.3	7
Vim	12.132	0.204	59.6	7
Dbi	9.931	0.287	34.6	7
Col28a1	9.651	0.022	444.1	6
Atp1a2	8.789	0.065	136.1	7
Cd9	8.684	0.043	201.7	6

Gene *(Table 7 Continued)*	Mean Glial Cell Expression	Mean Control Cell Expression	Ratio Glial/Control Expression	Number of Glial Cells Expressing Gene
Zeb2	7.448	0.098	76.0	6
Scd2	7.092	0.214	33.1	7
Iqgap2	7.079	0.140	50.6	7
Abca8a	6.844	0.067	102.1	6
Rarres2	6.717	0.056	119.5	6
Serpine2	6.376	0.153	41.6	6
Ptn	6.297	0.098	64.6	7
C4b	6.246	0.036	172.7	4
Lgi4	6.137	0.074	82.9	7
Plce1	6.011	0.061	98.0	7
Ttyh1	5.877	0.037	157.4	7
Ifi27l2a	5.812	0.078	75.0	4
Gbp2	5.775	0.034	169.8	5
Ahnak	5.617	0.213	26.3	7
Arpc1b	5.535	0.247	22.4	6
Pmepa1	5.447	0.041	133.2	5
Fxyd1	5.368	0.047	114.6	7
Gbp7	5.199	0.252	20.6	5
Chl1	5.070	0.040	125.9	6
Matn2	4.838	0.042	115.4	5
Clic4	4.556	0.140	32.6	6
Gatm	4.477	0.119	37.5	7
Cryab	4.406	0.031	140.9	7
Ifitm3	4.233	0.074	57.3	4
Col18a1	4.168	0.027	153.1	6
Col14a1	4.024	0.023	178.7	6
Cnn3	3.989	0.131	30.5	4
Ctgf	3.872	0.033	118.2	5
Olfml2a	3.865	0.004	865.5	6
Nnat	3.757	0.089	42.4	4
Col5a3	3.588	0.035	103.3	7
Col16a1	3.558	0.032	111.5	6
Abca8b	3.534	0.045	78.0	6
Entpd2	3.445	0.037	92.5	6
Col3a1	3.341	0.151	22.1	4
Fgl2	3.267	0.102	31.9	6
Cadm2	3.210	0.019	165.4	6
Hand2	3.193	0.051	62.1	6
L1cam	3.084	0.008	392.7	5
Rnd3	3.073	0.079	38.7	6

Gene *(Table 7 Continued)*	Mean Glial Cell Expression	Mean Control Cell Expression	Ratio Glial/Control Expression	Number of Glial Cells Expressing Gene
Lpar1	3.052	0.017	174.4	6
Akap12	2.842	0.075	37.9	5
S100a4	2.804	0.067	41.9	4
Adam23	2.788	0.048	58.6	6
Gas7	2.786	0.008	350.5	6
Pmp22	2.721	0.040	67.5	4
Nid1	2.710	0.032	84.4	5
Fbln5	2.676	0.019	140.9	5
Qk	2.669	0.114	23.4	4
Nrn1	2.635	0.005	582.9	4
Serpinh1	2.623	0.116	22.5	6
Hmgcs2	2.587	0.027	95.0	5
Mettl7a1	2.465	0.123	20.0	4
Gpm6b	2.454	0.038	64.2	6
Slc35f1	2.451	0.080	30.5	4
Parp9	2.332	0.105	22.1	4
Cdh19	2.296	0.005	501.2	4
Agrn	2.277	0.062	36.4	4
Mcam	2.273	0.101	22.5	4
Syn3	2.264	0.020	110.7	5
Aspa	2.220	0.014	159.7	5
Prex2	2.170	0.025	85.9	4
Adam11	2.137	0.004	540.1	6
Tmprss5	2.091	0.008	249.6	5
Tns1	2.036	0.030	67.7	4
Endod1	1.888	0.061	30.9	4
Calu	1.853	0.085	21.8	5
Casp12	1.847	0.004	413.6	4
Fads1	1.817	0.061	29.8	4
Gfra3	1.804	0.034	52.5	5
Cadm4	1.802	0.004	431.6	4
Lmo4	1.775	0.042	41.9	4
Sorbs1	1.673	0.020	81.6	4
Csrp1	1.595	0.027	58.8	5
Nkain4	1.576	0.007	223.7	4
Lamb1	1.528	0.040	38.4	5
Olfml2b	1.498	0.019	80.7	4
Lamb2	1.493	0.035	42.8	5
Col20a1	1.469	0.039	37.3	4
Htra1	1.444	0.041	35.6	4

Gene *(Table 7 Continued)*	Mean Glial Cell Expression	Mean Control Cell Expression	Ratio Glial/Control Expression	Number of Glial Cells Expressing Gene
Ptprs	1.434	0.037	38.7	5
Tgfb2	1.355	0.005	262.1	4
Fbln2	1.344	0.063	21.4	4
Mrpl18	1.301	0.049	26.3	4
Vgll4	1.299	0.024	53.3	5
Emp1	1.275	0.025	51.7	5
Slc1a5	1.266	0.042	29.8	4
Gpx8	1.202	0.022	53.8	4
Shc4	1.191	0.017	69.0	5
Cyp2j6	1.175	0.047	25.0	4
Rftn2	1.167	0.007	165.6	4
Lrrtm1	1.116	0.016	69.3	4
Ptprz1	1.108	0.023	48.2	4
Fabp5	1.006	0.009	115.9	4
Msn	0.995	0.049	20.3	4
Pik3ip1	0.981	0.028	35.6	4
Zfp536	0.936	0.015	63.9	4
Mmp14	0.917	0.030	30.1	4
Edil3	0.898	0.010	87.4	4
Lgmn	0.893	0.041	21.8	4
Sdc3	0.804	0.016	49.4	4
Srcin1	0.793	0.004	184.3	4

Notes: Glial and control cell expression was normalized on a per cell basis by dividing the unique transcript count for particular gene by the total number of transcripts in the cell. Mean glial cell expression was calculated by averaging the expression of all 7 glial cells; mean control cell expression was calculated with 168 control cells that lacked GFAP and/or GFP. Mean cell expression numbers were multiplied by 5000 as a last step; multiplying all average expression numbers by 5000 transforms the numbers into a number between 0-100 for easier reading in this table.

Table 8. Expression of glial-associated genes in potential glial cell from Drop-seq MiniSeq pilot

Gene	Cell Expression
Apoe	82.186
Sparc	55.531
Prnp	42.203
Plp1	39.982
Timp3	33.319
Ifi27l2a	22.212
Sfrp1	19.991
Kcna1	15.549
Vim	15.549
Iqgap2	15.549
Abca8b	15.549
Chl1	13.327
Synm	11.106
Scn7a	11.106
B2m	11.106
Dbi	11.106
Pmepa1	11.106
Cryab	11.106
Lpar1	11.106
Marcks	8.885
Slc35f1	8.885
Sostdc1	6.664
Lrrc4c	6.664
Apod	6.664
Cd59a	6.664
Zeb2	6.664
Scd2	6.664
Abca8a	6.664
Ttyh1	6.664
Fxyd1	6.664
Matn2	6.664
Col16a1	6.664
Lmo4	6.664
Msn	6.664

Figures

Figure Legends:

Figure 1. Endocrine and non-endocrine cells of the pancreatic islet

Overview of the endocrine cells (greyscale) and non-endocrine cells (color) of the pancreatic islet.

Figure 2. General appearance of GFAP+ islet glial cells

A. Immunofluorescence images of fixed frozen sections of pancreases from ~1 year old wild-type mice stained for GFAP (green) and insulin (red). Sections are 20 μM thick. **B.** Sections from the same pancreases as in A but stained for glucagon (blue), in addition to GFAP. Arrows in **i** point to GFAP processes surrounding glucagon-producing alpha cells, as also highlighted by the white oval in **ii.** Both A and B were imaged on an upright fluorescent scope, the Zeiss AxioImager Z1, in a single z plane. **C.** Islets isolated from 11.5 week old CD-1 mice and fixed with 4% PFA. Whole islets were stained with GFAP (green) and insulin (red) and were imaged on a confocal microscope. Z-stacks were set at the start and end of detectable fluorescence signal. Islet in **i** is shown as a maximum projection while a single z-plane is shown of the islets in **ii**. **D.** Islets isolated from a deceased, adult male human donor. Islets were fixed and stained for GFAP (green), insulin (red, as shown in **i**), and DNA (grey, as shown in **ii-vi**). Islets are shown as projected z-stacks of 10-30 layers (human islets only). All scale bars represent 100 μM.

Figure 3. Method development for studying pancreatic islet glial cells

A. Islets were mounted using ProLong Gold Antifade Reagent as standard practice (**ii**). However, using SunJin Lab RapiClear® clearing agent (**i** with zoomed inset for comparison with **ii**) allowed for improved visualization of fainter GFAP+ processes (red), as well as improved ability to image through the middle portions of the whole islet without loss of signal. Example

islets shown here were from fixed, isolated islets from 10-15 week old mice and shown as maximum projections. **B-D.** To assess whether the time of collagenase digestion during islet isolation effected the quality or amount of retained GFAP+ islet glial cells, 8 (**B**), 10 (**C**) and 12 (**D**) minute digestions were tested as shorter time periods than the standard 16 minute digestion. Islets were isolated from 7-8 week old wild-type C57BL/6J mice. Islets are shown as maximum projections with GFAP (green), insulin (red), and DNA (blue). All scale bars represent 100 μM.

Figure 4. Lineage tracing of GFAP+ islet glial cells

A-C. Fixed frozen sections of pancreases from 7-8 week old Wnt1-cre/mTmG mice. Sections were stained with GFP (green) and GFAP (red). The first image in each lettered row shows the merged image. **D.** Fixed frozen section from a 7-8 week old Wnt1-cre/R26R eYFP mouse stained with GFP (green) and GFAP (red). All images are maximum projections of the 20 μM thick sections and all scale bars represent 100 μM.

Figure 5. Lineage tracing of GFAP+ islet glial cells: individual nucleated cells

A. Zooming in on one GFAP+ glial cell in the Wnt1-cre/mTmG pancreas sections as described in Figure 4A-C. Section was stained with GFP (green), GFAP (shown here in blue), and Nkx6.1 (red; Nkx6.1 was imaged in a channel that also imaged tdTomato). **B.** Zooming in on nucleated GFAP+ glial cells in a section of Wnt1-cre/R26R eYFP pancreas as described in Figure 4D. GFAP is shown in red, DNA in grey, and GFP in green. White ovals highlight clearly nucleated, GFP+ cells that also stain for GFAP. All images maximum projections and all scale bars represent 25 μM.

Figure 6. Islet pericytes are not neural crest cell derived

Fixed frozen pancreas section, 20 μM thick, from a 7-8 week old mTmG mouse. The section was stained with NG2, a pericyte proteoglycan (red), and GFP (green). All images maximum projections and scale bar represents 100 μM.

Figure 7. Assessing using a GFAP-cre mouse line to study islet glial cells

A-D. Fixed frozen pancreas sections from male, 12-13 week-old GFAP-cre/R26R eYFP mice. Sections were stained for GFP (green) and GFAP (red). Merged images are shown on the far right in each letter row. A and B are images of islets while C is an image of the acinar area of the pancreas. Arrowhead in B points to a GFAP+ glial cell that also stained for GFP; arrow points to GFP+ cell that does not stain for GFP. **D.** Sections from the same pancreases as described in A-D but stained with GFP (green) and pericyte marker NG2 (red). All images are maximum projections of the 20 μM thick sections and all scale bars represent 100 μM.

Figure 8. Assessing using a GFAP-cre mouse line to study islet glial cells: vessel/duct close-up

A close-up of vessel/ducts from the GFAP-cre/R26R eYFP pancreas sections described in Figure 7A-D. GFP in green and GFAP in red. Image taken on an upright fluorescent scope, the Zeiss AxioImager Z1, in a single z plane at 20x magnification.

Figure 9. Proof of concept for ex vivo diphtheria toxin ablation in cultured isolated islets

A. Islets from female, 13-14 week old GFAP-cre/iDTR mice (**i-ii**) and GFAP-cre-negative/iDTR (**iii**) littermates were cultured for 72 hours in Matrigel® droplets with media without diphtheria toxin. **B.** Islet from GFAP-cre-negative/iDTR mouse cultured for 72 hours in Matrigel® droplet in media containing 100 ng/mL diphtheria toxin. Media with and without diphtheria toxin was

replaced every 24 hours. At the end of culture, islets were removed from Matrigel®, fixed, and stained for GFAP (green) and beta cell marker Nkx6.1 (red). All images are maximum projections and all scale bars represent 100 μM.

Figure 10. Assessing using a GFAP-GFP mouse line to study islet glial cells

A. Isolated islets from 10-11 week old GFAP-GFP mice were cultured in 50% Matrigel® droplets for 72 hours. Live islets were checked on a tissue culture fluorescent microscope every 24 hours. The 24 hour time point live brightfield (left) and GFP channel (right) images are shown in single z-planes. **B.** At the end of the culture period, islets were removed from Matrigel®, fixed, and stained for GFP (green) and GFAP (red). The stained islet is shown as a maximum projection. All scale bars represent 100 μM.

Figure 11. Assessing using TUJ1 as a pan-neuronal marker in pancreatic islets

A-C. Fixed frozen section of pancreases from 7-8 week old Wnt1-cre/R26R eYFP mice stained for GFP (green), TUJ1 (red), insulin (blue), and DNA (grey). TUJ1 stains for the neuron-specific class III β-tubulin and serves as a pan-neuronal marker. A is a single z-plane, while B and C are maximum projections. A confirms that these nucleated TUJ1+ cells are of neural crest cell lineage, as reiterated in C. B shows that these nucleated TUJ1+ cells are insulin negative. **D-F.** Fixed and stained isolated islets from 12-13 week old wild-type C57BL/6J mice were stained for TUJ1 (green), DNA (grey), and beta cell marker Nkx6.1 (blue). Islets **i** and **ii** in D are shown as maximum projections. Islet in E is shown as a single z-plane. The islet in F is shown as a maximum projection while the small inset in the white box shows the single z-plane to allow for visualization of the nuclei of the TUJ1+ cells in the attached peri-islet ganglia. All scale bars represent 100 μM.

Figure 12. TUJ1+ neurons and GFAP+ glial cells are in close contact in isolated islets

A. A close-up image of TUJ1+ cells in an isolated islet from 13-14 week old wild-type mouse stained for TUJ1 (green), GFAP (red), and DNA (grey), showing the close association between TUJ1+ neurons and GFAP+ glial cells. The arrows in the right-most image in A highlights GFAP+ cells that in very tight association with TUJ1+ cells (see left and middle images). **B.** More isolated islets stained for TUJ1 (green), GFAP (red), and DNA (grey), showing GFAP+ processes surrounding and following TUJ1+ cells bodies and processes. Islet **i** was isolated from a 13-14 week old wild-type mouse and islets **ii** and **iii** are a close-up images of the cleared, isolated islets from 12 week old wild-type C57BL/6J mice as shown in their entirety in Figure 13 viii and i, respectively. All islets in Figure 12 are shown as single z-planes and all scale bars represent 25 μM.

Figure 13. TUJ1+ neurons survive in isolated islet culture

Islets were isolated from 12 week old wild-type C57BL/6J mice and either fixed immediately (Time 0 h) or cultured for 72 hours in suspension culture with daily media and plate changes to assess the survival of TUJ1+ neurons in culture as compared to GFAP+ glial cells. Islets were stained for TUJ1 (green), GFAP (red), and insulin (blue). **A.** Islets **i-vii** are seven different islets at Time 0 h. **B.** Islets **i-iv** are four representative islets at Time 72 h. All islets besides B iv are shown as maximum projections. Islet B iv is shown as a single z-plane to allow for visualization of TUJ1+ processes in areas of the islet with minimal-to-no GFAP+ processes after 72 hours in culture. All scale bars represent 100 μM.

Figure 14. Retained TUJ1+ neurons generally match GFAP+ glial cell numbers in isolated islets

A-B. Isolated islets from the same experiment and time point as Figure 13B. Islets were cultured for 72 hours, fixed and stained for TUJ1 (green), GFAP (red), and insulin (blue). While TUJ1+ neurons may send out more processes in response to islet isolation and culture as compared to GFAP+ processes (as seen in Figure 13), the general number of retained TUJ1+ and GFAP+ cells are in roughly equal proportion to one another, ranging from dense TUJ1+ and GFAP+ patches (as seen in **i**) to less dense (**ii** to **iii**). Islets in A are shown as maximum projections. B. Islets **i** and **ii** are single z-planes and only contain a few neurons and glial cells. All scale bars represent 100 μM.

Figure 15. Outgrowth from adhesion cultured islets

A. Isolated islets from a Wnt1-cre/R26R eYFP mouse were grown on Permanox® plastic chamber slides for 5 days to allow islets to adhere and cells to grow out from the adhered islets. Slides were fixed with 4% PFA and stained for GFP (green), GFAP (red), and DNA (grey). The approximate number of outgrown cells that stained for GFP (indicative of being from neural crest cell lineage) ranged from only a few cells to nearly all outgrown cells, as shown by these three representative islets **i-iii**. **B.** GFAP (red) staining of islet ii in A, shown with exposure from A (left image) and with enhanced brightness and contrast (right image) to increase visualization of outgrown cells on the plastic slide.

Figure 16. Wnt1-cre/mTmG FACS Pilot and Drop-seq Pilot Sort

A. FACS plot from pooled, dissociated islets from four 4-5-month-old, mixed-sex Wnt1-cre/mTmG mice (three males and one female) and **B.** FACS plot from mTmG negative control mouse lacking Wnt1-cre. **C.** FACS plot from pooled, dissociated islets from three 13 week old male mice lacking any fluorescent protein expression (essentially wild-type mice). FACS

process was used to exclude doublets and cellular debris to generate single cells to practice Drop-seq droplet making and to generate two concentrations of cells: a high cell concentration at 225,000 cells/1.5 mL (150 cells/uL) and low cell concentration at 49,571 cells/1.5 mL (33 cells/uL).

Figure 17. Wnt1-cre/mTmG FACS for HiSeq Drop-seq

FACS plot from pooled, dissociated islets from four ~6 month old, mixed-sex Wnt1-cre/mTmG mice (three females and one male). Cells were sorted to exclude doublets and cellular debris and then sorted for FITC-high/dsRed-low cells (i.e. GFP-high/tdTomato-low cells; containing glial cells) and FITC-low/dsRed-high cells (i.e. GFP-low/tdTomato-high cells; control cells containing non-endocrine and endocrine cells types from non-neural crest cell lineages). A total of 204,251 cells were collected and brought up to 1.5mL with a HBSS/BSA solution (136 cells/uL) for Drop-seq droplet making. Only 4,251 of the collected cells (~2.1%) were GFP-high/tdTomato-low cells.

Figure 18. Heat map from Drop-seq gene expression data

A heat map of the HiSeq gene expression data from Wnt1-cre/mTmG Drop-seq experiment. Heat map was made using a subset of the 338 sequenced cells with over 1000 transcripts; 74 cells and 567 genes are shown here for visual clarity. Gene names are listed vertically and cell identification numbers are listed at the bottom. The right most 7 cells cluster together with glial cell markers and have the following identification numbers from right to left: 2.056, 1.087, 1.115, 1.058, 1.086, 1.076, and 1.065. Beta cells cluster on the far left, followed by delta cells (expressing Sst, somatostatin), PP cells (expressing Ppy, pancreatic polypeptide), and alpha cells (expressing Gcg, glucagon), moving left to right. Color scale: Red to blue through white.

Figure 19. Gene ontology and pathway analysis of Drop-seq gene expression data

Gene ontology and pathway analysis graphic created using the data from the HiSeq gene expression data from Wnt1-cre/mTmG Drop-seq experiment and the Max Planck Institute for Molecular Genetics' ConsensusPathDB-mouse online software program (http://cpdb.molgen.mpg.de/MCPDB). Analysis was run on the relative gene expression of the 7 identified glial cells from the clustering (see Figure 18) compared to 178 GFP-negative control cells.

Figure 1. Endocrine and non-endocrine cells of the pancreatic islet

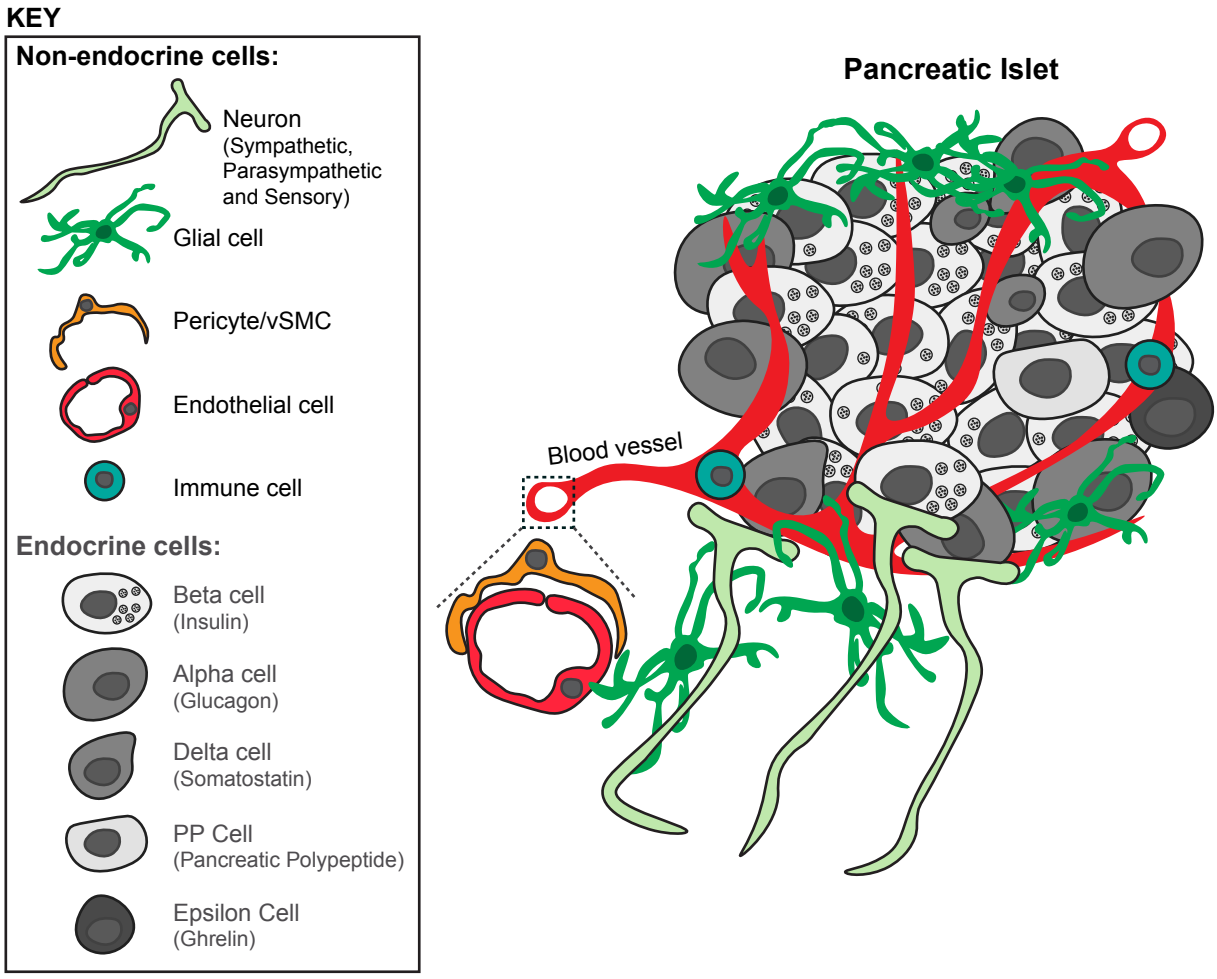

Figure 2. General appearance of GFAP+ islet glial cells

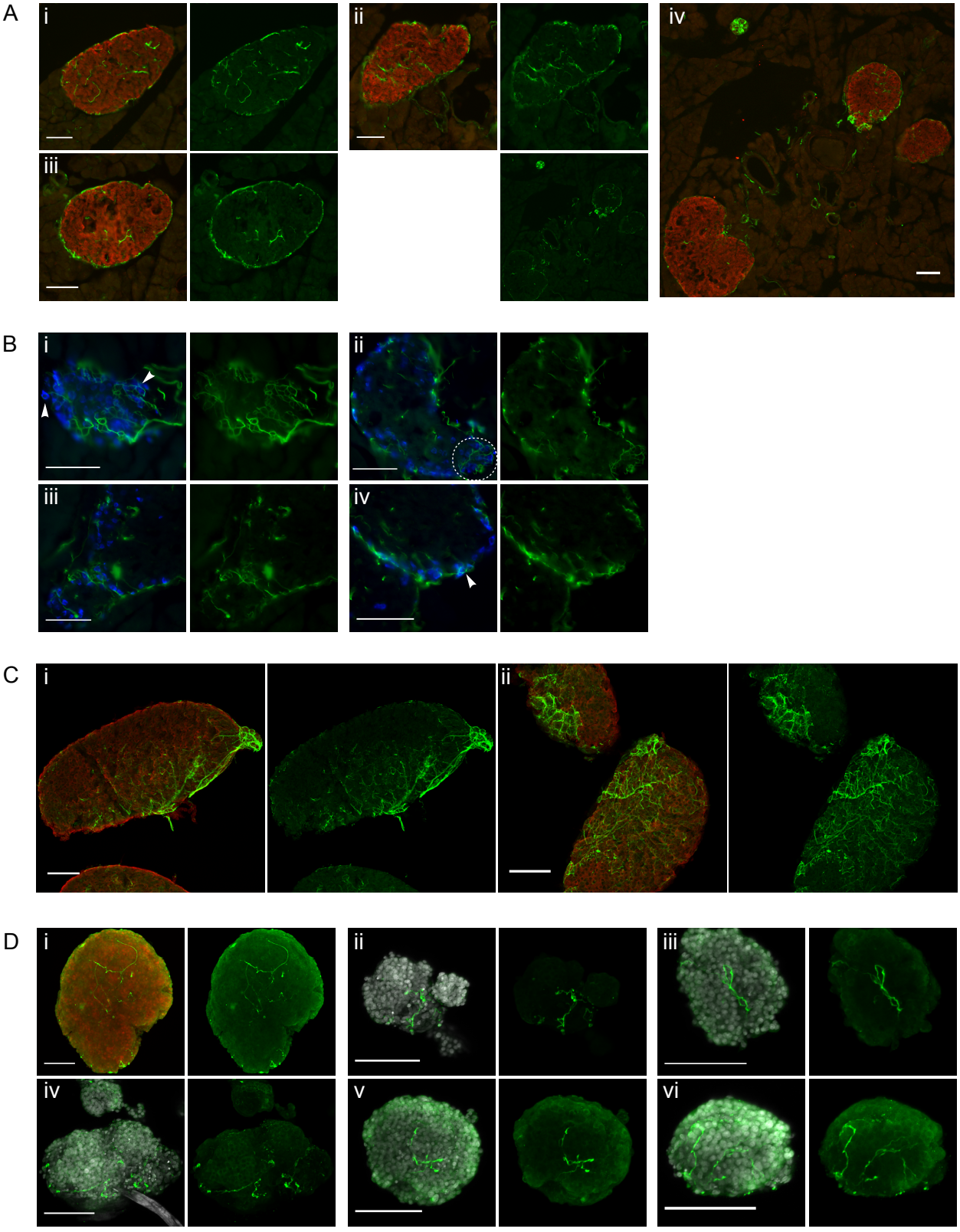

Figure 3. Method development for studying pancreatic islet glial cells

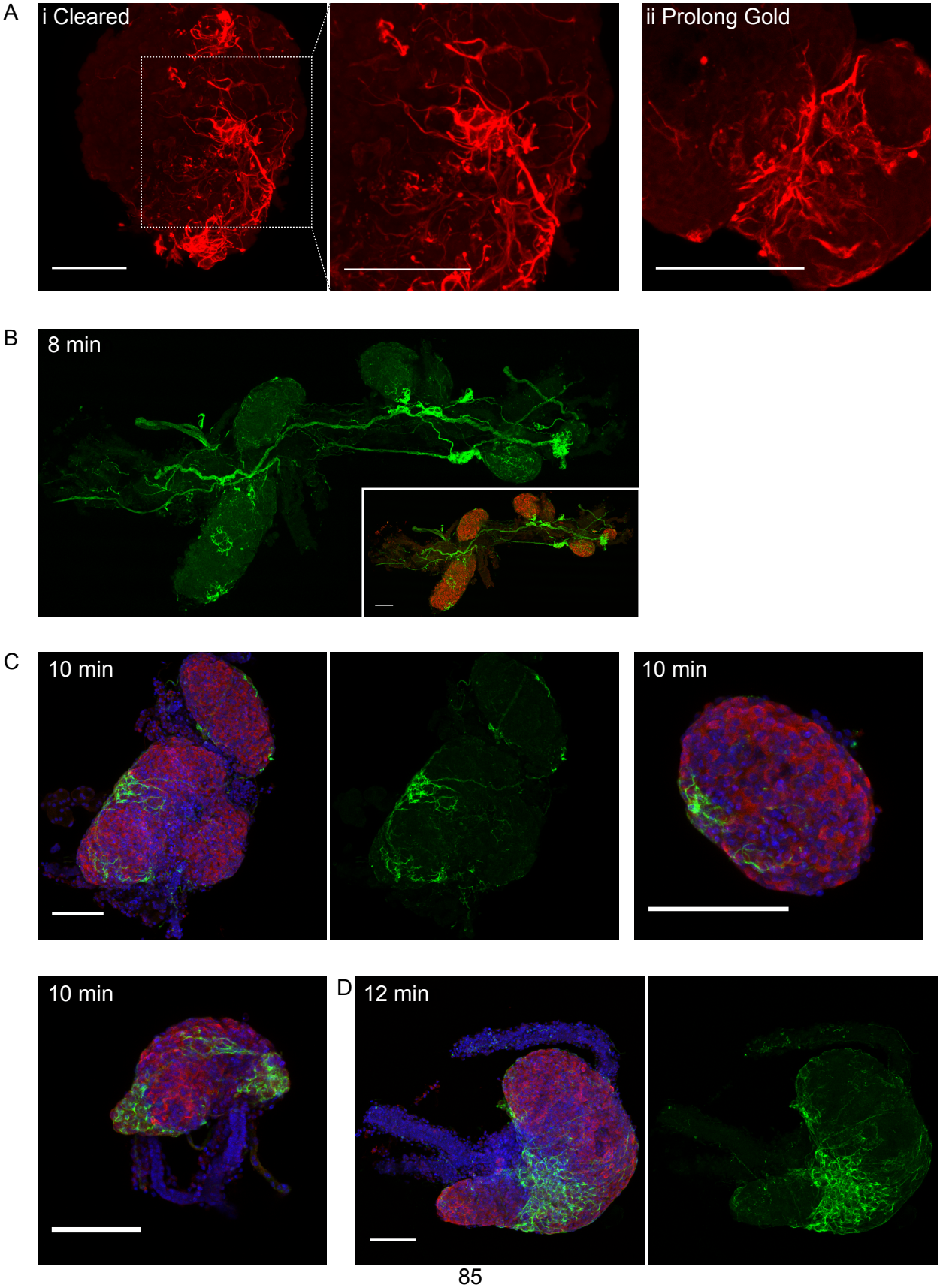

Figure 4. Lineage tracing of GFAP+ islet glial cells

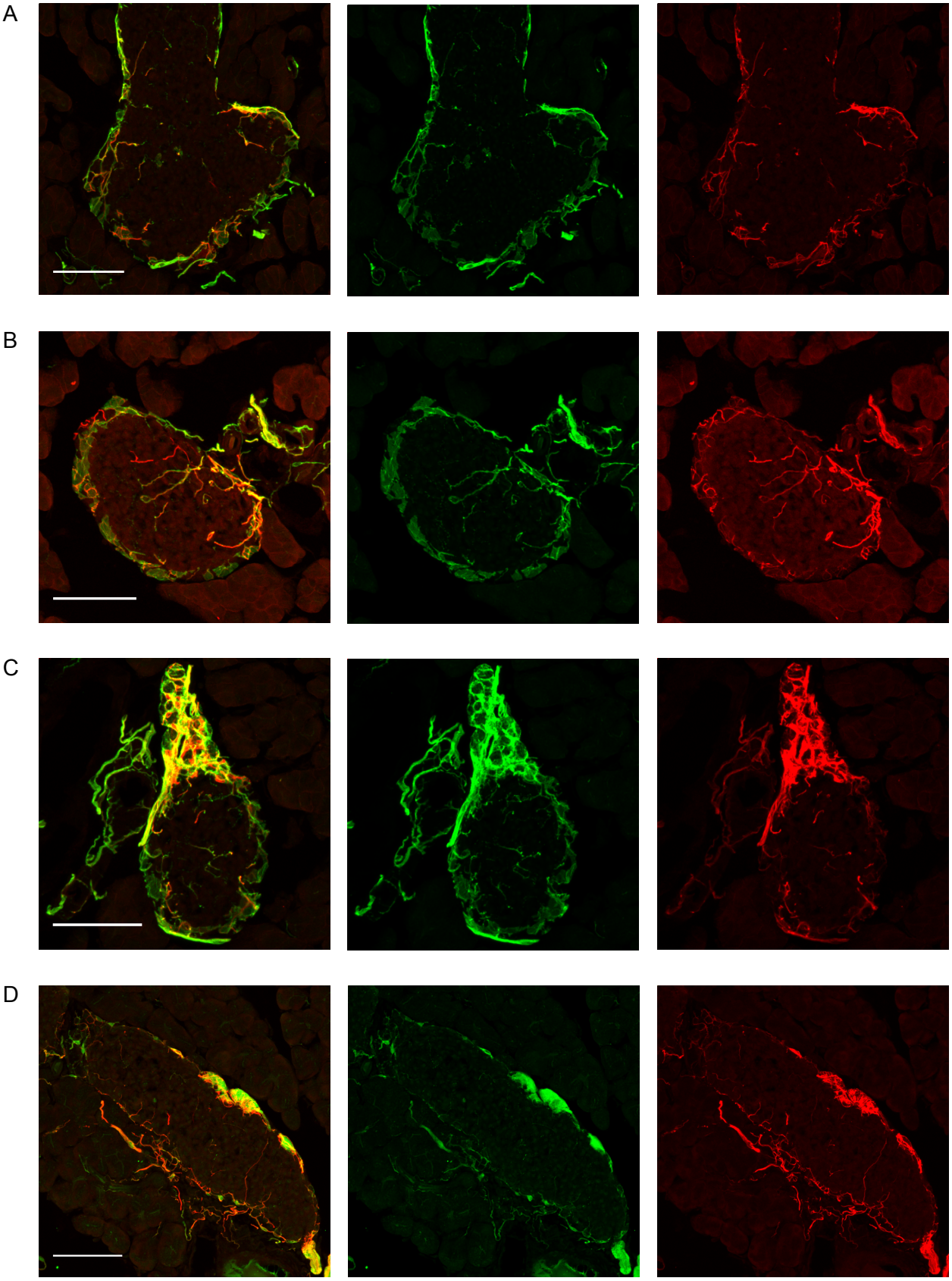

Figure 5. Lineage tracing of GFAP+ islet glial cells: individual nucleated cells

A

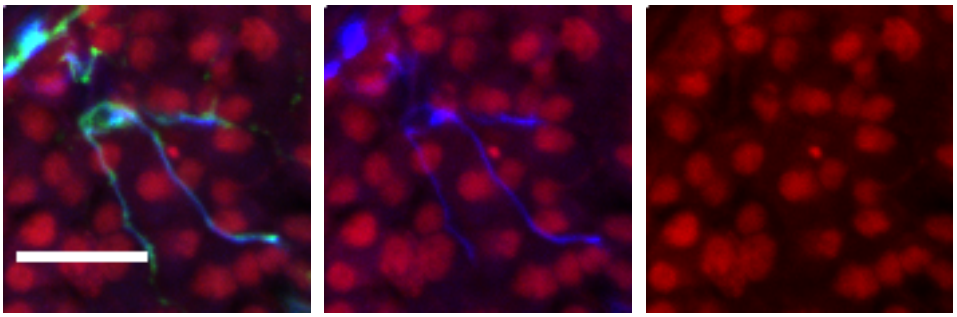

B

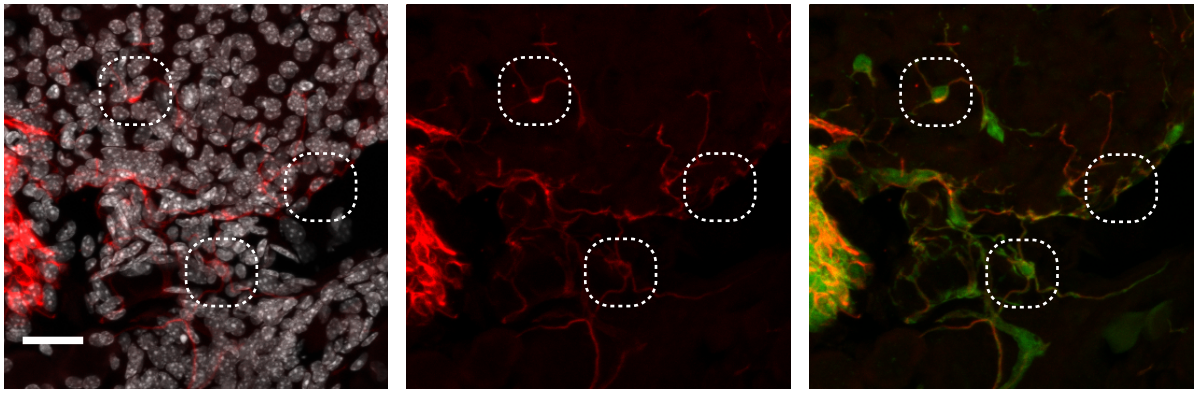

Figure 6. Islet pericytes are not neural crest cell derived

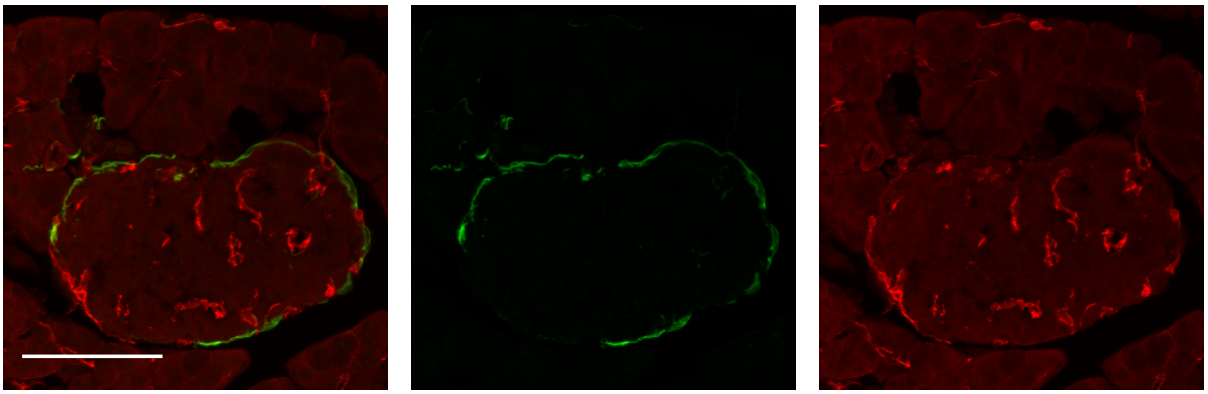

Figure 7. Assessing using a GFAP-cre mouse line to study islet glial cells

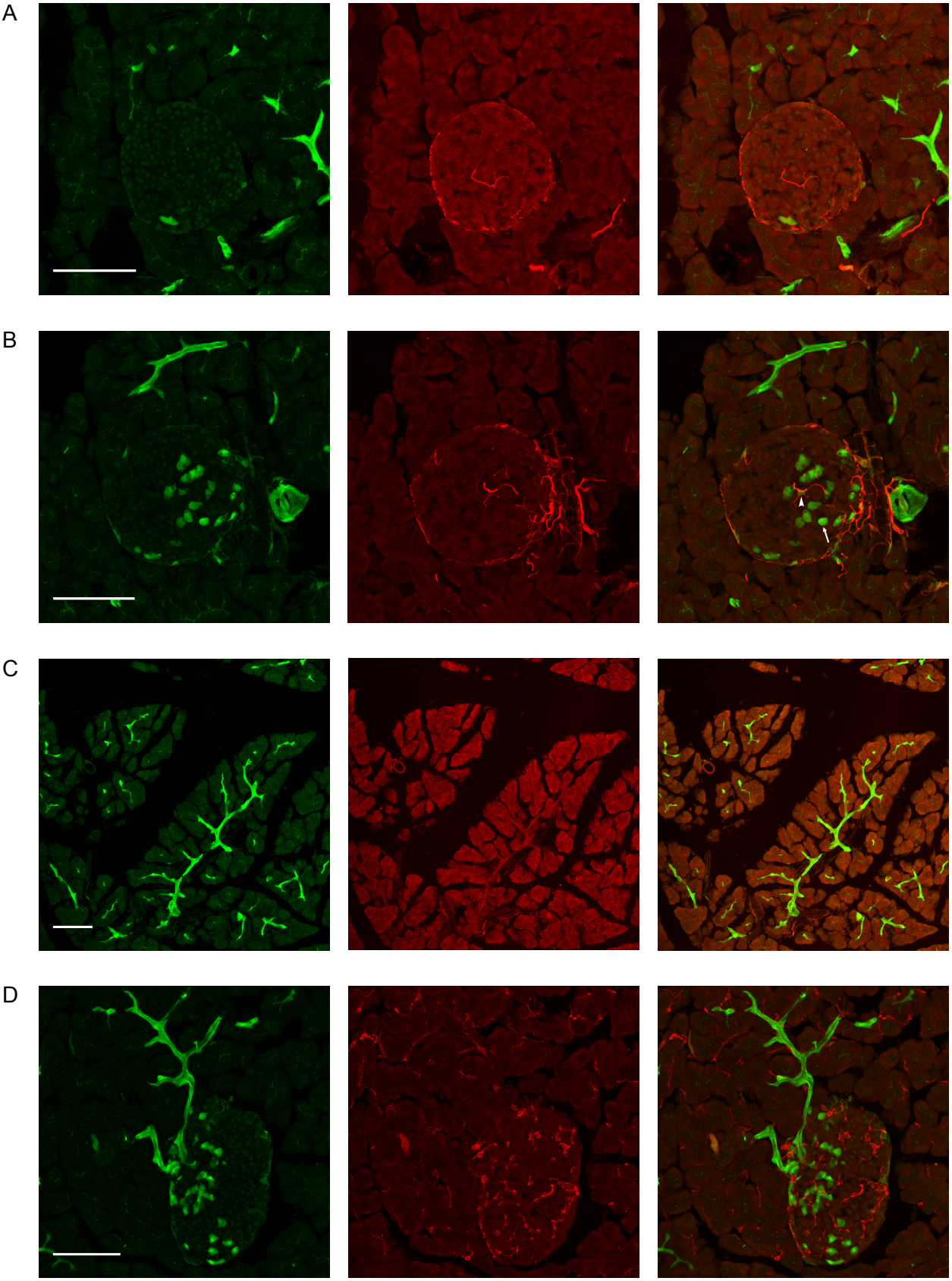

Figure 8. Assessing GFAP-cre mouse line to study islet glial cells: vessel/duct close-up

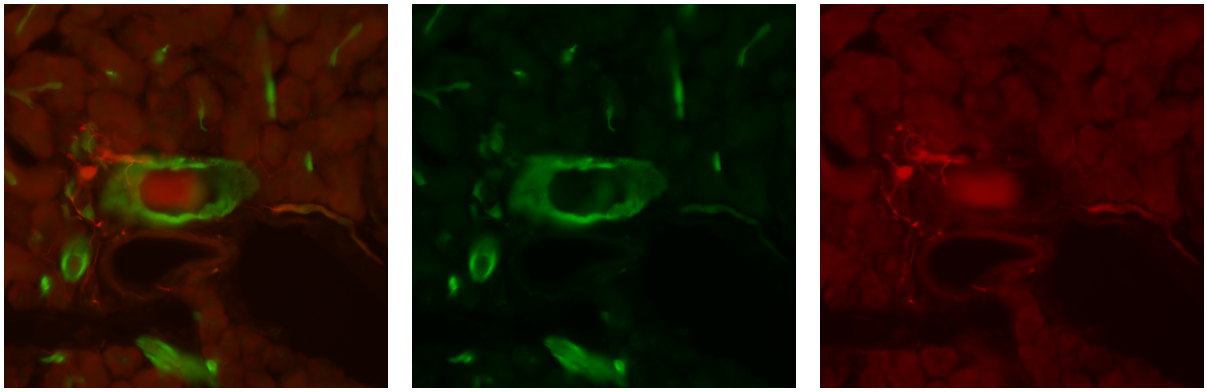

Figure 9. Proof of concept for ex vivo diphtheria toxin ablation in cultured isolated islets

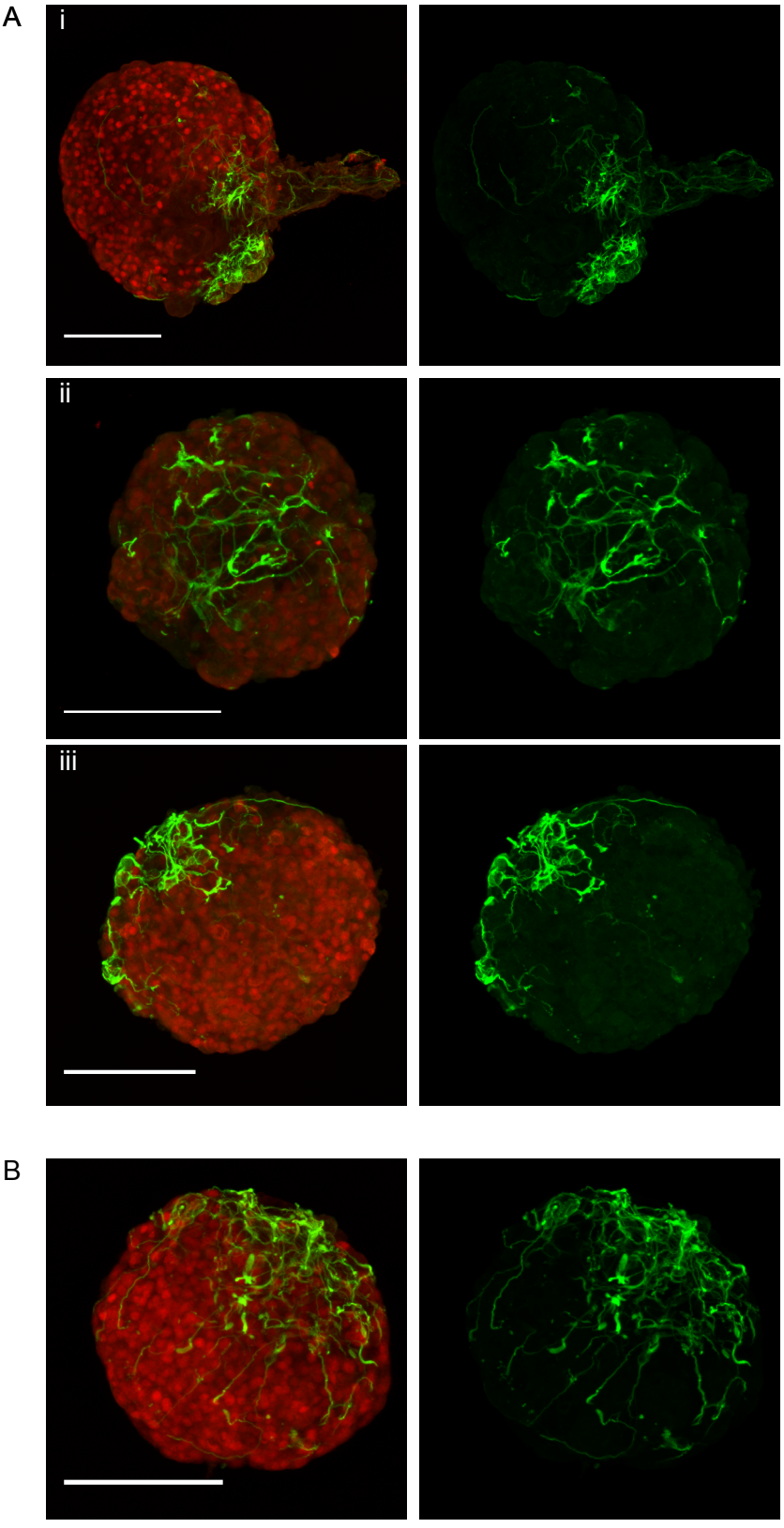

Figure 10. Assessing using a GFAP-GFP mouse line to study islet glial cells

A

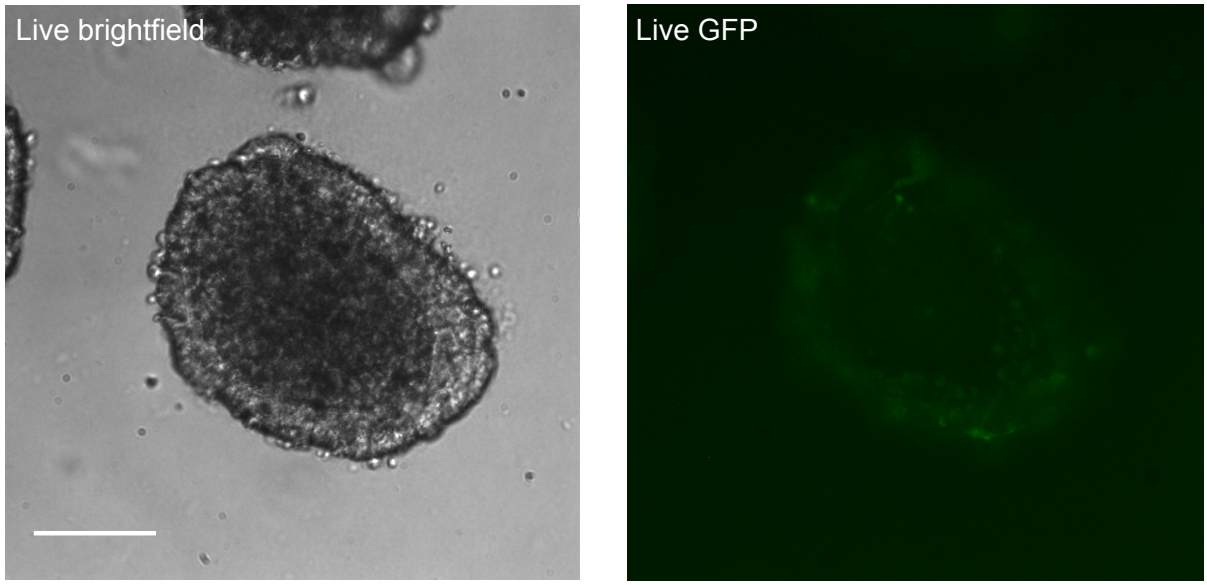

B

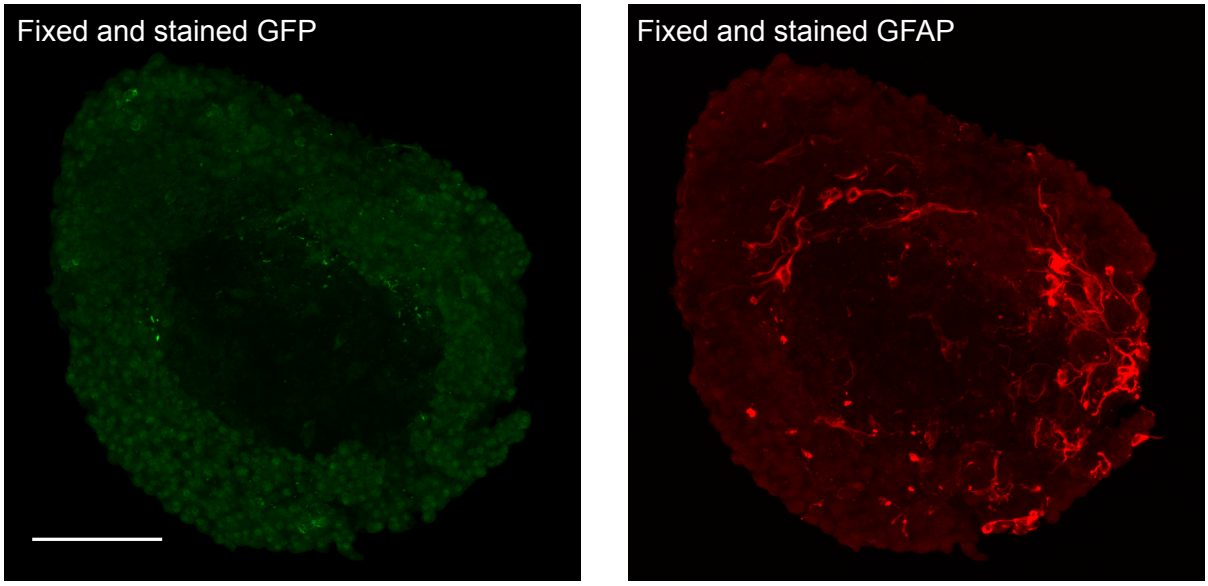

Figure 11. Assessing using TUJ1 as a pan-neuronal marker in pancreatic islets

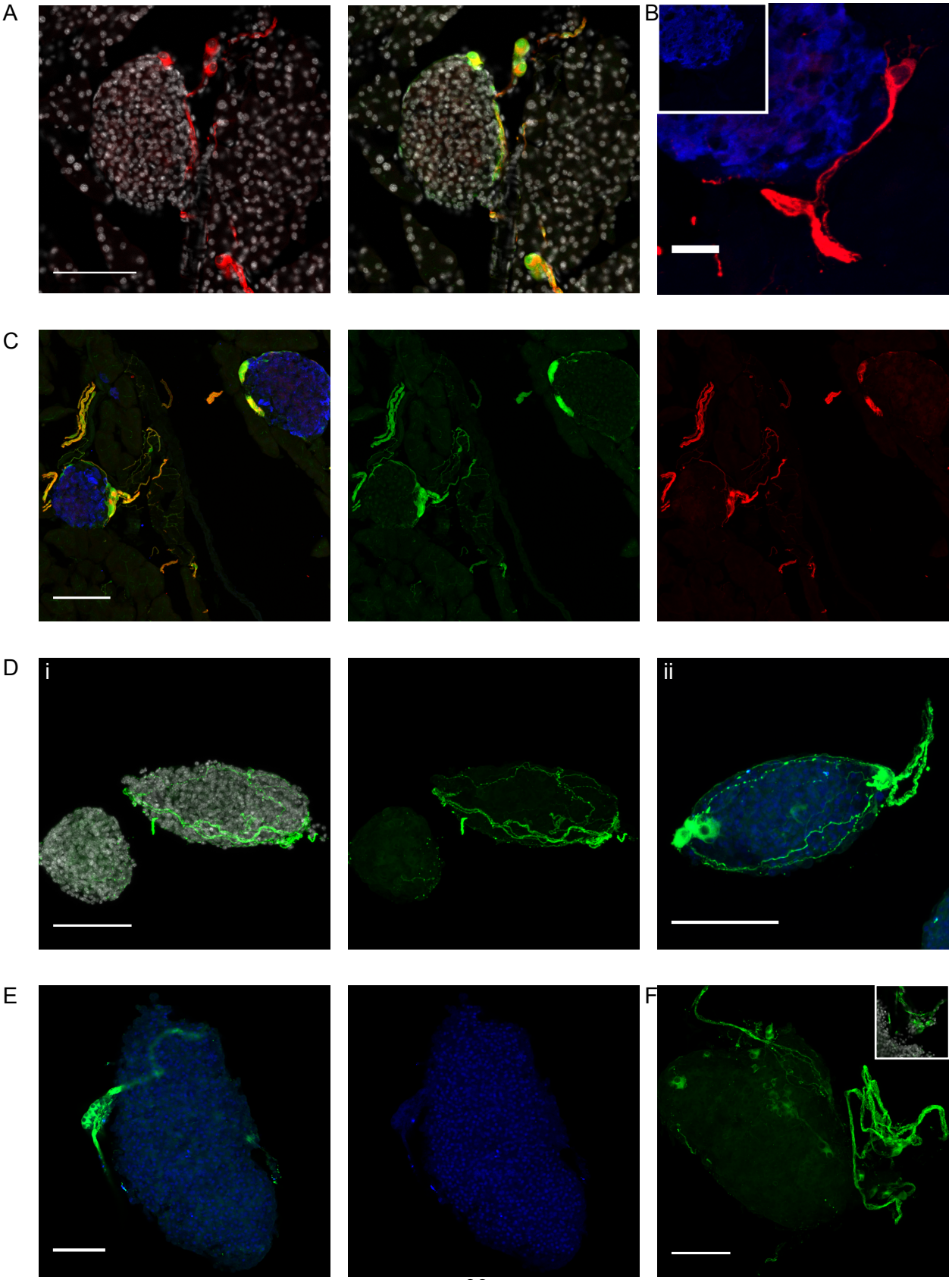

Figure 12. TUJ1+ neurons and GFAP+ glial cells are in close contact in isolated islets

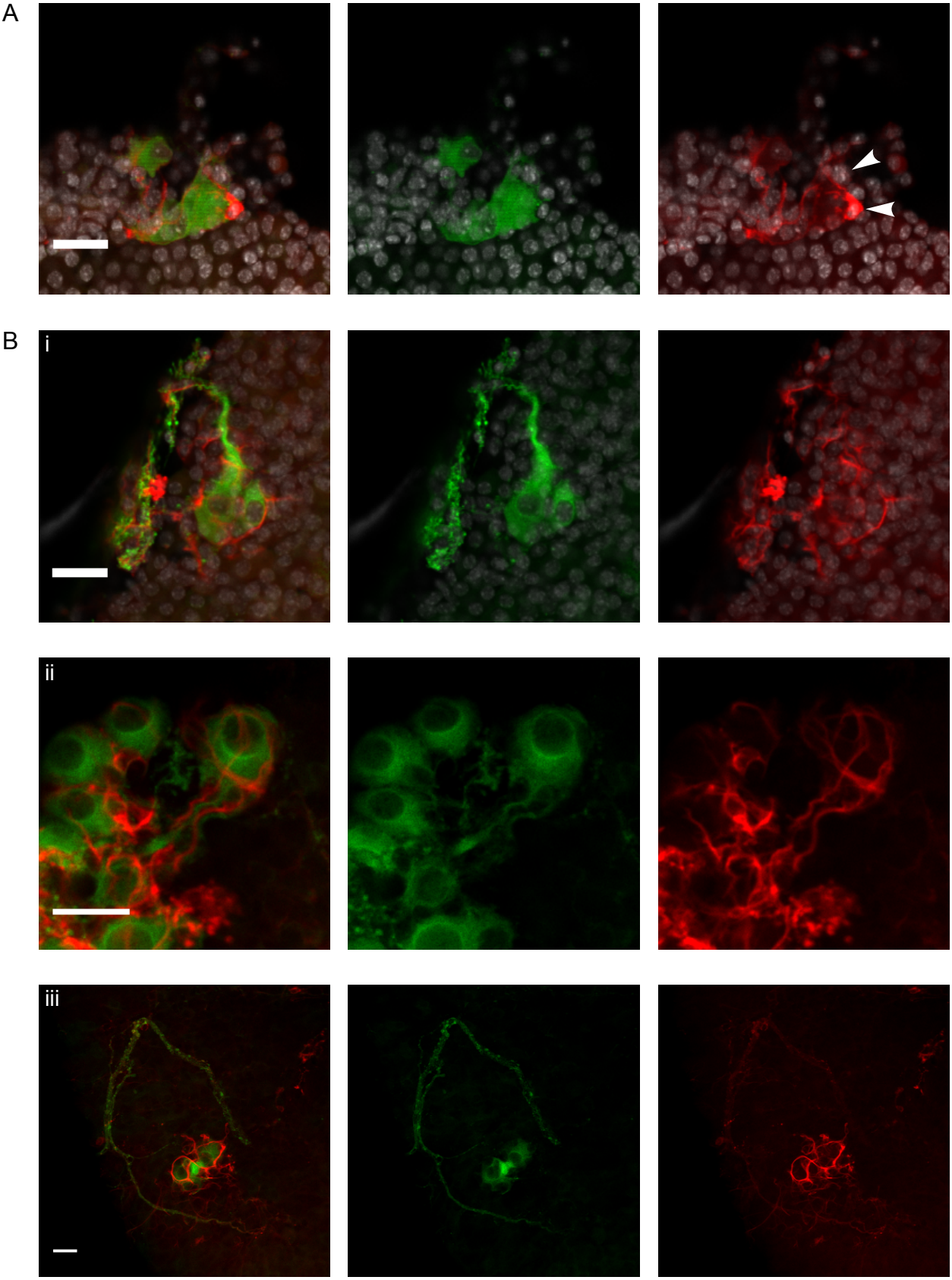

Figure 13. TUJ1+ neurons survive in isolated islet culture

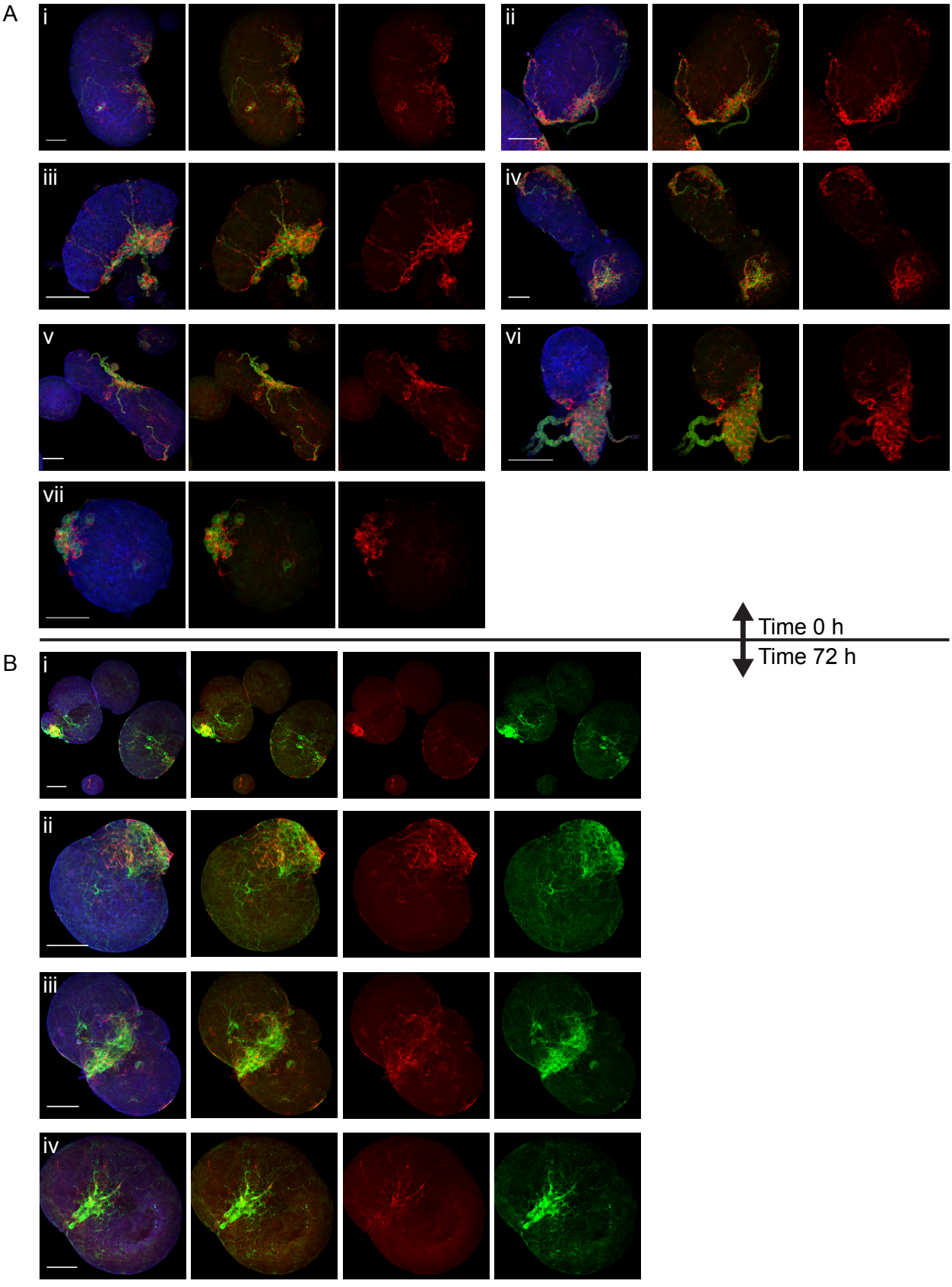

Figure 14. Retained TUJ1+ neurons generally match GFAP+ glial cell numbers in isolated islets

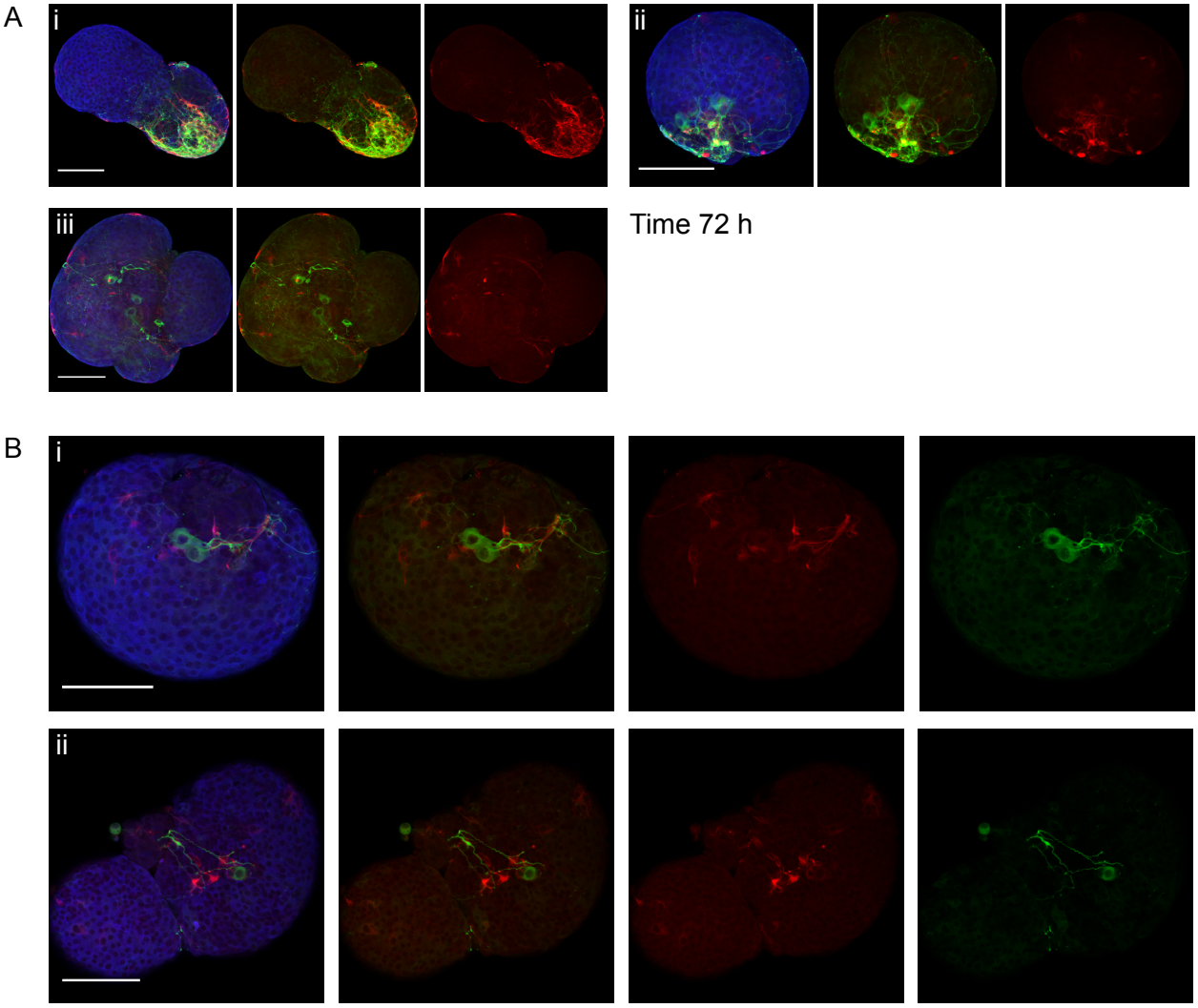

Figure 15. Outgrowth from adhesion cultured islets

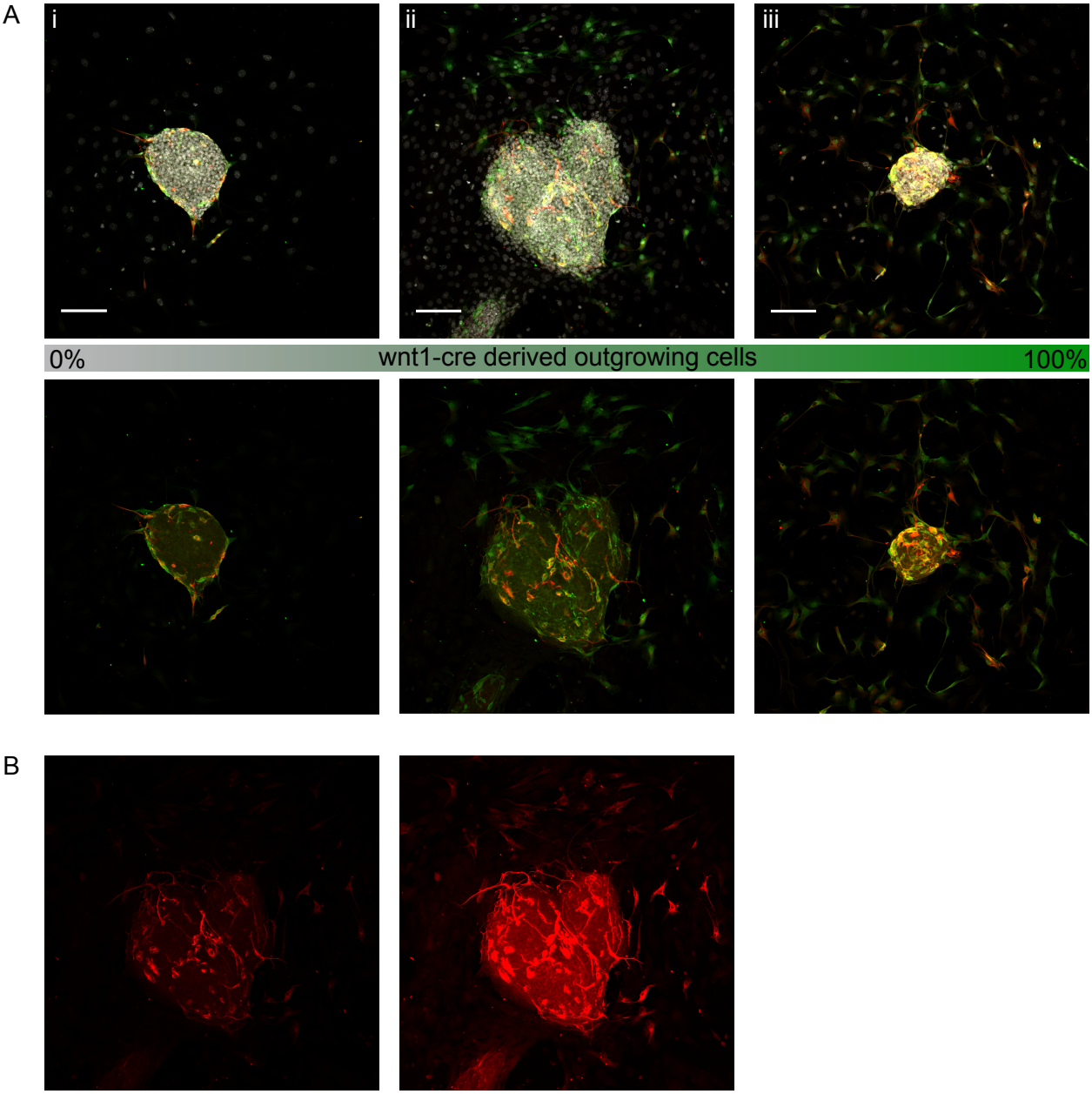

Figure 16. Wnt1-cre/mTmG FACS Pilot and Drop-Seq Pilot Sort

A

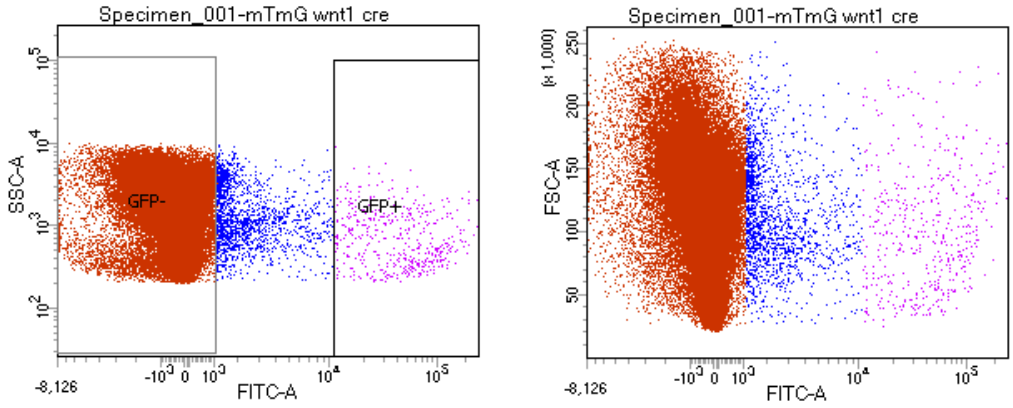

B

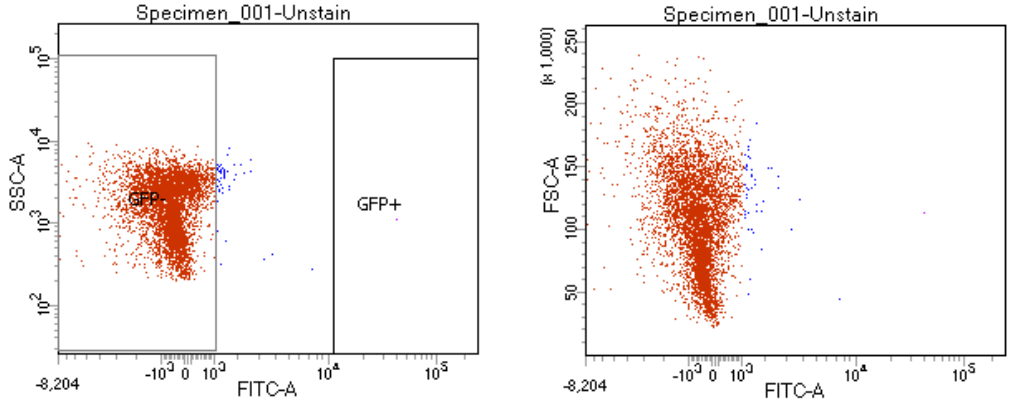

C

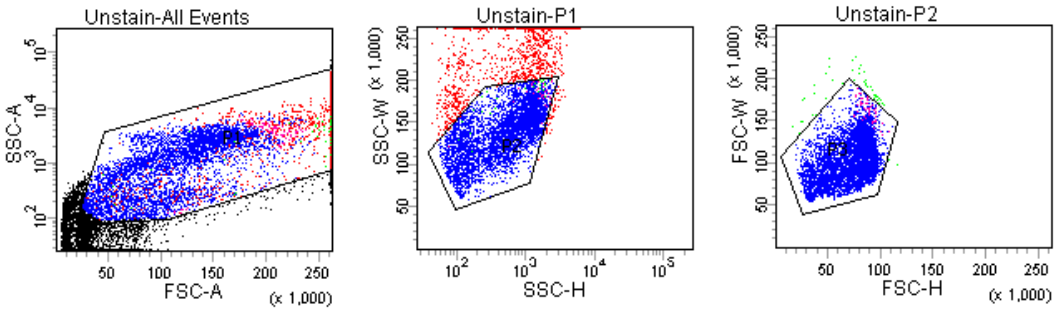

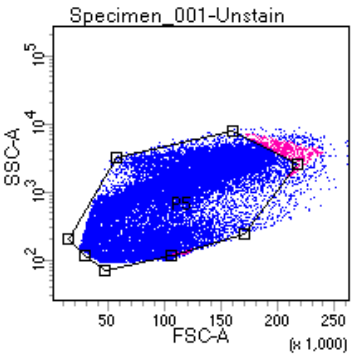

Tube: Unstain

Population	#Events	%Parent	%Total
All Events	100,000	####	100.0
P1	58,983	59.0	59.0
P2	45,383	76.9	45.4
P3	44,828	98.8	44.8
GFP+	####	####	####
GFP-	####	####	####
P4	40,727	90.9	40.7
P5	42,740	95.3	42.7

Figure 17. Wnt1-cre/mTmG FACS for HiSeq Drop-seq

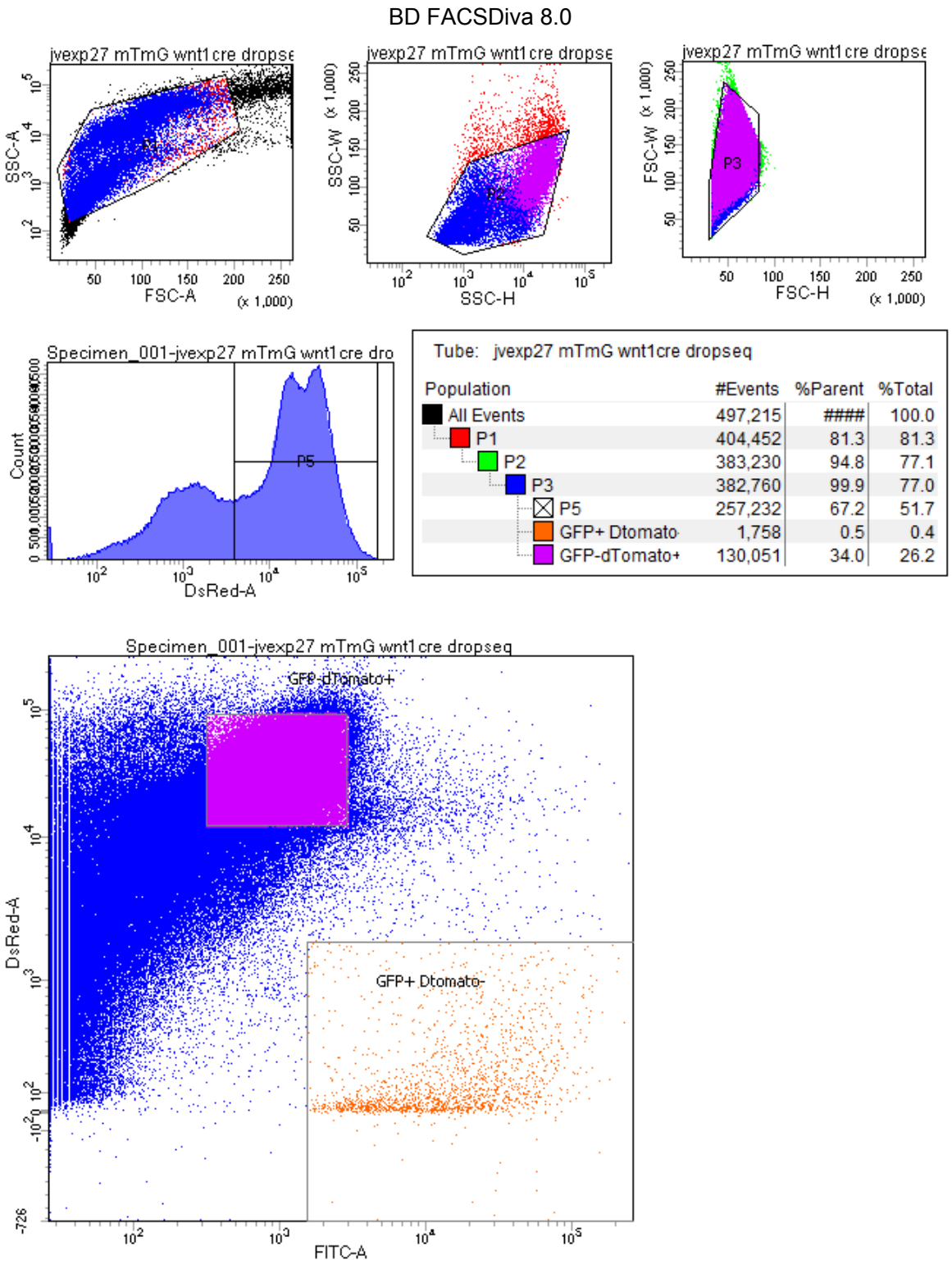

Figure 18. Heat map from Drop-seq gene expression data

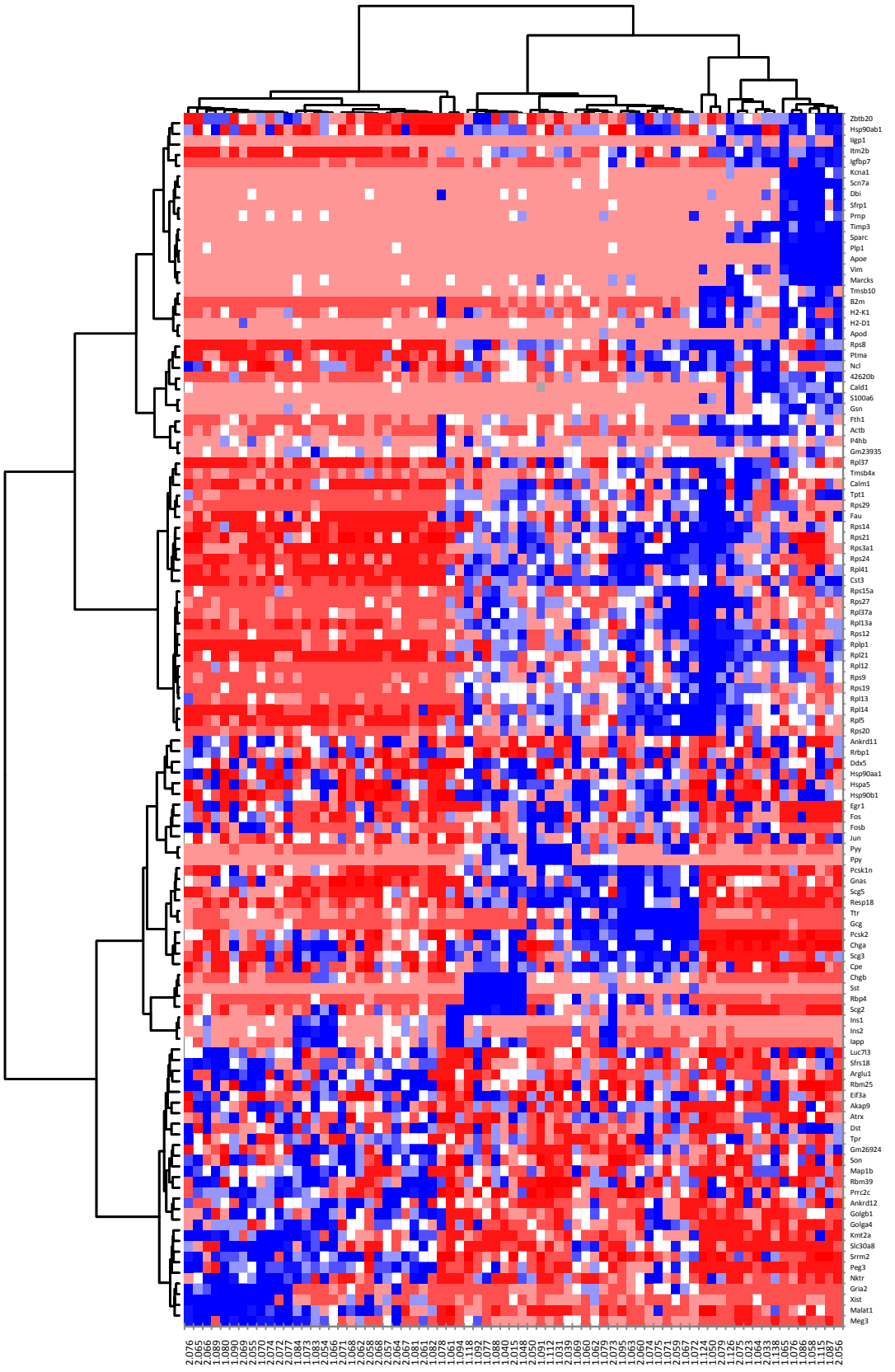

Figure 19. Gene ontology and pathway analysis from Drop-seq gene expression data

A.

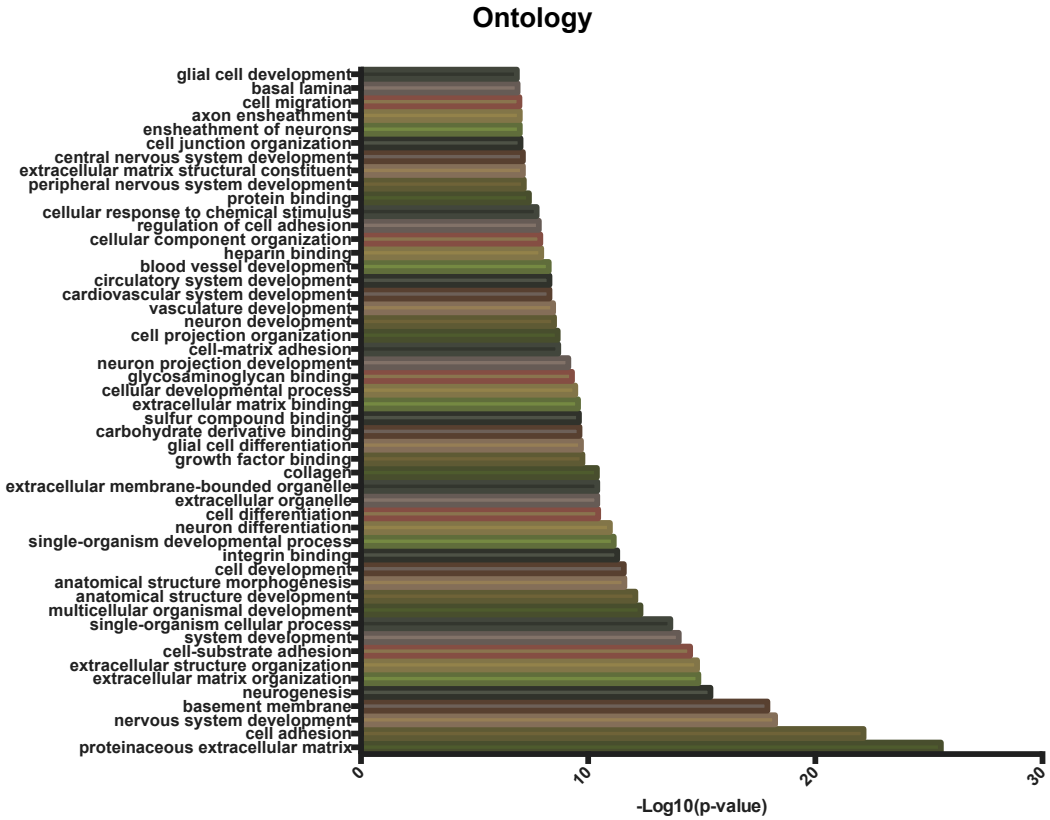

B.

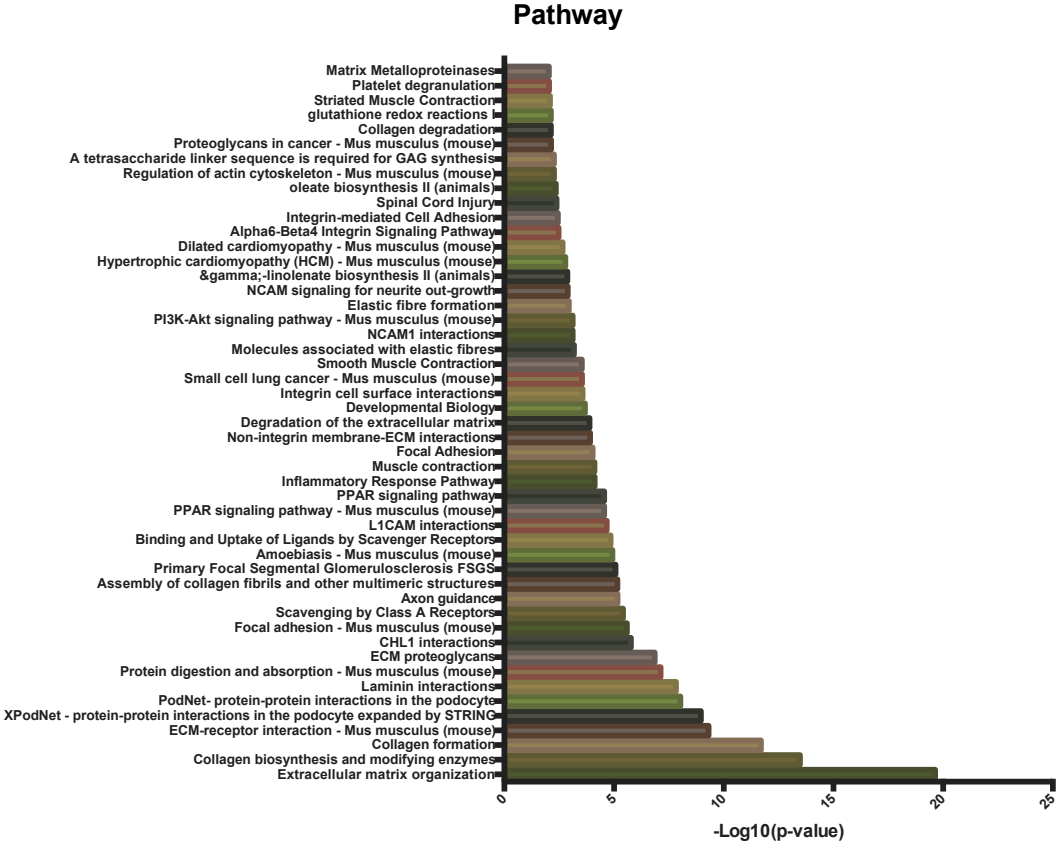

Publishing Agreement

It is the policy of the University to encourage the distribution of all theses, dissertations, and manuscripts. Copies of all UCSF theses, dissertations, and manuscripts will be routed to the library via the Graduate Division. The library will make all theses, dissertations, and manuscripts accessible to the public and will preserve these to the best of their abilities, in perpetuity.

I hereby grant permission to the Graduate Division of the University of California, San Francisco to release copies of my thesis, dissertation, or manuscript to the Campus Library to provide access and preservation, in whole or in part, in perpetuity.

Author Signature 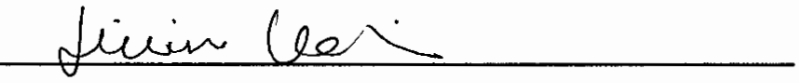

Date 12/27/16